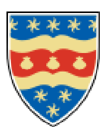

School of Geography, Earth and Environmental Sciences
Faculty of Science and Engineering

2021-01-01

Atomic Spectrometry Update: review of advances in elemental speciation

Robert Clough *School of Geography, Earth and Environmental Sciences*

Chris F. Harrington

Steve J. Hill *School of Geography, Earth and Environmental Sciences*

Yolanda Madrid

Julian F. Tyson

Let us know how access to this document benefits you

General rights
All content in PEARL is protected by copyright law. Author manuscripts are made available in accordance with publisher policies. Please cite only the published version using the details provided on the item record or document. In the absence of an open licence (e.g. Creative Commons), permissions for further reuse of content should be sought from the publisher or author.
Take down policy
If you believe that this document breaches copyright please contact the library providing details, and we will remove access to the work immediately and investigate your claim.
Follow this and additional works at: https://pearl.plymouth.ac.uk/gees-research

Recommended Citation

Clough, R., Harrington, C., Hill, S., Madrid, Y., & Tyson, J. (2021) 'Atomic Spectrometry Update: review of advances in elemental speciation', *Journal of Analytical Atomic Spectrometry*, 36(7), pp. 1326-1373.
Available at: https://doi.org/10.1039/d1ja90026a

This Article is brought to you for free and open access by the Faculty of Science and Engineering at PEARL. It has been accepted for inclusion in School of Geography, Earth and Environmental Sciences by an authorized administrator of PEARL. For more information, please contact openresearch@plymouth.ac.uk.

JAAS

ROYAL SOCIETY OF CHEMISTRY

ASU REVIEW

Cite this: J. Anal. At. Spectrom., 2021, 36, 1326

Atomic Spectrometry Update: review of advances in elemental speciation

Robert Clough, *[a] Chris F. Harrington, [b] Steve J. Hill, [c] Yolanda Madrid [d] and Julian F. Tyson [e]

Received 2nd June 2021

DOI: 10.1039/d1ja90026a

rsc.li/jaas

1 Topical Reviews
2 CRMs and Metrology
3 Elemental Speciation Analysis
3.1 Antimony
3.2 Arsenic
3.3 Cadmium
3.4 Chromium
3.5 Cobalt
3.6 Copper
3.7 Gadolinium
3.8 Gold
3.9 Halogens
3.10 Iron
3.11 Lead
3.12 Manganese
3.13 Mercury
3.14 Nickel
3.15 Phosphorous
3.16 Platinum
3.17 Selenium
3.18 Silicon
3.19 Silver
3.20 Sulfur
3.21 Tellurium
3.22 Thallium
3.23 Tin
3.24 Titanium
3.25 Uranium
3.26 Vanadium
3.27 Zinc
4 Biomolecular Speciation Analysis
5 Abbreviations used in this update
6 Conflicts of interest
7 References

[a]Biogeochemistry Research Centre, University of Plymouth, Plymouth, UK. E-mail: rclough@plymouth.ac.uk

[b]Supra-Regional Assay Service, Trace Element Laboratory, Surrey Research Park, 15 Frederick Sanger Road, Guildford, GU2 7YD, UK

[c]School of Geography, Earth and Environmental Sciences, University of Plymouth, Plymouth, UK

[d]Departamento de Quimica Analitica, Facultad de Ciencias Quimicas, Universidad Complutense de Madrid, Avda Complutense s/n, 28040 Madrid, Spain

[e]Department of Chemistry, University of Massachusetts Amherst, 710 North Pleasant, USA

This is the 13th Atomic Spectrometry Update (ASU) to focus on advances in elemental speciation and covers a period of approximately 12 months from December 2019. This ASU review deals with all aspects of the analytical atomic spectrometry speciation methods developed for: the determination of oxidation states, organometallic compounds, coordination compounds, metal and heteroatom-containing biomolecules, including metalloproteins, proteins, peptides and amino acids, and the use of metal-tagging to facilitate detection *via* atomic spectrometry. As with all ASU reviews, the focus of the research reviewed includes those methods that incorporate atomic spectrometry as the measurement technique. However, because speciation analysis is inherently focused on the relationship between the metal(loid) atom and the organic moiety it is bound to, or incorporated within, atomic spectrometry alone cannot be the sole analytical approach of interest. For this reason, molecular detection techniques are also included where they have provided a complementary approach to speciation analysis. This year the number of publications concerning As speciation remains similar to those covered last year, as do those for studies on Se speciation. The recent growth in work concerning Hg speciation has halted, although this is still a popular topic with the number of reports concerning Fe, halogen and sulfur speciation also rising. The number of elements covered this year reaches 30, showing the breadth of the elemental speciation field and how such work is now becoming more routine.

1 Topical reviews

This latest update adds to that from last year[1] and complements the five other annual Atomic Spectrometry Updates: advances in

 This journal is © The Royal Society of Chemistry 2021

environmental analysis,[2] advances in the analysis of clinical and biological materials, foods and beverages,[3] advances in atomic spectrometry and related techniques,[4] advances in X-ray fluorescence spectrometry and its special applications[5] and advances in the analysis of metals, chemicals and materials.[6]

There are no new textbooks featuring elemental speciation topics as the main theme published in this review period. However, several chapters in a recent book edited by Beauchemin, "Sample Introduction Systems in ICP-MS and ICP-OES", deal with the combination of separation techniques with plasma instrumentation.[7] The techniques covered include LC, GC, CE, FFF, VG, FIA, LA, ETV, and some electrochemical techniques. As might be expected, there is also a comprehensive chapter dealing with nebulisation and spray chambers. Each of the relevant chapters concludes with a substantial section entitled "applications". Although not specifically discussed in the preface, the book is clearly intended for practicing analytical chemists and features critical commentary (on for example, the advantages and shortcomings of various nebulisation systems) and guidelines for choosing a particular technique or system. The editor writes, "may it provide all the resources needed to enable, facilitate or enhance your specific application". The various review articles appearing during the review period may be broadly classified into those primarily concerned with (a) one analytical technique, (b) a particular method or stage in a method, (c) a particular area of application or sample type, or (d) a combination of a, b and c.

Three reviews have highlighted the impact of ICP-MS in the biological field. Pluhacek and Maier focused on the elucidation of the bioeffects of trace metals and their species on cellular metabolism and cell behaviour in a short (39 references) review of single-cell analyses.[8] They identified a number of methods, including time-resolved ICP-MS, ETV-ICP-MS, LA-ICP-MS, chip-based microextraction techniques, HPLC or CE coupled with ICP-MS, elemental tagging, and mass cytometry. The reviewers concluded that further developments are needed. Firstly, to improve LOD values so as to decrease the number of cells required. Secondly, techniques suitable for analysing the chemical composition of a single cell are needed, to allow for the study of the biotransformations of elements and species in a single cell. They suggested that a combination of multi-extraction and multidimensional separation techniques (*e.g.*, two-dimensional HPLC, HPLC, CE, or a combination of capillary isotachophoresis and CE) with ICP-MS techniques could be suitable. They also called for efforts to improve applications in structural biology, where more attention is paid to the application of molecular MS to the characterisation of biomolecules, including proteins, enzymes, and lipids. Xu *et al.* have summarised the contents of 57 articles concerning applications of ICP-MS to the understanding of the molecular mechanisms of metallodrug action.[9] They pointed out that metal/metalloid complexes are commonly used in medicine as either therapeutic or diagnostic agents and concluded that continued advances require the integration of multiple metalloproteomics approaches with other omics-based techniques. Lores-Padin *et al.* reviewed (157 references) the application of NPs as labels of specific-recognition reactions for the determination of biomolecules by ICP-MS.[10] The reviewers state that NPs offer higher amplification capabilities (and, therefore, greater sensitivity and improved detection capability) than other approaches, such as single metal chelates or commercial polymers containing metal complexes. They also suggest that one of the possible limitations identified, blank contamination in the determination of very low concentrations of analyte when the NPs consist of elements commonly present in the laboratory, can be overcome by sp-ICP-MS measurements. On the other hand, if the sample is digested before introduction, memory effects in the sample introduction system are minimised. It was pointed out that high backgrounds in LA-ICP-MS, due to the non-specific absorption of NPs on biological tissues, have been observed. The reviewers indicated that to avoid this, it is crucial to optimise the ligand density as well as to block any highly reactive sites remaining on the NP of the labelled probe. In looking to the future, they speculate that TOF-MS could detect about 100 parameters using a different nuclide for each parameter, and that with LA sampling, well-resolved images of the analytes in single cells and tissue sections could be rapidly acquired.

In a review (111 references) of elemental speciation analysis of foods by LC-ICP-MS and complementary techniques, the reviewers divided methods into two board categories: bespoke and nontargeted.[11] Bespoke speciation analysis involves the quantification of species that are expected to be found, based on results reported in the literature or previous experiments. Nontargeted speciation analysis also involves the identification of new species. In their introduction the reviewers identify two groups of elements: those attracting considerable research interest in the development of speciation methods (As, Cd, Cu, Hg, Pb, Se, and Zn) and those that, although they impact human health (Al, Co, Cr, Ni, Sb and Te), are not discussed in terms of their speciation. They point out that this latter group is definitely present in various chemical forms in several foods. Examination of one the summary tables reveals that complementary techniques are APCI-, ES- and MALDI-MS, SDS-PAGE, CE-ICP-MS and various X-ray techniques, which are also discussed in a separate section in the text. The nanoparticulate form of some elements is also considered. The review also contains a table that summarises the maximum permissible levels of elements in most common food types, according to four agencies: (a) General Standard For Contaminants And Toxins In Food And Feed (FAO/WHO); (b) Commission Regulation (EC) No. 1881/2006 of 19 December 2006 (EU); (c) Standard for Maximum Levels of Contaminants in Foods (China) and (d) Health Canada's Maximum Levels for Chemical Contaminants in Foods. The problems of ensuring that species do not interconvert during analysis is discussed and the pros and cons of IDA are presented. The reviewers conclude that instrumental development will be driven by the potential market, which will not open up until such time as countries establish food legislation that requires speciation analysis, rather than total measurements. For this to happen, they consider it necessary that there is convincing evidence of the toxic effects of individual species at concentrations typically encountered.

In a comprehensive review of solid sampling, some 626 articles published in the period 1990 to 2019 were surveyed, of which 251 were cited in the review.[12] Although speciation is mentioned in the abstract and in the concluding remarks as a "new possibility", the review contains only two examples (Cr and S) and a reference to an XRF based review. In the section on "ETV for sample introduction into plasmas", the reviewers consider that chelating agent modifiers permit the vaporisation of the complexed elements at lower temperatures, and are a possible route to selective reaction/vaporisation for potential speciation. In a review of *in situ* mapping of chemical segregation using synchrotron X-ray imaging, Feng *et al.* focus on the solidification of metallic alloys.[13] Although the reviewers consider that X-ray imaging techniques, which have steadily improved over the last decades allowing resolution at distance scales of sub-micrometres over sub-second time scales, can also give spatially resolved chemical information, elemental speciation is not featured in any of the 45 articles cited. They also pointed out that even relatively short synchrotron-based experimental campaigns already generate more data than can be analysed by a large team of researchers. They concluded that automated analysis and extraction techniques based on machine learning and artificial intelligence will become increasingly important.

Three reviews of sample pre-treatment emphasised applications for elemental speciation. Developments over the past 5 years in SPE by various nanomaterials (metallic, silica, polymeric and carbon-based) in the speciation analysis of As, Cr, Sb, Se were reviewed (135 references) by Pyrzynska.[14] The advantages of carbon nanotubes and graphene were highlighted in terms of the range of surface functionalisation that is possible, as were the superior separation features of magnetic NPs, whose surfaces can also be coated with a variety of materials and functional groups. Numerous examples of the use of such materials in the non-chromatographic speciation of the four elements mentioned were given. The increasing commercial availability of these materials is highlighted as indicative of the potential for continued application, not just to the elements mentioned but also for the speciation analysis of Mn, Sn, Tl and V. In a review (191 references) of CPE, elemental speciation was featured quite extensively.[15] Some 20 publications were discussed in a separate section that included a summary table for Cr that featured 8 procedures. Speciation procedures for other elements (As, Fe, Hg, Sb, Se, Te, Ti and V) were also discussed. The review also contained a short section (6 references) devoted to NPs (Ag, CuO and Au). A considerable portion of the review (maybe 20%) was given over to the CPE of organic analytes, and the review concluded with a discussion of newer methods, including micro-CPE, displacement CPE, rapid synergistic CPE, dual CPE, and acid-induced CPE. The reviewer pointed out that the CPE of anionic species has not attracted much attention, a comment that is perhaps directed more towards the determination of non-metal and non-metalloid species than towards species that would be quantified by an atomic spectrometry technique. Ricardo *et al.* reviewed (103 references) magnetic SPE in the sample preparation for the elemental speciation analysis of As, Cr, Hg, Se, for which the majority of methods have been developed.[16] The reviewers also included a smaller number of methods for Mn, Sb, Sn, Te and Tl. The obvious advantageous feature, ease of separation without filtration or centrifugation, was pointed out together with the fact that the sorbent material can be re-used and that the procedure has greatly benefitted from the use of NPs made from iron oxides, such as magnetite and maghemite, which have large magnetic moments, high surface areas and are easy to prepare. The review also mentions a small number of applications to the determination of Ag and Au NPs. The reviewers conclude by noting that as these materials are not yet commercially available, "inter-comparisons and harmonisations" are limited.

In one of two reviews of environmental elemental speciation, Chen *et al.*[17] devote a considerable part of the introduction to discussing what they mean by "environmetallomics" and they provide the following definition of the environmetallome: (i) the entirety of metal and metalloid species that can induce toxic effects on living organisms at an environmentally relevant concentration range; (ii) all metals and metalloids within a biological system which homeostasis could be directly or indirectly interfere and regulated to induce potential adverse effects. As the second part of this definition is hard to follow, the following may help "environmetallomics studies should underpin researches on the origins of metals and exogenous regulation of metal-associated biological responses in exposed organisms. In contrast to traditional metallomics studies, the scope of environmetallomics is extended from the interior of living organisms to a local habitat or ecosystem". The bulk of the review (total of 82 references) is taken up with a discussion of analytical approaches to environmetallomics (about 63 references) in which the reviewers highlight DGT as a popular and effective tool for estimating metal and metalloid bioavailability and bioaccumulation, thereby allowing identification of the factors controlling bioavailability. Elemental mapping techniques are also given prominence and the importance of the development of small molecule probes noted, as these allow *in vivo* metal imaging, so that metal transport and localisation inside organisms in real time can be followed. Single cell analysis, and metalloproteomics were also discussed. The review contains a very brief section (4 references) on bioinformatics and data mining. The reviewers conclude that environmetallomics needs analytical methods for not only the elemental chemical species, but also for associated molecular clusters, macromolecular complexes, and inert and semi-inert particles. They call for significant efforts to be made to improve the performance of analytical technologies, in terms of detection capability, coverage and interference tolerance. Finally, they note that the scarcity of reference genomes and proteomes for non-model organisms hinders data mining of sequencing data. In a slightly later article, three of the authors of the previous review are joined by three other reviewers to "revisit" the forms of trace elements in biogeochemical cycling to ascertain the analytical needs and challenges (77 references).[18] The reviewers make the point that the elements in the environment occur not only in different chemical species but also in species of different dimensions ranging from free ions,

 This journal is © The Royal Society of Chemistry 2021

ionic compounds, nanoparticles, macromolecular complexes and bulk materials (such as minerals). Much of the review is devoted to the characterisation of NP and macromolecules, species that are often lost in sample preparation procedures that involve centrifugation and/or filtration. The reviewers conclude that there is still lack of an efficient and reliable method for extraction of NPs and macromolecular complexes from complex matrices, such as soils and biological matrices, and that further research should be devoted to the development of *in situ* and non-destructive imaging of nanoparticles in organisms.

2 CRMs and metrology

Hijiki is unusual amongst macroalgae in that it contains significant proportions of iAs, MMA and DMA, as well as arsenosugars, whereas most seaweeds only contain arsenosugars. The first results from an inter-laboratory comparison covering the certification of a new CRM, a Hijiki seaweed which will be certified for various As compounds including arsenosugars, has been published.[19] Water-soluble As compounds were extracted from dried, ground Hijiki either by agitation overnight at room temperature, or for 1 hour with UAE or with a solution of 0.01% w/v pepsin in 0.07 mol L^{-1} and heating at 37 °C for 2 hours. In each case the extracts were then centrifuged and filtered before analysis. Separations used either by anion exchange or reverse phase HPLC columns with detection and quantification by either ICP-MS or ES-MS. Six As compounds, As^V, DMA and four arsenosugars, glycerol, phosphate, sulfonate and sulfate types, were detected in the extracts and method validation was by analysis of NMIJ CRM 7405a, a Hijiki seaweed certified for both total arsenic and As(v). The sum of the water soluble As species and those remaining in the candidate CRM residue was 104% of the total As content as determined by a MAE procedure with concentrated HNO_3 whilst the found and certified values for the NMIJ CRM 7405a were in statistical agreement. The found values for the candidate CRM were, total As 49.4 ± 1, As^V 24.4 ± 0.6, sugar-408 1.41 ± 0.05, sugar-328 0.45 ± 0.02, sugar-482 0.202 ± 0.007, sugar-392 0.157 ± 0.005 and DMA 0.239 ± 0.009 (all values in mg kg^{-1} and the uncertainty is the expanded uncertainty with a coverage factor of 2).

With recently legislated maximum levels of iAs in white and brown rice, which form a major part of infants' diet, there is a need for suitable CRMs to validate methods used to check product legislative conformity. To this end NRCC BARI-1, a baby cereal coarse rice flour CRM, certified for total As (0.248 ± 0.018 mg kg^{-1}), iAs (0.113 ± 0.016 mg kg^{-1}) and DMA (0.115 ± 0.010 mg kg^{-1}) with a reference value for MMA (0.0045 ± 0.0008 mg kg^{-1}) has been rapidly produced.[20] Trace amounts of an As compound, with a chromatographic retention time close to that of DMA were also observed, and despite extensive efforts this could not be identified but was not believed to be an analytical artefact. The CRM has also been certified for total Cd, Hg and Pb content. Participating laboratories in the certification exercise used their own in-house-validated extraction and/or digestion methods. Total metal quantifications were by ICP-MS whilst HPLC-ICP-MS was used for As speciation. Most methods used a weak HNO_3 solution and heat to extract the As species, often with added H_2O_2, whilst one laboratory used TFA and all As species separations appear to have been undertaken using anion exchange chromatography. The certification of NRCC BARI-1 was accomplished with a CRM rapid response approach in collaborative, focused effort completing the CRM development in few months instead of the typical multiyear project. The quantification of amyloid-beta (Aβ) biomarkers can contribute to an early diagnosis of Alzheimer's disease but there are still large variations among results obtained with different assays. To improve this two CRMs Aβ40 (GBW09874) and Aβ42 (GBW09875), with certified values and uncertainties of 7.58 ± 0.30 and 7.62 ± 0.30 μg g^{-1}, respectively, have been produced from high-purity Aβ.[21] Structural analysis of the Aβs was undertaken using UHPLC-q-TOF-MS whilst quantification was by both HPLC-ES-MS, using ^{13}C and ^{15}N labelled amino acids, and species unspecific ID-HPLC-ICP-MS in which a ^{34}S enriched spike was added post column to the HPLC eluent. Mass bias was evaluated using a natural isotopic S CRM. The values obtained by each analytical approach were in statistical agreement and the certified values and expanded uncertainties (U), with a coverage factor of 2, of the candidate Aβ40 and Aβ42 CRMs are reported as 7.58 ± 0.30 and 7.62 ± 0.30 μg g^{-1}, respectively. All three of these papers contain a wealth of information and deserve a detailed read.

There are also two other articles which may be of interest to the reader of this ASU. The first of these is a perspective paper, authored by one of the UK's leading metrologists, which covers traceability in analytical atomic spectrometry.[22] The paper gives a history of metrological traceability and the reasons why measurements need to be comparable, covers the international framework under which this now occurs, with a section on in-house methods also included and has a brief section on isotopic analyses and a further section on elemental speciation. Synchrotron radiation techniques are also being increasingly used to determine elemental speciation directly on solid samples, obviating the need for sample preparation procedures which require that species integrity is maintained during extraction from a sample. The uncertainty of these measurements is often lacking and this has been addressed in a paper which discusses the development of criteria for uncertainty analysis for these type of X-ray measurements.[23] The potential of the model was demonstrated by application to stacks of XRF maps collected around the Cu K-edge (pixel size: 3 × 3 μm^2, map sizes: 500 × 500 μm^2). The investigated samples included digested sewage sludge spiked with either CuO NPs or dissolved Cu_SO_4 and their corresponding ashes obtained through incineration. The chemical imaging data revealed differences in species distribution between the spiked sludges but not, as might be expected due to the temperatures involved, in the ashes of each spiked sample. Two benchmarks, score and correct largest Spectral Component Identified (CSCI), were used to assess the assess the reliability of the chemical images obtained and were evaluated using a synthetic dataset and applied to experimental data of a case study at different levels of uncertainty.

3 Elemental speciation analysis

3.1 Antimony

A number of research groups have published studies on *methods for Sb speciation.* Multielement approaches which include Sb have also become popular. An ultra-sensitive SCGD-OES method coupled with HG for the *determination of Sb valence state* has been described by Zhao *et al.*[24] By masking Sb^V with citric acid in HCl medium, stibine from Sb^{III} was selectively generated in a HG system. Total Sb was determined after reducing Sb^V to Sb^{III} with 0.3% L-cysteine in 0.01 mol L^{-1} HCl. The Sb^V concentration was calculated from the difference between total Sb and Sb^{III}. The main operational parameters and sources of potential interference that may affect the determination were optimised using a Sb^{III} standard solution. The LOD values obtained were 0.39 and 0.36 ng mL^{-1} for Sb^{III} and total Sb, respectively, and the RSDs were 2.1 and 1.7% at the 10 ng mL^{-1} level. The method was used to determine the valence state of Sb in water samples, and recovery experiments for different amounts of analytes were carried out. The recoveries were all in the range of 96.2 to 103.2% and were in good agreement with the corresponding ICP-MS values. An online simultaneous speciation method for the determination of ultra-trace iSb and Te in environmental waters using a polymer monolithic capillary microextraction combined with ICP-MS has been reported.[25] A poly(glycidyl methacrylate-ethylene dimethacrylate) monolithic capillary was functionalised with cystamine, and the resultant mercapto functionalised polymer monolithic capillary was then used to separate Sb^{III} and Sb^V. It was found that Sb^{III} was selectively retained on the capillary over a pH range 1 to 8, while Sb^V was not adsorbed in the pH range 3 to 8. Subsequently, Sb^V was pre-reduced to Sb^{III} and used to calculate total Sb; the Sb^V concentration was calculated by subtracting Sb^{III} from the total Sb. Under optimised conditions, the LOD for Sb^{III} was 3.9 ng L^{-1} with a RSD of 5.2 (0.1 μg L^{-1}, $n = 7$). The accuracy of the method was verified using two CRMs, Environmental Waters GSB07-1376-2001, and GBW(E) 080548. When using the method on river and lake water samples, sub-μg L^{-1} of Sb^{III} and Sb^V were found, and recoveries for spiked water samples for Sb^{III} and Sb^V were 87 to 113%. The method was also used to simultaneously determine Te^{IV} and Te^{VI}. A second report using dispersive μSPE for the speciation of Sb focused on cow milk.[26] In this study, fibrous TiO_2@g-C_3N_4 nanocomposites (FTGCNCs) were used. Samples were prepared with an artificial gastric juice for a bioaccessibility assessment as part of the study. The sample solution (20 mL) containing the Sb species was poured into a 30 mL centrifuge tube (pH 3.0) and then 10 mg of FTGCNCs were added to the tube. The mixture was sonicated for 4 min at room temperature. After complete extraction, the adsorbent was separated from the aqueous phase by centrifugation. The Sb^{III} retained on the adsorbent was eluted by adding 1.0 mL of 1.5 mol mL^{-1} HNO_3 solution and vortex mixing for 4 min. The elution solution was separated from the solid phase by centrifugation for ICP-MS detection of the Sb. The results showed that Sb^{III} was quantitatively adsorbed onto the FTGCNCs in the pH range 2.0 to 4.0, whilst Sb^V remained in the aqueous phase. The concentration of Sb^V was again based on subtracting Sb^{III} from total Sb. Total Sb was extracted and determined after the reduction of Sb^V into Sb^{III}. The main parameters affecting the separation and determination of the analytes were optimised, and under optimal conditions the LOD was 0.37 pg mL^{-1} for Sb^{III} with an RSD of 4.1% (1.0 ng mL^{-1}, $n = 9$). To validate the method, a CRM milk powder (GBW 10017, IGGE, China) was used and good agreement found with the certified values. A field-based speciation method for iSb in environmental water samples has been proposed using IE cartridges and ICP-MS.[27] The water samples were passed directly through an IE column cartridge on-site, and then taken back to the laboratory for separation and analysis. Two IE cartridge columns were evaluated to separate Sb^{III} and Sb^V. The first, a strong cation-exchange (SCX) column, on which all the Sb^{III} was retained whilst the Sb^V passed through, and a strong anion-exchange (SAX) column, on which both Sb^{III} and Sb^V were retained, but from which Sb^V can be eluted with 12% HNO_3. The two Sb species could be separated efficiently using the SCX and SAX columns in the pH range of 4 to 10 and 6 to 7, respectively. The LOD for Sb^V with the SCX column was 0.03 μg L^{-1} and 0.05 μg L^{-1} with the SAX column. The repeatability, expressed as the RSD, was 1.2 to 5.3% for the SCX column and 4.6 to 9.3% for the SAX column for two groundwater samples. The recoveries for Sb^V with spiked samples ranged from 91% to 103% for the SCX method and 85% to 120% for the SAX method. Potential coexisting ion interference was also evaluated and the SCX method exhibited a stronger matrix tolerance than the SAX method. Finally, ten natural water samples (two river water, five spring water, and three well water samples), collected from the Xikuangshan area (Hunan, China), were analysed using the proposed SCX method. The results show that the dominant species in all samples was Sb^V (64–12 000 μg L^{-1}), with Sb^{III} below the LOD (<1792 μg L^{-1}).

Although most published methods for determining Sb species utilise LC-ICP-MS, *a method utilising LC-ICP-OES* has been reported this year.[28] The separation was achieved on a Dionex AS15, 4 × 250 mm column used with a Dionex AG15, 4 × 50 mm guard column. The calibration curves showed good linearity at the three wavelengths tested (206.834 nm, 217.58 nm and 231.146 nm), although the LOQ varied depending on the wavelength used. The lowest LOQ for Sb^{III} (80.7 μg L^{-1}) and Sb^V (49.9 μg L^{-1}) was obtained at a wavelength of 217.582 nm. The method sensitivity for Sb^V was higher compared to Sb^{III} at all the wavelengths considered. Finally, samples containing different concentrations of Sb^{III} and Sb^V in three different matrices, *i.e.*, water, basal culture medium, and anaerobic sludge plus basal medium, were analysed. The CVs were low and ranged from 0.1 to 5.0 depending on the sample matrix. Recoveries of Sb^{III} and Sb^V were higher than 90% independent of the matrix analysed and the wavelength used.

Other *environmental applications of Sb speciation* have also been reported. The simultaneous separation of Sb^{III} and Sb^V in plants, soils, and sediments by HPLC-ICP-MS has been studied.[29] The chromatographic conditions using AEC (RP-X100, Hamilton, 4.1 mm 250 mm, 10 μm) including composition of the mobile phase and concentration of competing ion,

 This journal is © The Royal Society of Chemistry 2021

pH and flow rate of mobile phase, and the operating parameters for the ICP-MS were optimised by single factor experiments. The separation of the Sb species was achieved within 6 min using the optimised chromatographic conditions. The LOD values achieved by the method were 0.016 μg L^{-1} and 0.021 μg L^{-1} for Sb^{III} and Sb^{V}, respectively. The RSDs for replicate measurements ($n = 6$) of low (5 μg L^{-1}), medium (20 μg L^{-1}), and high (40 μg L^{-1}) concentrations of Sb^{III} and Sb^{V} were less than 4%. Spiking and recovery experiments on soil, sediments, and plants gave recoveries for the two species ranging between 92% and 103%. The spatial and temporal variability of five Sb and As species (Sb^{III}, Sb^{V}, $SbMe_3$, As^{III} and AsV) in water and sediments from a shallow, lowland dam in Kozlowa Gora Poland has been reported.[30] A total of fifteen elements plus the speciation of Sb and As, were determined in sediments using the BCR sequential chemical extraction method. Speciation was achieved using a Dionex IonPac AS7 column with ICP-MS detection and method validation was checked using four CRMs (NCS DC73309, NCS DC 73310, NCS DC 73312 from the NCS, China and NIST1643e). No methyl derivatives of Sb were found in the water or sediments of the reservoir, and the dominant Sb species was Sb^{V}, although often the Sb^{III} and Sb^{V} concentrations were similar as Sb^{III} could be released into the pelagic zone under appropriate conditions. Variability in the physicochemical conditions were also studied over a five-month period and changes in the speciation of Sb were found, with the levels of Sb^{III} increasing. The speciation of iSb and iAs in urban dust by fast sequential HG-AAS has been proposed.[31] Doehlert design and desirability function were used to find the optimum conditions for HG (1.0 mol L^{-1} HCl and 0.9% m/v $NaBH_4$). The accuracy of the method was evaluated using the CRM BCR 176R material fly ash, and a comparison with independent methods for Sb determination in urban dust samples also made. The LOQ values were 0.23 and 1.03 mg kg^{-1} for As and Sb, respectively, with an RSD of better than 4.7% ($n = 3$). The methodology was applied to eight samples of dust collected in urban areas of Salvador and Jaguaquara cities, Bahia, Brazil, with an aerodynamic size lower than 38 μm. Concentrations of iSb^{V} as high as 5.48 mg kg^{-1} were found, although the iSb^{III} was below the LOD in all samples. The high levels were attributed to intense industrial activities and vehicular traffic at the sampling locations.

One *industrial application of Sb speciation* has been reported this year, which was the determination of Sb species in Cu electrolyte samples, characterised by extreme acidity and high metallic content (Cu and Ni in the g L^{-1} range).[32] Separations were by HPLC-HG-AFS employing a PRP X100 strong anion-exchange column and a diammonium tartrate mobile phase. Linear calibration graphs ($r > 0.999$) were obtained for Sb in the range from 5 to 20 μg L^{-1}. The LOD values were 0.3 and 0.4 μg L^{-1} Sb^{III} and Sb^{V}, respectively. Antimony speciation of the Cu electrolyte samples showed that Sb^{III} was the predominant Sb species, with a concentration that ranged from 0.17 to 0.20 g L^{-1} depending on the sample. The concentration of Sb^{V} ranged from 0.10 to 0.13 g L^{-1}. The sum of the Sb species was 0.30 g L^{-1} for all the samples, which agreed with the total Sb content determined by ICP-OES (0.31 g L^{-1}). The stability of the Sb species in the samples prior to analysis was also studied over a period of 28 days with either aqueous dilution or acidification with HCl and different storage temperatures (4 °C, 25 °C and 65 °C). The dilution and the acidification with HCl caused partial oxidation of Sb^{III} to Sb^{V}.

3.2 Arsenic

A number of *reviews focusing on As speciation* have been published this year. A review of As speciation with an emphasis on chromatographic separations relating to the physicochemical properties of As species has been published by Reid *et al.*[33] The review, with 112 references, looks at the structure of common As species and a range of separation techniques (AEC, CEC, RP, ion pair and SEC). Recent work on HILIC, multiple separation mechanisms and the testing of fluorophenyl and graphene oxide stationary phases for the separation of As species were also covered. A useful table is included which gives details of specific types of column and their application. Sample preparation, extraction of As species, recovery of As species from separation columns, and method validation are also discussed. Recent developments in the speciation of As in environmental and biological samples have been reviewed by Yu *et al.*[34] The review (148 references) covered sample preparation, separation/pre-concentration processes and detection, with discussion on future development and prospects. Arsenic speciation analysis of environmental samples was the focus of a review by Ardini *et al.* covering the period 2004–2018.[35] The analytical methods developed to determine about fifty As compounds in environmental matrices, including soil, sediments, terrestrial and marine organisms, atmospheric particulate and various types of natural waters were covered. Various extraction/partitioning schemes were also discussed with reference to the As species (water- or lipid-soluble) and the matrix type (biotic or abiotic). The use of HPLC-ICP-MS was highlighted as the analytical technique of choice by most workers, although a significant number of studies also applied other couplings (LC to other atomic and MS techniques) or X-ray methods, and the review covers 240 publications. Environmental and biological applications of recently developed chromogenic and fluorogenic chemosensors for the detection of As species have also been reviewed, this time by Banik *et al.*[36] This review, with 126 references, focuses on strategies for design, sensing mechanisms, performance and potential bioimaging applications. The chemosensors were categorised into six types based on their sensing strategies: (i) chemosensors based on hydrogen bonding interactions; (ii) aggregation induced emission based chemosensors; (iii) chemodosimetric (reaction-based chemosensors); (iv) metal coordination-based sensing strategies; (v) chemosensors based on metal complex displacement and (vi) metal complexes used as chemosensors. A final, more specialised, review, published by Welna *et al.*, looked at the non-chromatographic speciation of As by HG techniques with a focus on sample types and matrices.[37] Literature published over the past 20 years was summarised and aspects of appropriate sample preparation before analysis and the selection of

adequate strategies for speciation purposes were emphasised. The review contained 86 references.

Two reviews focusing on *organoarsenicals in edible marine species* have been published by Luvonga *et al.*[38,39] The first, a comprehensive review with 308 references, covers the current analytical techniques for As speciation and considers oxidation states, interconversions occurring between chemical forms, matrix complexity, lack of standards and CRMs, and the lack of widely accepted measurement protocols. The requirement for high-quality As speciation data when establishing legislation and setting regulatory limits for As in food is also explored. The second review, with 255 references, provides an overview of the occurrence and assessment of human exposure to As toxicity associated with the consumption of seafood. There are sections on the metabolic transformations and toxicity of As, with subsections on methylated species, AB, AC, TMAO, tetramethyl arsonium ion, thioarsenicals, arsenosugars and arsenolipids. The last section covers considerations for risk assessment.

A number of *modifications and refinements to existing techniques for As speciation* have been reported. An attempt to improve existing HPLC related methods using UHPLC-ICP-MS in order to improve retention times, separation and resolution of As^{III}, As^{V}, DMAV and MMAV has been reported by Herath *et al.*[40] Two types of ammonium-based mobile phase ($NH_4H_2PO_4$ and NH_4NO_3) were evaluated at different eluent concentrations and pH to choose the most effective eluent system. The results demonstrated that a mixed mobile phase containing 8.5 mmol L^{-1} of $NH_4H_2PO_4$ and NH_4NO_3 (1 : 1) at pH 6.0 was the most effective eluent, achieving separation of the As species with improved resolution within 5 min. This compares well with many existing methods which take from 9 to 15 min. Unlike HPLC, UHPLC did not generate a higher column back pressure with increasing flow rates up to 2.5 mL min^{-1} resulting in faster separations and better peak resolution. The LOD values for As species were in the range from 0.3 to 0.5 μg L^{-1}. The proposed method was applied to successfully quantify As species present in the CRM ERM-BC211 rice, and several commercial varieties of rice from Australia and Sri Lanka. A study on the transformation kinetics of As^{III}, AB and AC has been carried out in aqueous solution using an ultrasonic treatment followed by the determination of the As species by HPLC-ICP-MS.[41] The separation was achieved on a Hamilton PRP-X100 AEC column. The results showed that the transformation of As species accorded with the 1st-order kinetic equation at different ultrasonic water bath temperatures (0–80 °C) and ultrasonic powers (150–750 W). At the ultrasonic power of 300 W, the reaction rate constants of As species at different ultrasonic water bath temperatures were: $k(20\ °C) > k(40\ °C) > k(0\ °C) > k(60\ °C) > k(80\ °C)$. At the ultrasonic water bath temperature of 60 °C, the reaction rate constants of As species at different ultrasonic powers were: $k(600\ W) > k(450\ W) > k(750\ W) > k(300\ W) > k(150\ W)$. The study provided a theoretical basis for the optimisation of UAE methods without altering the As speciation. The stability of As^{III}, As^{V}, DMA, and MMA during application of the BARGE UBM has been assessed by Tokalioglu *et al.*[42] The concentrations of As species in the UBM gastric and gastro-intestinal (gastric + intestinal) phases were determined using HPLC-ICP-MS whilst the total As content in the samples was determined using ICP-MS. These four As species were separated in 10 min using AEC (Hamilton PRP-X100) with a mobile phase containing 20 mmol L^{-1} $NH_4H_2PO_4$/1% methanol (pH 6.0). The recoveries of As species spiked into the gastric and gastro-intestinal fluids were in the range 90 to 108%. No interconversion between As species was observed as a result of applying the BARGE UBM, which is a particularly important finding for the reliability of As^{III} measurements. The accuracy of the BARGE UBM for *in vitro* extractable As^{V} was verified using British Geological Survey guidance material 102 (an ironstone soil). For a commercial rice sample, the bioaccessibility sequence of As was DMA > As^{III} > As^{V} for the gastric phase and As^{III} > DMA > As^{V} for the gastro-intestinal phase.

The development of *modified sorbents for extracting As species* have been reported. A hybrid adsorbent for As has been synthesised through intercalation of inorganic and organic surfactant cations onto kaolin clay interlayers.[43] The synthesised adsorbent was characterised using XRF, FTIR, SEM, and BET. Batch studies conducted to evaluate the As^{III} and As^{V} removal capacity showed that As^{III} was removed optimally at pH range of 4 to 6, whilst As^{V} was removal optimally at pH range 4 to 8. The data from adsorption kinetics fitted to a pseudo second order model, implied that the adsorption of As^{III} and As^{V} was chemisorption. Isotherm studies showed a better fit to the Langmuir isotherm model indicating that adsorption of both As^{III} and As^{V} occurred on a mono-layered surface. The maximum adsorption capacity for As^{III} and As^{V} at room temperature, as determined by the Langmuir model, were found to be 7.99 and 7.32 mg g^{-1}, respectively. The modified kaolin clay was successfully regenerated for up 7 adsorption–regeneration cycles using 0.01 mol L^{-1} HCl as the regenerant. The authors concluded that hybrid sorbent synthesised in the study was suitable for As removal from groundwater. Zinc oxide nanoparticles have been used in a photochemical reactor for As speciation by HG-AAS.[44] Optimisation studies showed that the analytical efficiency for the detection of As^{III}, As^{V}, and DMA was highly dependent on the physicochemical parameters (type of acid, acid concentration, semiconductor mass, and pH) and so these were carefully optimised. In use, As^{V} and DMA were photoconverted to As^{III} for arsine generation. A LOQ of 10.6 μg L^{-1} for As^{III}, 12.7 μg L^{-1} for As^{V}, and 22.0 μg L^{-1} for DMA was achieved. The optimised system was applied to the determination of As in environmental samples following the rupture of the containment system for mining waste in the state of Minas Gerais in Brazil. Concentrations of up to 103 ± 9.4 μg L^{-1} As^{V} were determined in surface water samples, and 84.1 ± 3.6 μg L^{-1} As^{III} and 112 ± 9.9 μg L^{-1} As^{V} in soil samples. A dual column packed with a magnetic metal–organic framework composite (MFC) and mercapto-functionalised MFC nanoparticles (MFC-SH) in microfluidic chip channels, has been described for array chip-based magnetic SPME of As species, As^{III}, As^{V}, MMA were determined together with total As in squamous carcinoma cells.[45] At pH 6, the MFC-SH adsorbed As^{III} while MFC quantitatively adsorbed As^{V}, DMA and MMA. The As^{III} adsorbed on the MFC-SH could be desorbed with a 2% solution of thiourea in 0.5 mol L^{-1} HNO_3. The As^{V}, DMA and

 This journal is © The Royal Society of Chemistry 2021

MMA were retained on the MFC but could be desorbed by ammonia. A sequential elution strategy was then employed to elute MMA, DMA, As^V and As^{III} in turn for subsequent on-line determination by ICP-MS. The LOD values were 4.8, 6.3, 3.8 and 7.1 ng L^{-1} for As^V, DMA, MMA and As^{III}, respectively. The enrichment factors were between 23 and 25, and the throughput was 7 samples per hour. The As species in (spiked) squamous carcinoma-7 cell samples were analysed by the online system with recoveries of 89 to 110%.

A novel *ionic imprinted polymer for As speciation* has been used in three applications by Jinadasa *et al.* The ionic imprinted polymer consisted of a template/bifunctional monomer/cross-linker with molar ratio fixed at 1 : 4 : 20 (1.6 mmol of $NaAsO_2$ (template), 6.5 mmol of 1-vinyl imidazole (bi-functional monomer), 32 mmol of DVB (cross-linker), and 20 mL 1 : 3 acetic acid/methanol porogen). In the first publication by the group, the synthesis of the surface ionic imprinting polymer on silica-coated Mn-doped ZnS quantum dots was described, and applied as a chemosensor for the selective quantification of iAs in fish.[46] Following optimisation and validation with the CRM BCR-668 (mussel tissue), the composite material was found to offer high selectivity (high imprinting factor) for iAs species with a LOQ of 29.6 μg kg^{-1}. Other ions, including organo As compounds, did not interact with the composite material. In the second paper, low levels of As^{III} and As^V were selectively isolated from fish extracts (1.0 g of wet fish samples pre-treated with 10 mL of 1 : 1 methanol/water under sonication at 25 °C for 30 min) using the ionic imprinted polymer incorporated into a SPE procedure (on-column mode).[47] Optimised pre-concentration conditions of the fish extract (10 mL), pH adjustment to 8.5, and elution with 2 mL of ultrapure water at 0.50 mL min^{-1} were used, and this facilitated a pre-concentration factor of 50 after evaporation to dryness (N_2 stream) and re-dissolution in 0.2 mL of ultrapure water. Separation of the As species and their determination was then by HPLC-ICP-MS. The method gave LOQ values of 1.05 and 1.31 μg kg^{-1} for As^{III} and As^V, respectively, with RSDs better than 12% in fish extracts spiked at different levels of As^{III} and As^V. The final publication combined UAE and VAME and the ionic imprinted polymer as a selective sorbent for the isolation and pre-concentration of As^{III} and As^V in extracts from rice samples prior to their determination, again by HPLC-ICP-MS.[48] The analytical performance of the procedure was studied at optimised conditions: ultrasound sonication at 40% amplitude for 2.0 min using 1 : 1 methanol/ultrapure as an extractant, 50 mg of sorbent, extract at pH 8.0, vortex loading at 1000 rpm for 1.0 min, and elution with ultrapure water by vortexing at 1000 rpm for 1.0 min. The final preconcentration factor was 10. The LOD values obtained for As^{III} and As^V were 0.20 and 0.41 μg kg^{-1}, respectively, well below the maximum levels set by the EU for rice and rice containing products. The accuracy of the method was confirmed by analysing the rice CRM ERM-BC211 with good agreement with the certified values.

There has been an increase in *simultaneous multielement speciation methods involving As* this year, and several examples may be found in this review under the appropriate element heading. One of the more comprehensive is the simultaneous determination of As^{III}, As^V, DMA, MMA, Hg^{II}, MeHg, EtHg and PhHg, Pb^{II}, TML and TEL, which were separated and analysed within 8 minutes.[49] The resolution using a 15 cm Diamonsil C_{18} column (4.6 mm i.d. × 5 μm) was reasonable, although the composition of the mobile phase proved critical for separation of the species. Various mobile phase compositions were evaluated and 2 mmol L^{-1} TBAH + 20 mmol L^{-1} Cys + 1 mmol L^{-1} Na 1-pentanesulfonate at pH 5.0 offered promising results. The method offered LOD values from 0.036 to 0.20 μg L^{-1} for As-species, from 0.023 to 0.041 μg L^{-1} for Hg-species, and from 0.0076 to 0.14 μg L^{-1} for Pb-species. The method was applied to speciation measurements of the above species in five lotus seed samples, indicating the presence of DMA (19.6 to 28.2 μg kg^{-1}), TML (1.4 to 2.9 μg kg^{-1}), MeHg (1.2 to 4.8 μg kg^{-1}) and EtHg (0.8 to 2.2 μg kg^{-1}).

To *preconcentrate gas phase iAs species in situ* a dielectric barrier discharge trap (DBDT) has been utilised in the construction of a LC-HG-DBDT-AFS system.[50] The trap was fabricated using a three-cylinder concentric quartz tube DBDT in place of the original AFS atomiser. After LC separation, only As^V was trapped by a 11 kV discharge operating with 110 mL min^{-1} air mixed with Ar. This was followed by sweeping with Ar gas for 190 s since excessive moisture generated from the HG proved detrimental to sustaining the DBD plasma. The iAs was then released at 13 kV, and 180 mL min^{-1} H_2-rich Ar used to transport the analyte to the AFS for measurement. To test the performance for As speciation, a series of 5 mg L^{-1} standards (As^{III}, As^V, DMA, and MMA) were measured. The LOD for As^V was 0.05 mg L^{-1}, which compared well with the LOD without the DBD in place of 0.6 mg L^{-1}. The measured iAs in CRMs were within their certified values, and the spike recoveries were in the range 93 to 102%. Other As species could also be pre-concentrated and detected by the proposed method by precisely synchronising the DBD trap and release with chromatographic retention times.

Solid-phase As speciation using XANES has been reported for the preservation of species in environmental risk assessment.[51] Characterisation of As species was by SR-XAS in 14 different matrix CRMs and candidate materials, from the Korea Research Institute of Standards and Science (KRISS). Materials included sediments, ash, ore tailings, seafood, commodity plastics, and cosmetic products. The validity of the method was successfully evaluated by comparison with the results obtained using IC-ICP-MS. The use of XANES revealed details of both the composition and distribution of As species in the intact solid samples. This approach would seem to offer potential for development as a complementary technique to existing methods where non-destructive microscopic analysis is required.

The speciation of As in a range of foodstuffs has been investigated this year, with rice, mushrooms and seafood remaining the most popular matrices. Arsenic speciation in sea cucumbers has been reported by Gajdosechova *et al.*[52] Three species of sea cucumbers, *Cucumaria frondosa, Apostichopus californicus* and *Apostichopus japonicus* were collected from three geographical regions, the Atlantic and Pacific coasts of Canada and the Yellow/East China sea in China. The organisms were sectioned into parts (body wall, tentacles, internal organ, skin and

muscle) and then analysed for total As by ICP-MS and As species by HPLC-ICP-MS. Normal and reversed phase separations were optimised to address As distribution between lipids (polar and nonpolar) and water-extractable fractions. The results revealed that the total As concentration and As species distribution varied significantly between the sea cucumbers species. Total As in the body parts ranged between 2.8 ± 0.52 and 7.9 ± 1.2 mg kg^{-1}, with the exception of the muscle tissue of *A. californicus*, where it reached 36 ± 3.5 mg kg^{-1}. The most abundant As species in *A. californicus* and *A. japonicus* was AB. However, iAs represented over 70% of total recovered As in the body parts of *C. frondosa*. Arsenosugars 328 and 482 were found in all of the studied body parts whereas arsenosugar-408 was only found in the skin of *A. californicus*. This is the first time that such a variation in As species distribution between sea cucumber species has been reported. The accumulation and transformation of As species in the hydroponic cultivation of strawberry plants has been studied.[53] Cultivation experiments were performed by adding iAs at concentrations of 10, 100 and 1000 μg L^{-1} *via* root irrigation. The total As content was determined by HG-AFS. The accumulation was found to be dependent on the concentration of As added and the As species used and As^{III} accumulated at higher rates than As^{V}. A greater accumulation of As was found in roots, from 0.44 to 4.10 mg kg^{-1}, than in stems, from 0.43 to 1.27 mg kg^{-1} and fruits from 0.22 to 0.30 mg kg^{-1}. Speciation results from HPLC-HG-AFS analysis indicated that the addition of As^{III} resulted in a partial methylation producing MMA and DMA. After As^{V} addition, only MMA was observed, accompanied by a notable reduction in the ratio of As^{V} to As^{III}. Arsenic speciation in the endangered catfish *Genidens barbus* has been reported.[54] The catfish is consumed in parts of S. America. The iAS, MMA, DMA, and AB were determined by HPLC-ICP-MS after extraction (microwave extraction with 10 mL of 2% v/v HNO_3 and 5 mL of 1% v/v H_2O_2) from muscle, liver and gill of catfish samples collected from Argentina ($n = 12$) and from Brazil ($n = 11$). Concentrations (mg kg^{-1}) of non-toxic As species were 10.4 ± 2.89 and 14.9 ± 5.94 for muscle, 1.48 ± 0.58 and 2.21 ± 1.24 for liver, and 0.66 ± 0.39 and 2.44 ± 1.93 for gill, for Argentinian samples and Brazilian samples, respectively. This represented 95.5% to 99.5% of the total As for each tissue and included three unknown organo As species. The iAs levels (mg kg^{-1}) were 0.048 and 0.013 for muscle, 0.24 and 0.011 for liver, and 0.037 and 0.012 for gill, representing from 0.45 to 4.93% of the total As for the Argentinian samples and from 0.24 to 0.60% for the Brazilian samples. The authors calculated a potential health risk from chronic consumption. The simultaneous speciation analysis of As^{V}, As^{III}, AB, DMA, MMA and MeHg in edible oil by HPLC-ICP-MS has been reported.[55] A RP C_{18} ODS column was used for the separation with a single mobile phase containing ion-pair reagent and L-cysteine. The LOD values for iAs and MeHg were 0.05 ng g^{-1} as As and 0.09 ng g^{-1} as Hg, respectively. The simultaneous extraction from the edible oil was achieved using 2% w/w TMAH solution. The proposed method was also applied to the several CRMs (NMIJ CRM 7402-a cod fish tissue, NMIJ CRM 7503-b white rice flour, NMIJ CRM 7533-a brown rice flour, and NMIJ CRM 7405-a hijiki seaweed). Finally, five types of edible oil were analysed (fish liver oil, krill oil, whale oil, whale fat and sardine oil). The iAs and MeHg were in the concentration range from 0.001 mg kg^{-1} to 0.010 mg kg^{-1} and from 1.21 ng g^{-1} to 10.18 ng g^{-1}, respectively. All of the iAs was found as As^{V}, DMA was found in all of the samples, and MMA and AB at low levels in three of the samples.

Continuing on the topic of *As speciation in foodstuffs* a study of As speciation and the associated health risk from consumption of the Chinese mitten crab (*Eriocheir sinensis*) has been reported.[56] A total of 2130 crabs were collected from seven locations in China and the sample extracts analysed by HPLC-ICP-MS for As^{V}, As^{III}, AB, AC, DMA and MMA. The target hazard quotient was utilised to evaluate the human health risk. The total As concentration and totals for the six As species were from 0.25 to 1.66 mg kg^{-1} and from 0.05 to 1.19 mg kg^{-1} wet mass, respectively. Arsenobetaine was found to be the most predominant As species in the crabs, comprising from 50.0 to 90.0% of the sum of six As species measured. The iAs ranged from 0.01 to 0.21 mg kg^{-1} wet mass. The target hazard quotient values of iAs through the consumption of the Chinese mitten crabs were all less than 1, indicating no appreciable hazard risk to human health. Both cooking and/or the digestion process have been shown to alter the forms of As present in food. Solid state speciation with XANES has been used to investigate As species in rice, asparagus, and garlic boiled in water containing As^{V}, and in their bio-accessible fractions (solubilised As after gastrointestinal digestion).[57] The raw samples of these three foods contained low concentrations of total As (rice: 0.11 mg kg^{-1} w/w; asparagus: 0.28 mg kg^{-1} w/w; garlic: 0.08 mg kg^{-1} w/w) as determined by FI-HG-AAS following dry ashing. However, since the detection of As by means of XAS requires concentrations of higher than 10 mg kg^{-1} dry mass in the matrix analysed, the samples were heavily spiked. L-cystine and glycerol were also added to reflect work in previous studies on the reduction of As^{V}. The analysis revealed the presence of As^{III} in the cooked foods and in their bioaccessible fractions. The percentage of As^{III} species (12 to 55%) followed the order asparagus $\gg$ rice $\sim=$ garlic. In the asparagus and garlic samples, part of the As^{V} (tetrahedral form) that had been added appeared in the form of an octahedral As^{V} compound (As^{V} – glycerol). Such changes could considerably modify the risk associated with ingestion of As-contaminated food. In addition to the changes shown in the food matrices, the authors noted that in the presence of L-cystine, a standard solution of As^{V} was transformed into As^{III}–Cys. This may also have important implications with respect to diets where water is the main source of As exposure. Total As, As^{III} and As^{V} have been determined in flavoured and bottled drinking waters using HPLC-ICP-MS and ES-MS-MS and the method detailed in ISO 17294-2:2016 to investigate contamination from the packaging and Cr^{VI}, Sb^{III}, and Sb^{V} were also included in the study.[58] The concentrations of total As in the waters studied were in the range from 0.0922 ± 0.0067 to 8.37 ± 0.52 μg L^{-1}. Of the two iAs species, As^{V} was found to be dominant in flavoured waters, although in unflavoured waters higher concentrations of As^{III} were observed in the majority of the tested samples. The As^{III} concentrations ranged from 0.580 ± 0.055 μg L^{-1} to 0.133 ±

0.012 μg L^{-1}, with means of 0.292 μg L^{-1} and 0.349 μg L^{-1} for flavoured and unflavoured water, respectively. The As^V ranged from 3.26 ± 0.30 μg L^{-1} to 0.0600 ± 0.0055 μg L^{-1} with means of 0.904 μg L^{-1} and 0.218 μg L^{-1} in flavoured and unflavoured water. In some of the samples AB was detected whilst MMA or DMA was not detected. An unknown As species was also detected in about half of the samples.

Following the trend in recent years, the *speciation of As in rice and rice based products* remains a popular area of research. The transport of As from soil through to the edible crop has been reported for the rice plant, *Oryza sativa*, by Foulkes *et al.*[59] Samples of soil, irrigation water and plant, were collected from an agricultural site in the Middle East. Total As, As speciation and DNA fractionation were evaluated using HPLC-ICP-MS in samples which included the root, stem, leaf and grain of the rice plant. The methodology was validated using CRMs (EU ERM-CC141 loam soil and GBW10015 spinach). The highest concentration of As was found in the root of the plant and the lowest in the grain. The total As concentrations reported were: soil (aqua-regia extractable) 2.88 μg g^{-1}, irrigation water 0.58 μg L^{-1}, roots 8.28 μg g^{-1}, stem 4.00 μg g^{-1}, leaves 2.93 μg g^{-1} and grain 1.02 μg g^{-1}. Levels of iAs^V and As^{III} were quantified in the soil and plant material, whilst the DMA, MMA were below the LOD values. The 'plant available' levels of As in the soil (14%) were determined as part of a full, validated three-step BCR sequential extraction procedure. Since As can behave as a phosphate analogue, a method was developed for the extraction of vegetative DNA to determine the different forms of As associated with, or integrated within, the DNA fractions. Measurement of As in the DNA extracts were above the LOD (0.019 μg kg^{-1}) for the root, stem, and leaf samples. The concentration of both weakly and strongly associated As with DNA obtained from the root, stem and leaf decreased with decreasing total As concentrations. A narrow, near-constant ratio for the strongly associated As value (As/total As DNA) in all root, stem and leaf DNA samples (41.3 ± 0.3%) was proposed by the authors as further evidence for the incorporation of As into the DNA. An *in vitro* digestion method with dialysis has been used to estimate the relation between As ingested and the As absorbed from rice.[60] The estimation of As species bioavailability was made with an *in vitro* digestion procedure with dialysis membranes. Dried and pulverised rice samples (0.5 g) were weighed into Erlenmeyer flasks and 20 mL of ultra-pure water was added. After 10 min, the pH was adjusted to 2.0 with 0.1 mol L^{-1} HCl solution. Then, 0.15 g of gastric solution (pepsin 16.0% m/v prepared in 0.1 mol L^{-1} HCl) was added, and the simulated gastric digestion was carried out under orbital-horizontal shaking (37 °C, 150 rpm) for 120 min. In order to stop the enzymatic activity, the flasks were introduced into an ice bath at the end of the gastric digestion. The intestinal stage began with the addition of 5 mL of intestinal solution (4.0% m/v pancreatin and 2.5% m/v bile salts solution prepared in 0.1 mol L^{-1} sodium hydrogencarbonate). Dialysis membranes filled with 20 mL of 0.15 mol L^{-1} PIPES solution (pH 7.5) were then placed inside the flasks. The simulated intestinal digestion was also performed under orbital-horizontal shaking (37 °C, 150 rpm) for 120 min followed by the use of an ice bath again. The As species were determined in both the rice samples and in the dialysate fraction by HPLC-ICP-MS. The LOD and LOQ obtained for the As determination in the dialysates were 0.007 and 0.020 μg per As per L respectively (2.8 and 8.0 μg kg^{-1} dried rice). The iAs concentrations found in the samples ($n = 16$) varied from 82 to 165 μg kg^{-1} (dried rice), although the low bioavailability of As species (As^V 10 to 31%, As^{III} 7 to 12%, DMA 11 to 14%) found in the study using the proposed *in vitro* digestion method and simulated gastrointestinal conditions indicated a low risk from rice consumption. The study was prompted by EU regulations which have established a maximum level of iAs of 100 μg kg^{-1} in rice destined for the production of food for infants and young children. A bioavailability study of As species in rice was also performed in order to evaluate changes in As speciation occurring during the gastrointestinal digestion process. The results showed mainly decreases in As^{III} and increases in As^V. A hydroponic study has been carried out to examine the influence of iAs and DMA on the concentration and distribution of C, Cu, Fe, Mn, N, Ni, S, and Zn in rice caryopsis at maturity using laser confocal microscopy and SR-XRF.[61] The results showed that treatments with iAs and DMA did not change the distribution characteristics of the above elements in rice grains. It was also found that Fe, Mn, and iAs were mainly limited to the ventral ovular vascular trace, while Cu, Zn, and DMA extended into the endosperm. This implied that milling processes were likely to remove the majority of the Fe, Mn, and iAs, but not Cu, Zn, and DMA. In addition, the analysis revealed a significant 12.7% increase for N and 8% reduction for S in DMA-treated rice caryopsis and a significant decrease of 24.0% for S in iAs-exposed rice caryopsis. These findings suggested that Cu, Zn, and S are more easily impacted by iAs, while N is mostly affected by DMA. In another study of the total iAs concentrations and dietary exposure to rice-based infant food in Australia, the total As concentrations were determined by nitric acid digestion and ICP-MS while iAs was determined by acid extraction, followed by HG-ICP-MS.[62] Nearly 75% of samples had iAs exceeding the EU maximum levels for infants and children (0.1 mg kg^{-1}) and the mean iAs percentage of total reached as high as 84.8%. In a study of As in rice from Brazil, total iAs was determined by ICP-MS (34.4 to 86.5 ng g^{-1}), and then HPLC-HG-ICP-MS used to determine As^{III}, As^V, MMA and DMA with LOD values of 0.004 μg L^{-1} for DMA, 0.003 μg L^{-1} for MMA and As^{III} and 0.010 μg L^{-1} for As^V.[63] The mass balance, total of the As species compared with the total As content, for ten analysed samples were satisfactory in most cases, ranging from 90.1 to 127% with a mean of 107%, although recoveries were high for two of the samples (127% for Red Rice variety and 122% for "Marabá" variety). The mean percentages of As species in the ten rice varieties were 65% As^{III}, 16% As^V, 24% DMA and 12% MMA. The mean estimated daily intake through rice consumption were calculated to be 3.88 μg for total As, 2.88 μg for iAs and 0.92 μg for DMA. Finally, a study to evaluate iAs concentrations in 55 different types of rice sold in the UK and to quantify the health risks to the UK population has been reported.[64] The authors first analysed all of the rice samples for total As concentration from which 42 rice samples with total As > 0.1 mg kg^{-1} were selected for As speciation using HPLC-ICP-MS. Statistically significant

differences were found between organically and non-organically grown rice. Brown rice contained a significantly higher concentration of iAs compared to white or wild rice. Notably, 28 rice samples exceeded the 0.1 mg kg^{-1} iAs limit stipulated by the EU, with an average iAs concentration of 0.13 mg kg^{-1}. Based on the average concentration of iAs in the samples, the authors calculated values for the Lifetime Cancer Risk, Target Hazard Quotient and Margin of Exposure which indicated that infants up to 1 year must be restricted to a maximum of 20 g per day for the 28 rice types with higher As levels to avoid carcinogenic risks. The determination of As in rice milk has attracted attention this year, perhaps reflecting the increase in consumption, mainly by individuals intolerant to lactose or allergic to cow milk.[65] In this study, As^{III}, As^{V}, DMA and MMA species in rice milk were determined using LC-ICP-MS. The LOQs ranged from 0.25 to 0.43 μg L^{-1} As, with recoveries of 81 to 116% for samples spiked to 1.00 μg L^{-1} or 5.00 μg L^{-1} As. The RSD was better than 5%. A limited number of samples were analysed (two rice milks, one wholegrain rice milk and one rice milk with coconut). All four species were detected in the analysed samples. The mean concentration of iAs ($As^{III} + As^{V}$) found in the study ranged from 10.2 to 19.5 μg L^{-1}, although the pattern of distribution of As^{III}, As^{V} and DMA varied significantly between the samples and MMA was only detected in two of the samples, both at low levels.

The *speciation of As in mushrooms* has proved a popular topic of research in recent years. A review of As speciation in mushrooms has been presented by Zhang *et al.*[66] A systematic literature search was carried out on studies reporting As speciation in mushrooms from China, using sources published in both English and Chinese. Associated environmental and health risks were also discussed. Several other groups from China have reported on As speciation in fungi. In one such paper, workers have developed a HPLC-ICP-MS-MS method for As speciation in eight varieties (266 samples) of edible mushrooms.[67] Six As species (As^{III}, As^{V}, AB, AC, DMA, and MMA) were extracted ultrasonically from the mushrooms using ultrapure water at 60 °C as the solvent, and then separated on a PRP-X100 AEC column (4.1 × 250 mm, 10 μm), with 20 mmol L^{-1} NH_4HCO_3 and 50 mmol L^{-1} $(NH_4)_2CO_3$ as the mobile phase, before being quantified using ICP-MS-MS in oxygen reaction mode. The LDRs of the method were from 0.5 to 100 μg L^{-1} with LOD and LOQ values of from 2.5 to 10 μg kg^{-1} (S/N = 3), and from 8 to 33 μg kg^{-1} (S/N = 10), respectively. The results indicated that most wild edible mushrooms contained organic As, mainly AB and AC, although the iAs content of *Armillariella tabescens* (3.63 mg kg^{-1}) and parts of the cultivated *Agaricus blazei murrill* (up to 4.50 mg kg^{-1}) were relatively high, presenting a potential health risk for consumers. The speciation of As in the so called caterpillar fungus, *C. sinensis*, and the potential health risks if digested (the fungus is used in traditional Chinese medicines) have been investigated.[68] The analyses were by SEC-HPLC-ICP-MS and a number of unknown As species were identified. The As in *C. sinensis* was mainly found in alkali-soluble proteins. The authors postulate that the unknown As species in *C. sinensis* may be converted into iAs, which may lead to enhanced toxicity. The Violet Crown Cup mushroom, *Sarcosphaera coronaria*, has an interesting history in that it was originally considered edible, but was then associated with several poisonings in the early 20th century. The reason for this seemingly sporadic toxicity is still unknown, although *S. coronaria* is known to accumulate As. Braeuer *et al.*[69] have investigated the As speciation in *S. coronaria* using HPLC-ICP-MS and found it to contain up to 0.9% As (dry mass). Most of the As was present as methylarsonic acid (As^{V}), although low concentrations of the more toxic methylarsonous acid (As^{III}) were also detected. The amounts found were too low to pose an acute risk for consumers, but the concentration of As^{III} significantly increased during simulated gastric digestion. The authors could not unambiguously identify As as the toxic constituent of *S. coronaria*, but demonstrated that As^{III} can be formed under certain circumstances.

The *As species and As transformation pathways in marine plants* have been studied by Lorenc *et al.*[70] Five types of seaweed sample were selected including two CRM materials. The seaweed CRM 7405-a was used for method validation and verification of total As, extractable total As and As speciation by HPLC-ICP-MS. The kelp powder (*Thallus laminariae*) NIST SRM 3232 was used for the identification of As-sugars by an ultra-performance LC-ES-MS-MS method. The total As content in the edible algae samples was found to range from 19.3 ± 0.45 mg kg^{-1} up to 72.6 ± 2.7 mg kg^{-1}. The As speciation identified As^{III} ranging from <LOD (0.61 mg kg^{-1}) to 8.97 ± 0.59 mg kg^{-1}, As^{V} from <LOD (0.55 mg kg^{-1}) to 5.95 ± 0.29 mg kg^{-1} and DMA from <LOD (0.57 mg kg^{-1}) to 0.766 ± 0.040 mg kg^{-1}. Mass balance calculations carried out on the basis of total As and As speciation results showed that the amount of unidentified As species in the algae samples varied from 28% to 100% of extracted total As. These unidentified As species in the algae samples were shown to consist of a high variety of As–sugars (12 compounds) and the presence of simple inorganic and organic As species such as As^{V} and DMA along with 8 more simple organic As compounds.

Studies on *As speciation in terrestrial plants*, other than food crops, have looked at ferns, lichen and algae this year. The fern *Pteris vittata* has been widely studied due to its As hyper-accumulation characteristics and two further studies on this plant have been reported this year. Arsenic redox transformations and cycling in the rhizosphere of the plant have been reported.[71] Using a combined approach of 2D sub-mm scale solute imaging of As^{III}, As^{V}, Fe, Mn, O_2 and P the authors found localised patterns of As^{III}/As^{V}, redox transformations in the rhizosphere (As^{III}/As^{V} ratio of 0.57) compared to bulk soil (As^{III}/As^{V} ratio of ≤0.04). The data indicated that high As root uptake, translocation and accumulation from the As-rich experimental soil (2080 mg kg^{-1}) to the fronds (6986 mg kg^{-1}) induced As detoxification *via* As^{V} reduction and As^{III} root efflux, leading to As^{III} accumulation and re-oxidation to As^{V} in the rhizosphere porewater. This As cycling mechanism was linked to a reduction of O_2 and $Mn^{III/IV}$ (oxyhydr)oxides which resulted in decreased O_2 levels and increased Mn solubilisation along the roots. The study also looked at *Pteris quadriaurita* which had a 4-fold lower As translocation to the fronds (1611 mg kg^{-1}), 2-fold lower As^{V} depletion in the rhizosphere, and no As^{III} efflux from the roots, suggesting that this plant

 This journal is © The Royal Society of Chemistry 2021

effectively controls As uptake to avoid toxic As levels in roots. The study demonstrated that two closely-related As-accumulating ferns had distinct mechanisms for As uptake, modulating As cycling in As-rich environments. In the second study looking at *Pteris vittate*, van der Ent *et al.*[72] combined planar and confocal μXRF imaging and fluorescence computed μ-tomography to study the localisation of As in the endodermis and pericycle surrounding the vascular bundles in the rachis and the pinnules of the fern. Arsenic was also accumulated in the vascular bundles connecting into each sporangium, and in some mature sori. The use of 2D XANES imaging provided information on the As speciation across the tissues, revealing As^V in the vascular bundles and As^{III} in the endodermis and pericycle. The distribution patterns of As species in the lichen biomonitor *Parmotrema austrosinense* have been reported.[73] Chromatographic separations of As in lichen using HPLC-ICP-MS and the use of sequential extractions have historically been shown to have low analyte recoveries and poor analyte selectivity respectively. In this study a four-step sequential extraction of the lichen material, involving ultrasonic extraction and chromatographic separation of As followed by a traditional sequential extraction procedure improved the selectivity and recoveries of As species. A mass balance was calculated for each sample using the sum of As concentrations from the extraction steps compared to the total As concentration. The stability of the four As species (As^V, As^{III}, AB and DMA) in the lichen matrix was also evaluated over 1 month in the water-extractable fraction. This evaluation excluded MMA since it was below the LOD in each extraction. The results showed variations in the concentrations of the As species with an increase in As^V. This is somewhat counter intuitive given previous studies, but the authors propose that for lichens the presence of oxalic acid could reduce and make readily available As which was previously bound to carbonates and oxides thereby explaining the increase in As^V in the water-soluble fraction. The developed method was applied to lichen collected from two sites in South Africa which had different potential sources of As (urban and rural sources). In the modified extraction step, AB, DMA and an unknown As species were statistically ($p < 0.05$) higher in the urban site than the rural site. Analyte recoveries using the combined method were higher than other studies reported in literature, with percentage recoveries of 104% and 111% of As in the urban and rural sites respectively. The As concentrations were found in the following order of abundance at both sites: oxidisable > reducible > water-extractable > residual. Concentrations of total As in the oxidisable and non-bioavailable fraction were statistically lower ($p < 0.05$) in the rural site than in the urban site. Arsenosugars have been extracted from algae to prepare standards for identification and quantification purposes.[74] Several commercial algae samples were characterised (total As and speciation) to select the most appropriate for use in relation to their arsenosugar contents. Water extracts from the selected sample (*Fucus vesiculosus*) were fractionated using a Hamilton PRP-X100 preparative column, and the presence of As species in the isolated fractions ascertained by IC-ICP-MS. Two of the fractions presented As species corresponding to sulfate and sulfonate arsenosugars at suitable concentrations. To unequivocally confirm the presence of both compounds, ES-TOF-MS was used, and the exact mass determined with errors lower than 0.5 ppm. The standard solutions obtained were successfully used to identify and quantify SO_4-sug and SO_3-sug in several edible algae samples purchased from a local market. Total As content for analysed samples ranged from 34 to 57 mg kg^{-1}, concentration values found for SO_3-sug ranged from 5 to 36 mg As kg^{-1} and SO_4-sug was only found in fucus with a concentration of 9.3 mg As kg^{-1}.

A diverse range of *environmental studies involving As speciation* have been reported. The removal mechanisms for As^{III} and As^V by Fe-modified biochars, have been studied using SR-XAS and confocal μXRF imaging.[75] Biochars are materials recently shown to have potential for the removal of As from aqueous environments due to their porous structure and various functional groups. Batch experiments followed by solid-phase analyses at different pyrolysis temperatures (300, 600, and 900 °C) were used and revealed that the As removal by Fe-modified biochars was best described by pseudo-second order kinetic and Langmuir isotherm models. The As removal increased from 73.8 to 99.9% for As^{III} and from 86.8 to 99.9% for As^V as the pyrolysis temperature increased. For As^{III}-spiked systems, XANES data indicated 20.2 to 81.5% of As^{III} was oxidised to As^V as the pyrolysis temperature increased; an increase of oxidation efficiency was observed after adding calcite. For As^V-spiked systems, no As^V reduction was observed. Overall, As^{III} and As^V removal using Fe-modified biochars was affected by the spatial distribution and As speciation. In the marine environment the toxicity of As^V and As^{III} in marine zooplankton, the rotifer *Brachionus plicatilis* and the copepod *Paracyclopina nana*, has been investigated.[76] The As metabolites were determined by HPLC-ICP-MS and *in vivo* toxicity and antioxidant responses recorded. While As^{III} was more toxic than As^V in both organisms, the rotifer *B. plicatilis* exhibited stronger tolerance, compared to the copepod *P. nana*. The As speciation analysis revealed differences in biotransformation processes in the two species, with *B. plicatilis* having a less complicated process than *P. nana*, contributing to a better As tolerance. Moreover, the levels of GSH content and the regulation of omega class glutathione S-transferases were different in response to oxidative stress. The spatial variability of As speciation in the Gironde Estuary in the South West of France has been studied.[77] The focus of the study was the dynamics (potential bioavailability) of As^{III} and As^V fractions, quantified in the estuary using an antifouling gel-integrated gold microelectrode interrogated by square wave ASV(GIME-SWASV). The concentrations of dissolved As^{III} and As^V were determined by HG-FI-AAS and ICP-MS in collected samples following filtration, through 0.2 μm as well as 0.02 μm pore size filters. The concentrations of As^{III} in the dynamic fraction, As^{III} (dyn), ranged from 1.3 to 3.3 nmol L^{-1}, accounting for nearly all of the dissolved As^{III}. The As^{III} (diss) ranged between 0.9 and 3.1 nmol L^{-1} in the 0.2 μm fraction, and between 1.2 and 3.7 nmol L^{-1} in the 0.02 μm fraction. Concentrations of As^V in the dynamic fraction, As^V (dyn), ranged from 0.9 to 22.9 nmol L^{-1}, and contributed from 4 to 73% of the 0.2 μm fraction and from 5 to 90% of the 0.02 μm fraction for As^V. The concentrations of As^V (dyn), in the 0.2 μm

fraction were between 14.5 and 36.2 nmol L^{-1}, and between 15.2 and 34.9 nmol L^{-1} in the 0.02 μm fraction. The determination of As species in different fractions, together with the results from dissolved Mn and Fe, particulate suspended matter, and measurement of physicochemical parameters (temp, pH, O_2, redox E), helped to broaden the understanding of biotic and abiotic processes governing the distribution of As, especially its potentially bioavailable forms, in the estuary. The export of e-waste from industrialised to developing countries has led to the formation of a large-scale informal e-waste recycling sector in Agbogbloshie, Accra, Ghana. During the recycling process, workers are exposed to several hazardous substances, including iAs and a study to assess exposure to iAs in e-waste workers has been presented by Yang *et al.*[78] A group of 84 e-waste workers and 94 control subjects were included in the study which determined iAS in urine samples using HPLC-ICP-MS. The E-waste workers showed higher median concentrations of As^{III}, As^{V}, DMA, MMA, and the sum of iAs in comparison to the control group. More than 80% of the e-waste workers exceeded the acceptable concentration (14 μg L^{-1}), which was significantly higher in comparison to the control group (70%). The tolerable concentration (40 μg L^{-1}) was exceeded in 17.2% of the participants, meaning a statistically relevant risk of developing cancer due to As exposure throughout their (working) life.

Several reports have focused on *As speciation in atmospheric particles*. A study of the occurrence, seasonal variation, and size resolved distribution of As^{V}, DMA, MMA and TMAO in atmospheric particulate matter in an urban area in SE Austria has been reported.[79] The paper presents results from more than 300 daily PM_{10} and further size-resolved atmospheric PM samples in the size range from 15 nm to 10 μm collected over the course of a year. Both AEC and CEC were used as part of the HPLC-ICP-MS system. A significant amount of iAs was present in all samples with the highest concentrations found during winter, but all organoarsenicals were detected throughout the year. The dominant As species was found to be As^{V} in each individual analysed daily PM_{10} sample ($n = 325$), corresponding to 89.1 ± 6.9% of the total water + H_2O_2 extracted species in terms of total As. Other As species, DMA, MMA and TMAO, make up the remaining 11%, corresponding to 2.6 ± 2.2, 0.4 ± 0.2 and 7.9 ± 5.5%, respectively. Only DMA showed a clear seasonal trend throughout the year and MMA was detected in 277 out of the total 325 samples. The speciation of iAs in urban dust collected in the cities of Salvador and Jaguaquara, NE Brazil has been reported using slurry sampling and detection by fast sequential HG-AAS.[31] Doehlert design and desirability function were used to find the optimum conditions for HG (1.0 mol L^{-1} HCl and 0.9% m/v $NaBH_4$). The accuracy of the analytical method was evaluated using the CRM BCR 176R fly ash, and recovery tests for iAs species made using urban dust samples. The LOQ for As was 0.23 mg kg^{-1}. The concentrations of total iAs in urban dust samples ranged between 2.67 ± 0.07 and 23.30 ± 0.02 mg kg^{-1}, with an average concentration of 7.90 ± 6.76 mg kg^{-1}. Most of the As was found as As^{V}, although some samples had up to 42% As^{III}. The authors suggested that the high levels of As reflected intense industrial activities and vehicular traffic in the area. A first report of As speciation in e-liquids (solution used for e-cigarettes) and aerosols generated from vaping the e-liquid has been presented by Liu *et al.*[80] Seventeen e-liquid samples of major brands, purchased from local and online stores in Canada and China, were analysed for As species using HPLC-ICP-MS. Aerosols condensed from vaping the e-liquids were also analysed and the As speciation compared. Six As species were detected; As^{III}, As^{V}, MMA, and three new As species not reported previously, and As^{III} was detected in 59% of the e-liquids, As^{V} in 94%, and MMA in 47% of the samples. In the condensate of aerosols from vaping the e-liquids, As^{III} was detected in 100%, As^{V} in 88%, and MMA in 13% of the samples. The concentration of As^{III} in the condensate of aerosols (median 3.27 mg kg^{-1}) was significantly higher than that in the e-liquid (median 1.08 mg kg^{-1}) samples. The concentration of iAs in the vaping air was approximately 3.4 mg m^3, which approaches the permissible exposure limit (10 mg m^3) set by the United States Occupational Safety and Health Administration. According to the EPA's unit risk factor (4.3×10^{-3} per mg m^3) for inhalation exposure to iAs in the air, the estimated excess lung cancer risk from lifetime exposure to iAs in the e-cigarette vaping air (3.4 mg m^3), assuming e-cigarette vaping at 1% of the time, is as high as 1.5×10^{-4}. These results clearly raise health concerns over the exposure to As from electronic cigarettes.

Industrial applications of As speciation are uncommon, although there has been one report this year. A method based on HPLC-HG-AFS has been proposed for the determination of As^{III} and As^{V} redox couples in Cu electrolyte samples, characterised by extreme acidity and high metallic content (Cu and Ni in the g L^{-1} range).[32] The stability of As species in the samples prior to analysis was also studied over a period of 28 days considering aqueous dilution, acidification with HCl and different storage temperature (4 °C, 25 °C or 65 °C). Dilution and acidification with HCl did not lead to oxidation the As species. The proposed method was successfully applied to industrial electrolyte samples, indicating that As^{V} was the predominant species in the electrolyte with a concentration that ranged from 7.72 to 8.42 g L^{-1} depending on the sample. The As^{III} had a concentration ranging from 0.51 to 0.78 g L^{-1}, and the sum of the As species (8.50 to 8.93 g L^{-1}) was in agreement with the total As content determined by ICP-OES (8.52 to 8.95 g L^{-1}).

Few reports of *As speciation in geological samples* other than soils and sediments have been published in this review period. The bioleaching of arsenopyrite, an iron arsenic sulfide, by the moderately thermoacidophilic strain *Sul fobacillus thermosulfidooxidans YN-22* has been reported.[81] A number of analytical techniques were used including As/S K- and Fe L-XANES, SR-XRD, and SEM, and FTIR and ICP-OES were also used in the determination of the leaching parameters. The results showed that the presence of bacteria significantly promoted the dissolution of arsenopyrite. The As and Fe in the bioleaching solutions mainly existed as As^{V} and Fe^{III}, whilst in the chemical leaching tests they were found mainly as As^{III} and Fe^{II}. The surface of the arsenopyrite was gradually corroded, and some secondary products were formed during bioleaching. In the sterile control experiment, the mineral surface was only slightly corroded, and only a few products were found after 10 days of

 This journal is © The Royal Society of Chemistry 2021

chemical leaching. The As^{III}-oxidising microbes existing in an abandoned iron ore mine in India have also been investigated.[82] The authors cultured 13 morphologically distinct bacterial strains, of which 6 grew in high concentrations and showed the ability to transform As^{III}. Analysis of the amplified 16S rDNA gene sequences of the isolates revealed them to belong to alpha-, gamma-proteobacteria and firmicutes particularly the genera *Paenibacillus, Pseudomonas, Ochrobactrum, Enterobacter* and *Bacillus*. A qualitative silver nitrate screening assay and quantification by HPLC-ICP-MS indicated that these strains could transform As^{III} to As^{V}. The isolates were also genetically analysed for the presence of the As transporter gene (arsB) which indicated the genetic ability of bacteria to tolerate As species.

Several workers have reported on *As speciation in soils and sediments.* A study to investigate the chemical speciation and extractability of As in 24 soil samples from sites potentially affected by anthropogenic pollution in Japan has been reported by Itabshi *et al.*[83] The results of As K-edge XANES demonstrated that naturally contaminated soils were grouped into two types: (i) soils containing FeAsS-like and As_2S_3-like species (average 53%) and (ii) soils with no or minor As–S species (average 3%). Clear differences were found in As, Fe, and S fractionation by sequential extraction. In naturally contaminated soils enriched with As–S species, more than 50% of As was extracted in the oxidisable fraction. Arsenic was mainly recovered in the reducible fraction for naturally contaminated soils with no or minor As–S species and in anthropogenically contaminated soils. The use of μXRF and μXAFS revealed that the naturally contaminated soils containing As–S species were abundant in pyrite framboids (about 20 μm in diameter) in which As occurred in multiple oxidation states. The results suggested that framboidal pyrite becomes a source of As in naturally contaminated soils after being excavated and exposed to the surface environment. The development of a non-destructive method to directly observe the local behaviour of metal(loid)s, in this case As, in the oxidative-reductive layer typically found in waterlogged soil such as flooded paddy soil, has been described.[84] A soil chamber was constructed from titanium plate and glass with low gas permeability and high corrosion resistance, to facilitate the anoxic environment in waterlogged soil. The soil chamber could be mounted directly in a SR-μXRF-μXAFS beamline to allow observations of the intact paddy soil without physical and chemical disturbance. The μXRF imaging of As-contaminated paddy soil showed that the As in the soil was strongly accumulated in the topsoil layer (millimetre scale) during 1 month incubation under flooded conditions. The μXAFS analysis of As and related metals also indicated that the As accumulation was closely attributed to the change in the oxidation state of As with soil depth and the coexistence of the most favoured sorbent (Fe^{III} hydroxides) in the oxidative-reductive layer of the paddy soil. The speciation of iAs in soil and vegetables irrigated with treated municipal wastewater has been investigated.[85] Samples were prepared using VAME based on a DES followed by GF-AAS. The DES was prepared by mixing choline chloride and citric acid monohydrate at a molar ratio of 1 : 1. Under optimal conditions, the proposed method gave an enrichment factor of 175. The LDR was from 0.3 to 100 μg kg^{-1} and the LOD was 0.10 μg kg^{-1}. The repeatability and reproducibility of the method based on seven replicate measurements of 50 μg kg^{-1} As^{III} in analysed samples were 4.2% and 6.5, respectively. The relative recoveries from soil and vegetables that were spiked with different levels of As^{III} and As^{V} were from 94.2 to 104.3 and from 91.0 to 107.0%, respectively. The accuracy of the proposed procedure was evaluated by speciating the As in two SRMs; GBW10014 cabbage and GBW10015 spinach. In another study, the optimum extraction parameters, chromatographic separation conditions, and interference correction, for the simultaneous extraction and quantification of As^{III}, As^{V}, DMA, MMA and Cr^{VI} from sediment by HPLC-ICP-MS has been reported.[86] A gradient mobile phase employing 10 mmol L^{-1} and 70 mmol L^{-1} NH_4NO_3 at pH 8.7 enabled baseline separation of the species within a total run time of 18 minutes. The optimum extraction conditions, a mixture containing 0.375 mol L^{-1} $(NH_4)_2HPO_4$ and 50 mmol L^{-1} EDTA at pH 7 as an extraction buffer, extraction temperature of 150 °C and volume of 15 mL were attained by factorial design. The LOQ values were ranged from 0.064 to 0.682 ng g^{-1}. San Joaquin Soil SRM 2709a was used to evaluate the accuracy of the developed procedure and recoveries of 96.8% were achieved for As^{V}. Spiking and recovery studies at 3× and 25× the LOQ gave recoveries from 84.9 to 104% for As species. The method was used to investigate sediments in the Mokolo River, South Africa. The As speciation in water and bottom sediment samples collected from the dam at Kozlowa Gora Reservoir (Poland), an area known to be heavily contaminated by anthropogenic sources, have been studied using the simultaneous determination of As^{III}, As^{V} and Sb^{III}, Sb^{V}, $SbMe_3$ species by HPLC-ICP-MS.[30] The extraction efficiency for As and Sb from the bottom sediments was checked using the CRM, NCS DC 73310, sediment. The total As concentration in the reservoir water did not show significant temporal or spatial variation, with on average 0.98 μg L^{-1} As^{III} and 1.02 μg L^{-1} As^{V}. For the bottom sediments, the average As content was 33 mg kg^{-1}, with more As^{V} in most months, although the concentration of both iAs forms in bottom sediments was comparable in May and June. The maximum concentration of As^{III} (18.7 mg kg^{-1}) occurred in August. The sediments were also heavily polluted with Cd, Cu, Ni, Pb, and Zn.

As noted in previous years, *clinical studies investigating the impact of As exposure* are a popular area of research. *Polymorphisms in As^{III} methyltransferase* (AS3MT) has again attracted interest this year. These polymorphisms have been shown to be related to interindividual variations in As metabolism and to influence adverse health effects in acute promyelocytic leukemia (APL) patients treated with As_2O_3. The occurrence of hyperleukocytosis with As_2O_3 treatment seriously affects the early survival rate of APL patients, but no definite explanation for such a complication has been clearly established. This has been evaluated by Liu *et al.*[87] who used AS3MT polymorphisms 14 215 (rs3740390), 14 458 (rs11191439), 27 215 (rs11191446), and 35 991 (rs10748835) and profiles of plasma As metabolites in a group of 54 newly diagnosed APL patients treated with single-agent As_2O_3. In this work HPLC-HG-AFS was used to determine the concentrations of plasma As metabolites. Plasma As methylation metabolism capacity was evaluated by the

percentage of iAs, DMA, MMA, primary methylation index (MMA:iAs), and secondary methylation index (DMA:MMA). The results showed that APL patients who developed hyperleukocytosis had a higher plasma iAs%, but a lower MMA% and primary methylation index than those who did not develop hyperleukocytosis during As_2O_3 treatment. In addition, patients with the AS3MT 14215 (rs3740390) CC genotype had significantly higher plasma iAs% and incidence of hyperleukocytosis, but lower primary methylation index than patients with the CT + TT genotype. Conversely, the authors did not observe statistically significant associations between the occurrence of hyperleukocytosis and AS3MT 14458 (rs11191439), 27215 (rs11191446), and 35991 (rs10748835) polymorphisms in the study subjects. The results indicated that AS3MT 14215 (rs3740390) might be used as an indicator for predicting the occurrence of hyperleukocytosis in APL patients treated with As_2O_3. An assessment of the influence of polymorphic variants of AS3MT and glutathione-S-transferase on urinary As metabolites in people exposed to As in groundwater has also been reported.[88] Twenty-two groundwater wells for human consumption from municipalities in Colombia were analysed for As^{III}, As^{V}, DMA, and MMA by HPLC-HG-AFS. An assessment of the exposure by lifetime average daily dose (LADD) (μg per kg per bw per day) was made and surveys on 151 participants aged between 18 and 81 years old conducted to collect demographic information. In addition, genetic polymorphisms (GSTO2-rs156697,GSTP1-rs1695,As3MT-rs3740400,GSTT1andGSTM1) were evaluated by real time and/or conventional PCR. The median of total As concentration in groundwater was found to be 33.3 μg L^{-1} and the median of LADD for the high exposure dose was 0.33 μg per kg per bw per day. Univariate analyses of the As metabolites and genetic polymorphisms showed MMA concentrations higher in heterozygous and/or homozygous genotypes of As3MTcompared to the wild-type genotype. The DMA concentrations were lower in heterozygous and/or homozygous genotypes ofGSTP1compared to the wild-type genotype. Both DMA and MMA concentrations were higher in GSTM1-nullgenotypes compared to the active genotype. Multivariate analyses showed statistically significant association among interactions gene–gene and gene-covariates to modify the MMA and DMA excretion. The authors suggested that interactions between polymorphic variants As3MT*GSTM1and GSTO2*GSTP1 could be potential modifiers of urinary excretion of As and that covariates such as age, LADD, and alcohol consumption contribute to variations in individual As metabolic capacity in exposed people. The combined effect of polymorphisms of methylenetetrahydrofolate reductase (MTHFR), methionine synthase (MTR), As methylation capacity, plasma folate and vitamin B-12 levels on the developmental delay in preschool children in Taiwan has also been studied.[89] A total of 178 children with developmental delay and 88 without developmental delay were recruited. Urinary As species were determine using HPLC-HG-AAS whilst plasma folate and vitamin B-12 concentrations were measured by SimulTRAC-SNB radioassay. Polymorphisms of MTHFR C677T, MTHFR A1298C, and MTR A2756G were examined by PCR and restriction fragment length variation. The results showed that MTHFR C677T C/T and T/T genotypes had a lower risk of developmental delay than the C/C genotype (odds ratio [OR] = 0.47; 95% confidence interval, 0.26–0.85). Subjects with the MTHFR C677T C/C genotype had significantly lower plasma folate and vitamin B-12 levels than those with the MTHFR C677T C/T and T/T genotype. The MTHFR C677T C/C genotype combined with high total urinary As and poor As methylation capacity indices significantly increased the OR of developmental delay in a dose-response manner. The authors reported this to be the first study to show the combined effect of MTHFR C677T genotype and poor As methylation capacity on developmental delay. A study to evaluate the metabolic potency of human gut microbiota toward As^{V}-sorbed goethite and jarosite, different behaviours of As release, and the solid–liquid transformation and partitioning has found a higher degree of As^{V} and Fe^{III} reduction by human gut microbiota in the colon digests of goethite than jarosite.[90] The release of As occurred mainly in the small intestinal phase for jarosite and in the colon phase for goethite, respectively. Speciation analysis using HPLC-ICP-MS and XANES, revealed that 43.2% and 8.5% of total As was present as As^{III} in the liquid and solid phase, respectively, after goethite incubation, whereas almost all generated As^{III} was in the colon digests of jarosite. The study helped elucidate the role of Fe minerals in human health risk assessment associated with soil As exposure. The effects of chronic As exposure on inflammatory immune-related homeostasis has been studied.[91] Kunming mice were treated with 25 and 50 mg L^{-1} As^{III} for 1, 3 and 12 months *via* drinking water. At different endpoints of As exposure, all animals and the whole spleen of the mice were weighed. The total As levels in the spleen were determined by HPLC-HG-AFS. Splenic NF-kappa B, MAPK and NRF2 protein levels by treatment of 25 mg L^{-1} $NaAsO_2$ for 1, 3 and 12 months and 25 mg L^{-1} and 50 mg L^{-1} $NaAsO_2$ for 12 months were assessed by the western blot test. The results indicated that chronic As exposure induced a time-dependent modulation of the inflammation and immunosuppression in spleen, which may be related to the activation of Tregs induced by MAPK/NF-kappa B as well as the increased transcription level of Foxp3andIl-10. It has been previously reported that iAs methylation capacity is associated with breast cancer and the risk factors may vary according to immunohistochemical subtype. A study by Lopez-Carrillo *et al.*[92] has investigated this relationship in women from northern Mexico. Patients with available information about breast cancer subtypes ($n = 499$) were age-matched with healthy controls. Sociodemographic, reproductive and lifestyle characteristics were also obtained. Tumour marker information was obtained from medical records. Cases were classified as HR + [estrogen receptor (ER+) and/or progesterone (PR+), and human epidermal growth factor receptor 2 (HER2−)], HER2+, or triple negative (TN). Urinary As species (As^{III}, As^{V}, DMA and MMA) were determined by HPLC-ICP-MS, and the methylation capacity parameters calculated. The results showed that the urinary total As varied from 0.60 to 303.29 μg L^{-1} and that altered iAs methylation capacity which resulted in higher % MMA was associated with HR+ and TN breast cancer, but not with HER2+. The metabolite more likely to be related to breast cancer was MMA, although further work is needed to confirm

 This journal is © The Royal Society of Chemistry 2021

these results and elucidate the underlying biological mechanisms. Finally, the As concentrations, diversity and co-occurrence patterns of bacterial and fungal communities in the faeces of mice under sub-chronic As exposure through food has been studied.[93] The mice were exposed *via* animal feed prepared with four As species; As^{V}, As^{III}, DMA, and MMA with the ratio of 7.3%, 72.7%, 1.0%, and 19.0%, respectively, according to the proportion of major As species in rice. The levels of total As and As species in mice faeces and urine samples were determined using ICP-MS and HPLC-ICP-MS. At 30 days and 60 days exposure, the total As levels excreted from urine were 0.0092 and 0.0093 mg per day, and total As levels in faeces were 0.0441 and 0.0409 mg per day, respectively. The authors found significant differences in As species distribution in urine and faeces ($p < 0.05$). In urine, the predominant As species were As^{III} (23% and 14%, for 30 and 60 days respectively), DMA (55% and 70%, for 30 and 60 days respectively), and uAs (unknown arsenic, 14% and 10%, for 30 and 60 days respectively). In faeces, the proportion of major As species were more evenly distributed (As^{V}, 26% and 21%; As^{III}, 16% and 15%; MMA, 14% and 14%; DMA, 19% and 19%; and uAs, 22% and 29%, for 30 and 60 days respectively). Microbiological analysis (MRPP test, alpha- and beta-diversities) showedthat the diversity of gut bacteria was significantly related to As exposure through food, but the diversity of gut fungi was less affected. Further analysis showed that the diversity of gut bacteria was significantly related to As exposure through food, but the diversity of gut fungi was less affected. Arsenic exposure significantly changed the microbial taxa, which might be directly associated with As metabolism and diseases mediated by As exposure, such as *Deltaproteobacteria*, *Polynucleobacter*, *Saccharomyces*, *Candida*, *Amanitaceae* and *Fusarium*. The results demonstrated that subchronic As exposure *via* food can significantly change the gut microbiome.

Several studies on the *impact of As exposure during pregnancy and childhood* have been reported. Prenatal As exposure has been associated with reduced foetal growth and increased risk for preterm birth, but most studies have been conducted in highly exposed populations. The impact of early pregnancy exposure to As on birth weight and gestational age at birth in a predominately lower income Hispanic pregnancy cohort in urban Los Angeles USA, has now been reported.[94] The study also compared multiple biomarkers of As exposure (blood, urine, and hair) assessed in early pregnancy. Total As (blood, hair) was measured by ICP-MS and iAs, DMA and MMA (urine) were measured by HPLC-ICP-MS. The associations between log e-transformed As measures and birth outcomes were evaluated using multivariable linear regression. A doubling in hair As levels was associated with a lower birth weight, after adjusting for potential confounders and gestational age at birth. A similar, but non-significant trend was observed for blood As, but not urine As. The inverse association between hair As and birth weight was more pronounced among infants whose mothers gained greater amounts of weight during pregnancy. The study provided evidence that even at relatively low exposure levels, As exposure (measured in hair samples collected in early pregnancy) may adversely affect foetal growth in this population, particularly in combination with greater gestational weight gain. The associations of dietary intakes and serum levels of folate and vitamin B-12 with the methylation of iAs in 7 year old children from Montevideo, Uruguay, has also been reported.[95] The work had two objectives: firstly to compare the associations of serum concentrations and estimated intake of folate and vitamin B-12 with indicators of iAs methylation; and secondly to highlight the implications of these different B-vitamin assessment techniques on the emerging evidence of the impact of dietary modifications on iAs methylation. Serum folate and vitamin B-12 levels were measured on a benchtop analyser and urinary iAs, DMA and MMA were measured using HPLC-ICP-MS. Dietary intakes were assessed using the average of two 24-h dietary recalls and models were adjusted for age, sex, body mass index, total urinary As, and rice intake. The results indicated that serum folate and vitamin B-12 levels were above the adequacy threshold for 99% of the participants. No associations were observed between serum folate, serum vitamin B-12, or vitamin B-12 intake and iAs methylation. The folate intake was inversely associated with urinary % MMA. The authors concluded that additional studies on the role of B-vitamins in iAs methylation are needed to develop a deeper understanding of the implications of assessing folate and vitamin B-12 intake compared to the use of biomarkers. In addition, where possible, both methods should be employed because they reflect different exposure windows and inherent measurement error, and if used individually may contribute to a lack of consensus. Table 1 shows other applications of As speciation presented in the literature during the time period covered by this ASU.

3.3 Cadmium

The first reports for several years of cadmium speciation have appeared and the two reports describe very different approaches (synchrotron X-ray techniques and CE/HPLC-ICP-MS), though the applications were both to biological materials: rice grain and cancer cell cytosol, respectively.

Gu *et al.* described[100] the *speciation and distribution of Cd in rice grain* by measurements made with the 100-element solid-state Ge detector at the XAS beamline at the Australian Synchrotron, Melbourne that has the capability to detect Cd at the concentrations encountered in the samples studied. To assess bulk Cd speciation by XANES, grains were ground to a powder and pressed into pellets (no details were provided) and for the distribution of Cd species, grains were embedded in epoxy and cut into 100 μm thick longitudinal and transverse sections that were placed between two pieces of 4 μm thick Ultralene film and analysed by μ-XRF and micro μ-PIXE. Elemental μ-XRF maps were collected at the μ-XRF beamline at the Australian Synchrotron whose maximum excitation energy of 27.2 keV allows mapping of Cd at the K-edge (26.7 keV). The μ-PIXE analysis was performed with the upgraded CSIRO-MARC high-excitation quintuplet nuclear microprobe at the University of Melbourne. Air-dried rice grains were manually dehusked and subsamples of the brown rice were polished using a laboratory rice milling machine (details given). They found that the

Table 1 Applications of speciation analysis: arsenic

Analyte species	Matrix	Technique	Sample treatment	Separation	LOD	Validation	Reference
As^{III}, As^{V}, DMA^{V}, MMA^{V}	Rice	HPLC-HG-AFS	Species in ground rice extracted with 10 mL 0.28 mol L^{-1} HNO_3 at 92 °C for 90 min	AEC, Hamilton PRP-X100, isocratic 20 mmol L^{-1} (K_2HPO_4 + KH_2PO_4) pH 6.2	0.09–2 μg kg^{-1} in rice	NIST SRM 1568 (rice flour), spike recovery	96
As^{III}, As^{V}, DMA^{V}, MMA^{V}	Algae (kelp)	HPLC-HG-AFS	Extraction with 0.15 mol L^{-1} HNO_3 (90 °C, 2 h), cooled, centrifuged, hexane clean-up, filtered	AEC, Hamilton PRP-X100, isocratic KH_2PO_4 + NaH_2PO_4, pH 6.0	5–10 μg kg^{-1}	Spike recovery	97
11 As species As^{III}, As^{V}, DMA, MMA, AB, AC, TMA, TMAO, DM-dithioarsinic acid, MM-monothioarsinic acid, and trimethylarsine sulfide	Fish, crustacean, mussel, cephalopod and mushroom	HPLC-ICP-MS	Freeze-drying, UAE (30 min, 35 W, 44 kHz) into H_2O, centrifugation filtration	RP C-8, 1.2 mmol L^{-1} TMAH, 4 mmol L^{-1} malonic acid, 6.2 mmol L^{-1} sodium butane-1 sulfonate, and 0.05% methanol	1.4–4.0 μg kg^{-1}	ERM Belgium CRM BC211 (rice), spike recovery	98
As^{III}, As^{V}, DMA^{V}, MMA^{V}, AB, AC	Urine	HPLC-ICP-MS	10 fold dilution with H_2O	Hamilton PRP-X100, 20 mmol L^{-1} ammonium acetate, 4-step pH (5–9) gradient	0.1 μg L^{-1}	Proficiency test samples. Institut National de Santé Publique, Quebec	99

majority of the Cd (66–92%) was present as Cd–thiolate complexes, probably in the form of Cd bound to thiol-rich proteins. The remainder was present as Cd-carboxyl compounds and Cd-histidine. Elemental mapping showed two different patterns of Cd distribution: an even distribution throughout the entire grain, and a preferential distribution in the outer tissues (aleurone layer and outer starchy endosperm). The researchers pointed out that the distribution pattern is important as it affects the removal of Cd during milling, which decreased the Cd concentrations by anything between 22 and 65%. They also observed that the variation in the distribution pattern of Cd in the rice grain correlated with temporal changes in the supply from the soil porewater during grain filling.

The *transformations of CdSeS/ZnS-based QDs in cancer cytosol were examined with CE- and HPLC-ICP-MS.*[101] The CE separation (based on the group's previous work) was at 37 °C in a polyimide-coated fused silica capillary (i.d. 75 μm, o.d. 375 μm, length 70 cm) at 15 kV in a 20 mmol L^{-1} HEPES buffer at pH 7.4 with ^{72}Ge as an internal standard. The spectrometer was equipped with a low-volume spray chamber fitted with a CEI-100 nebuliser and a crosspiece to merge the flow of sheath liquid. The electrical circuit was completed *via* a grounded platinum wire. Details of the pre-treatment of new capillaries and of cleaning between runs were given. The HPLC separation was on a polymeric RP column PLRP-S400 column (150 mm × 4.6 mm, 8 μm particle and 400 nm pore size) with a mobile phase of 1 mmol L^{-1} Na_2HPO_4, 1 mmol L^{-1} NaH_2PO_4, 5 mmol L^{-1} SDS, and 1% MeOH at a flow rate of 0.3 mL min^{-1} and an injection volume of 20 μL. Despite the RP designation, the separation was, in fact, by SEC. Although the separation was based on a previously published method (reference given), further optimisation was considered necessary in terms of the MeOH concentration (to increase the column life-time) and the SDS concentration (to prevent QD adsorption onto the stationary phase). The LOD values of the CE and HPLC methods were 4×10^{-10} and 5×10^{-12} mol L^{-1}, (45 and 0.6 ng L^{-1}) respectively. The procedures were applied to the Cd speciation in the cytosolic fraction obtained after incubation of Hep G2 cells with QDs. The researchers found that regardless of the initial dose, nearly all the Cd was in the low molecular-weight (dissolved) fraction. Similarly, for the QD–serum protein conjugates incubated in simulated cancer cytosol: no Cd in the nanoparticulate form was found. The effect of serum proteins on the surface of QDs on the uptake by Hep G2 cancer cells, investigated by ICP-MS, showed that conjugated proteins greatly decreased the particle internalisation.

3.4 Chromium

In a *review of Cr speciation in foodstuffs, biological and environmental materials* (105 references), Milacic and Scancar first discussed spectrophotometric methods, then the relatively small number of electrochemical methods, and then devoted the bulk of the review to (a) non-chromatographic separations with atomic spectrometry and (b) chromatography with atomic spectrometry (mostly HPLC-ICP-MS).[102] The review opens with an account of the biogeochemistry of Cr which sets the scene for the need and challenges for Cr speciation analysis. The reviewers presented summary tables of relevant topics in which (adverse) critical comments are made. The reviewers pointed out that several reports of the presence of Cr^{VI} in biological materials are erroneous because of “wrongly applied analytical methodology”. They also concluded, about methods involving LLE and SPE that these are, in general, not selective enough to be reliable when applied to Cr speciation in complex matrices.

 This journal is © The Royal Society of Chemistry 2021

The importance of SSID ($^{50}Cr^{III}$ and $^{53}Cr^{VI}$ enriched isotopes) was stressed, particularly for following any reduction of Cr^{VI} during the sample preparation stages. Separation by ion-pair HPLC was criticised on the basis that negatively charged Cr^{III} species can form ion-pairs that may co-elute with Cr^{VI} species. The reviewers endorsed AEC as the separation method of choice, drew attention to the need to quantify Cr in the procedural blanks, and provided a list of the limited number of RM certified for the Cr^{III} content. In the conclusion, the situation regarding Cr^{VI} in foodstuffs and in human biological samples was emphasised: appropriate procedures (AEC-HPLC-ICP-MS and isotopically enriched Cr^{III} and Cr^{VI} tracers) show that Cr^{VI} does not exist. The review is highly recommended.

Two research groups have devised *separations of Cr^{III} and Cr^{VI} by LLE involving deep eutectic solvents* (DESs). A DES is characterised by a significant depression in melting point compared to those of the neat constituent components. Rajabi and co-workers extracted Cr^{III} as the 1-(2-pyridylazo)-2-naphthol (PAN) complex into either (a) choline chloride-phenylethanol,[103] by an air-assisted emulsification microextraction procedure, or (b) choline chloride-phenol[104] by either vortex-assisted or UAE microextraction. The researchers concluded that the UAE procedure was superior. In both methods, the DES (about 200 μL) was aspirated directly into a FAAS. The air-assisted procedure involved repeated withdrawal from and re-injection into a test tube of 100 μL of the mixture of sample solution (10 mL) and extracting solvent (250 μL). The resulting finely dispersed mixture was separated by centrifugation (4000 rpm for 4 min). In the UAE procedure, the phases were also separated by centrifuging, but in this case 400 μL of THF was added so that the extracting solvent was floating on top of sample solution. The LOD for both procedures was 0.4 ng mL^{-1}, and the UAE procedure was validated by the accurate analysis of a CRM (TMDW water) containing 20 μg L^{-1} Cr. Spike recoveries were also undertaken with several real samples (tap, river and mineral waters, rice, sausage mushroom and soybean) in which Cr^{III} was detected in the tap water, river water and sausage, and Cr^{VI} was detected in the river water and sausage. Recoveries ranged from 87–106% for spike concentrations between 0.2 and 400 μg L^{-1}. For the determination of total Cr, Cr^{VI} was reduced to Cr^{III} with ascorbic acid. A DES procedure based on the UAE of the Cr^{VI} complex with APDC into a DES of choline chloride–phenol has been devised.[105] Phase separation was by the addition of THF and centrifugation with aspiration of the organic phase, diluted to 5 mL with methanol, into an FAAS. The LOD was 0.8 μg L^{-1}. Total Cr was determined after oxidation of Cr^{III} with hot acidified permanganate. Spike recoveries (94–104%) of concentrations of 500 and 1000 μg L^{-1} of both species were obtained from two real samples (desert water and the acid digest of black tea), in which both species were found. In the light of the comments by Milacic and Scancar,[102] the values for Cr^{VI} in sausage and tea should perhaps be taken with a grain of NaCl.

A *microextraction procedure* based on "continuous sample drop flows and solidification of switchable hydrophilic fatty acid" has been reported in which the Cr^{VI} (as the 1,5-diphenylcarbazide complex) in the extraction phase, diluted to 1 mL with acetonitrile, was determined by ETAAS.[106] The LOD was 0.3 μg L^{-1} and the procedure was applied to the analysis of river, tap, and well water and industrial wastewater, in which both Cr^{VI} and Cr^{III} were detected (except in the tap water), though no procedure was given for the Cr^{III} determination. Spike recoveries of concentrations from 3–30 μg L^{-1} ranged from 96 to 105%. The article badly needed some editorial input. There are so many sentence-level problems that many of the key passages are incomprehensible.

Rajabi and co-workers devised a *dispersive SPE procedure* in which Cr^{VI} was extracted by NPs of layered double hydroxides of zinc and aluminium into which APDC was intercalated during the preparation.[107] The air-assisted procedure described above was used to disperse 30 mg of the extractant in 10 mL of sample solution (pH adjusted to 5.0). Phase separation was by syringe filtering and the entire solid phase dissolved in 200 μL of 6.0 M HNO_3, 100 μL of which was injected into a FAAS. The LOD was 2 μg L^{-1} and the method was applied to the analysis of hair, nail, saliva, plasma and urine, in all of which Cr^{VI} was detected. Spike recoveries of 10 μg L^{-1} ranged from 96 to 101%. All results were given in solution concentration units, which in the case of solid samples were presumably for the sample digests (2 g of sample in a final volume of 50 mL). As the sample preparation for both hair and nail included heating with concentrated HNO_3, followed by evaporation to dryness, then heating with concentrated $HClO_4$ or H_2O_2, it is possible that some oxidation of the Cr species occurred, and the comments made earlier[102] also apply to these results. No results for Cr^{III} were presented. For the ETAAS determination of Cr species leached from textiles, Cr^{VI} was selectively extracted onto micrometre-sized silica spheres coated with a layer of Cr^{VI}-imprinted methylimidazolium IL.[108] Samples were prepared according to ISO method 105-E04 (10 mm squares were shaken with 50 mL artificial perspiration solution for 12 h at 37 °C) using a water bath. Following filtration and acidification to pH 3 with 0.1 mol L^{-1} HNO_3, sorbent particles (50 mg) were added to a 10 mL subsample that was shaken for 10 min. After centrifugation, the supernatant was removed, and the Cr^{VI} eluted (for 10 min) with 2 mL of 3 mol L^{-1} ascorbic acid + 2 mol L^{-1} HNO_3. The LOD was 0.015 μg g^{-1} and the RSD was 3–8% for concentrations Cr^{VI} that ranged from 0.015–0.5 μg g^{-1} in line with the requirements of international textile regulations. The recovery of Cr^{VI} (concentration not given) in the presence of 10 mg L^{-1} Cr^{III} was 98% and recoveries of Cr^{VI} spiked at concentrations of 2 and 5 μg L^{-1} into the extracts of five different textiles ranged from 93 to 103%. No information about the possible determination of Cr^{III} was given.

A method for the *ICP-MS determination of Cr^{VI} by CVG* (by reaction with BH in acid solution) has been reported, in which the sensitivity was increased substantially by the addition of DDTC (which the researchers refer to as diethylaminodithioformate).[109] The generation efficiency was 28% and the LOD was 0.2 ng mL^{-1}. The substantial interference from copper was significantly decreased by the addition of excess DDTC. The typical polyatomic interferences encountered at *m*/*z* 52 with conventional solution nebulisation were also decreased because the analyte was introduced predominantly as

a vapour phase molecular species rather than dissolved, along with other matrix components, in aerosol droplets. The procedure was validated by the accurate analysis of Beijing Century Aoke Biological Co., Ltd SRM GEW(E)080197 (water), which contains 16.7 ± 0.7 μg mL^{-1} Cr^{VI}, and by recoveries, which ranged from 90–116%, of 20 ng mL^{-1} spikes from three real water samples (tap, drinking and sea), in none of which was Cr^{VI} detected. The method was also able to determine Cr^{III}, following oxidation of all species with permanganate.

A previously developed *electrodialysis separation method* has been improved giving an ETAAS LOD of 0.01 μg L^{-1} for both Cr^{VI} and Cr^{III}.[110] The ion-transfer device consisted of five thin solution channels separated by ion-permeable membranes. The sample solution was delivered to the central channel and, under the action of a dc electric field of 15 V, anionic Cr^{VI} and cationic Cr^{III} migrated in opposite directions into two acceptor channels. A comprehensive description of the unit and a detailed diagram are included in the paper, together with references to prior work with the device. Problems with high blanks were overcome by passing the relevant acceptor solutions through ion-exchange columns. The procedure was applied to the analysis of soil extracts, prepared according to Japanese Environmental Agency notification number 46 that was operated in a continuous recycling mode with periodic sampling for analysis, which allowed plots of species concentrations as a function of extraction time to be constructed. The method was validated by (a) comparison of the results with those obtained by an SPE-ICP-MS method in which Cr^{III} was selectively retained on a cation-exchange resin with determination of the unretained Cr^{VI}, followed by determination of the Cr^{III} in the HNO_3 eluent, and (b) spike recoveries of 99% for 2 μg L^{-1} Cr^{VI}. The researchers point out that the device is field-deployable and thus the accuracy of determination of the separated species at a later time is unaffected by any interconversion that may occur during transport and storage. To study Cr speciation in soils contaminated by tannery waste, Shi *et al.*[111] applied (a) US EPA method 3060A (alkaline extraction) and US EPA method 7196A (spectrophotometry with DPC), and (b) synchrotron-based XANES and spatially resolved XRF. The XANES results indicated that a significant portion of the Cr^{VI}, was not removed by the phosphate buffer extraction, and the XRF maps showed that Cr was associated with both Mn and Fe. The researchers concluded that Cr^{III} was oxidised to Cr^{VI} by Mn oxides, that both Cr^{III} and Cr^{VI} were immobilised onto Fe (hydr)oxides, and that Cr^{VI} immobilisation involved precipitation as $CaCrO_4$.

During this review period 8 articles have appeared in which *Cr species were separated by LC and detected by ICP-MS*. As this is not a new concept, it is disappointing to note that most of the articles did not contain citations to any prior work or explain what advances in the chromatography had been achieved, and so it appears as though essentially the same analytical method is being published multiple times. As the procedures were applied to different sample materials, the novelty is considered to be in the application. Seven of these are summarised in Table 2. In addition, Lorenc *et al.*[58] applied previously published HPLC-ICP-MS methods to the determination of inorganic and organic species of As, Cr, and Sb in flavoured and functional drinking waters. They found for about one-half of the 42 samples, the sum of the concentrations of As^{III} and As^{V} was equal to about 80% of the total with other 20% made up of AsB and unknown organic species. In the remaining samples, the concentrations of As^{III} and As^{V} corresponded to 34–75% of the total, with the remainder consisting of AsB and unknown organic species. For one sample, Sb^{V} corresponded to 100% of the total; in all the others, it was present as unknown organic species. No Cr^{VI} was detected in any sample; thus, Cr was present as either Cr^{III} or unknown organic Cr species. In a study of Cr species in milk, dairy and cereal products to assess dietary exposure, the researchers reported that there was no Cr^{VI} in any of the 68 products analysed.[112] The LOD values were 0.3–0.4 μg kg^{-1} in the original samples. No Cr^{VI} was found in Cr-enriched yeast, but, curiously the Cr^{III} content was not given.[113] Nor was Cr^{VI} found in either of two lobster hepatopancreas CRMs.[114] In a study of blood serum,[115] it was shown that Cr^{VI} reduction was slow: 48 h after spiking, about 20% of the added $^{50}Cr^{VI}$ remained in the serum, while the resulting $^{50}Cr^{III}$ was bound predominantly to Tf. Table 2 shows other applications of Cr speciation presented in the literature during the time period covered by this ASU.

3.5 Cobalt

The Co *species content of various in biological materials has been determined by HPLC-ICP-MS.* To investigate the possible use of inorganic Co^{II} as a "blood dopant" (to improve an athlete's aerobic capacity and endurance performance by stimulating the production of red blood cells), Knoop *et al.* speciated the Co in urine, and determined total Co in plasma and concentrated red blood cells.[119] As several organic Co-containing compounds, such as cyanocobalamin (vitamin B_{12}), are not prohibited in sports, the method must be able to discrimination between the contributions from permitted and banned substances to urinary concentrations. The column, at 35 °C, was an Agilent Poroshell Ec-C18 (2.1 mm × 50 mm, 2.7 μm), the sample volume was 50 μL (of neat urine) and elution (400 μL min^{-1} flow rate) was by a gradient created from (A) 0.1% formic acid and (B) methanol containing 0.1% formic acid that started at 20% B, increased to 50% over 2 min followed by an increase to 80% over 0.5 min then held constant for 1 min. To maintain a constant composition of solvent entering the plasma, the eluent from a second HPLC system, with an inverse gradient, was merged with the chromatographic eluate and the flow split downstream to maintain that entering the spectrometer at 400 μL min^{-1}. A Micromist™ nebuliser and cooled (−5 °C) Scott-type spray chamber were used. For total Co analyses, in was used as an internal standard, but it is not clear whether this was also done for the speciation analysis. Nor is it clear whether any collision gas was needed. The speciation procedure was based on those described in previous cited publications. No information on the LOD or validation was provided, though it was clear that inorganic Co and cyanocobalamin spikes could be readily distinguished, though it turned out that cyanocobalamin was not detected in urine following oral administration of 1000 μg of cyanocobalamin per day (over a period of 14 days).

 This journal is © The Royal Society of Chemistry 2021

Table 2 Applications of speciation analysis: chromium

Analyte species	Matrix	Technique	Sample treatment	Separation	LOD	Validation	Reference
Cr^{VI}	Rice	HPLC-ICP-MS,	Ground <150 μm. UAE with 5% (v/v) TMAH, centrifuge, filter	Hamilton PRP-X100, 80 mmol L^{-1} NH_4NO_3, 1% methanol, pH 8.8	0.06 μg L^{-1}	Spike recoveries. Comparison with results of a RP-HPLC-ICP-MS procedure	116
Cr^{III}, Cr^{VI}	Yeast	HPLC-ICP-MS	UAE with boiling weakly alkaline EDTA	Two IonPac AG7 (50 mm × 4 mm) 0.6 mmol L^{-1} EDTA + 76 mmol L^{-1} NH_4NO_3, pH 7	0.05 (Cr^{III}), 0.4 (Cr^{VI}) μg L^{-1}	None	113
Soluble Cr^{III}, total Cr^{VI} and bound Cr	Hepatopancreas material	HPLC-ICP-MS	Shaking with alkaline EDTA at room temperature	PRP-X100 30 mmol L^{-1} NH_4NO_3 pH 6	0.03 μg g^{-1}	NRCC CRM LUTS-1 (lobster hepatopancreas) and TORT-2 (lobster hepatopancreas)	114
Cr picolinate and Cr^{VI}	Multivitamin and mineral supplements	HPLC-ICP-QQQ-MS	Extraction with dilute NH_4OH at pH 10 (for Cr^{VI}) or acetonitrile/water (for Cr picolinate)	Cr^{VI}. PRP-X100 50 mmol L^{-1}, NH_4NO_3 pH 8. Cr picolinate. RP XDB-C18 ACN/H_2O	0.13 μg g^{-1}	NRCC candidate RM VITA-1 and VITB-1 and spike recovery	117
As^{III}, As^{V}, DMA, MMA, Cr^{VI}	River sediment	HPLC-ICP-MS	MAE with $(NH_4)_2HPO_4$ + EDTA	AEC PRP-X100 4 step gradient 10–70 mmol L^{-1} NH_4NO_3 pH 8.7	0.06–0.7 ng g^{-1}	NIST SRM 2709a (San Joaquin soil) and spike recovery	86
Cr, Mn protein bound	Plants traditionally used to treat diabetes mellitus	HPLC-ICP-MS	Water (80 °C) pH 4 shaken (24 h), centrifuged, filtered	SEC two columns. TSK HW 55S and TSK HW 40S 9:1 50 mmol L^{-1} NH_4 acetate, pH 5.8, 500 mmol L^{-1} NH_4 acetate, 10 mmol L^{-1} Tris, 5% MeOH, pH 8.0	Not given	None. Comparison with previously reported ranges	118
Cr^{III} Cr^{VI} Cr–Tf, Cr-HAS	Serum	HPLC-ICP-MS with ID	Blood, centrifuged, serum separated, stored frozen, thawed, diluted with mobile phase A	AEC monolithic column disks Gradient A: 50 mmol L^{-1} Tris–HCl + 10 mmol L^{-1} $NaHCO_3$ (pH 7.4). B: A + 2 mol L^{-1} NH_4Cl (pH 7.4). C: 0.2 mmol L^{-1} Tris–HCl (pH 7.4)	0.15 (Cr^{VI}), 0.13 (Cr–Tf) 0.20 (Cr-HAS) μg L^{-1}	SSID ^{50}CrVI, ^{53}CrIII	115

This was attributed to biochemical conversion, photolytic degradation, and insufficient detection capability. The method was rapid: peak separation was within 2 min and the overall run including column re-equilibration took 4 min. The bio-accessible fraction of Co species, extracted from berries and seeds, was determined by SEC-ICP-MS.[120] Total Co determinations showed that acai berries and chia seeds (both with 0.35 ± 0.04 μg g^{-1}) had higher concentrations than acai seeds or goji berries. Samples were extracted with simulated gastric and intestinal digestion (full details given) and the diluted extract injected into a Superdex 200 (10 × 300 mm, 10 μL) column (held at 24 °C) that was coupled to the cross-flow nebuliser of the ICP-MS instrument by PEEK tubing. The mobile phase was 10 mmol L^{-1} ammonium acetate (at pH 7.4) at a flow rate of 0.7 mL min^{-1}. No prior references to the chromatographic separation were given. The instrument was optimised for the lowest level (≤0.2%) of polyatomic oxide interferences to minimise possible interferences from $^{43}Ca^{16}O^+$, $^{42}Ca^{16}O^1H^+$ and $^{40}Ar^{18}O^1H^+$ on ^{59}Co. No internal standard was used. The LOD was 0.02 μg L^{-1} and the method was validated by spike recoveries (concentrations not given) of between 75 and 103%. In addition, following ultracentrifugation through 3 kDa molecular weight cutoff (to separate enzymatic proteins from small molecules) samples were analysed by μ-HPLC-ES-MS. The column (not exactly micro) was a Zorbax SB C18 (4.6 × 150 mm, 5 μm) and gradient similar to that of Knoop *et al.*[119] described above, was used. The injection volume was 0.2 μL and the flow rate 5 μL min^{-1}. In addition to extractions with the simulated gastric and intestinal fluids, samples (0.05 g of dry powder) were also subject to UAE with 2 mL of 10 mmol L^{-1} ammonium

acetate (pH 6.8), or 30 mmol L^{-1} Tris HCl (pH 7.4), or 2% SDS in water followed by centrifugation (20 min at 15 000 rpm at 15 °C) and filtration (0.45 μm). Bilberries and goji berries were also studied; the former had the highest concentrations of cobalamin species, including methylcobalamin and adenosylcobalamin.

To characterise the *elemental distribution and chemical speciation of Co and Cu and in three metal-tolerant plants, a range of X-ray techniques* were employed together with SEM-EDS with the determination of total extractable elements (in soils as well as the plants) by ICP-OES.[121] Plants were also examined by optical microscopy after fixing and staining. For XFM at the Australian Synchrotron, frozen leaves, held between two sheets of Kapton thin-film stretched over a plastic U-frame, were examined at −140 °C with a beam spot size of 10 μm. For XANES, samples and standards (14 for Co) were analysed in either polycarbonate or poly-lactic acid cuvettes, covered with Kapton tape, maintained at 5–15 K by a closed-cycle He cryostat, at the XAS beam line at the Australian Synchrotron. Nuclear μ-PIXE measurements were made at the Materials Research Department, iThemba LABS, South Africa, and proton backscattering spectrometry was performed simultaneously. The proton beam was focussed to a 3 μm spot. Of the plants studied, *Persicaria puncata* is a Co-hyperaccumulator (up to 1060 μg g^{-1} in the leaves), whereas *Persicaria capitata* and *Conyza cordata* are Co-excluders; all three are Cu-accumulators. The researchers found that the highest concentrations of Cu–Co were in the epidermal cells, whereas in *Persicaria puncata* Co was also enriched in the phloem. They found that an aqueous Co^{II} tartrate complex the predominant species in all plant tissues, together with a minor component that was a Co^{II} compound with oxygen donor ligands, and they observed considerable variation in the Cu speciation in the various tissues across the three species. They concluded that the study revealed different biopathways for transition elements (Cu, Co) in hyper-tolerant plant species.

3.6 Copper

Copper is an essential element for biological functions within humans and animals and there are several known *diseases associated with Cu deficiency or overload*, such as Menkes disease and Wilson's disease, respectively. Consequently, Cu in the clinical field is still a topic of much research. In this line a method to determine extractable Cu in serum was developed by employing HPLC-ICP-MS.[122] The Cu compounds were extracted from serum of Wilsons disease rats (Atp7b−/−) and control rats (Atp7b+/−). Chromatographic separations of bound and extractable Cu species were carried out using an Elemental Scientific CF-Cu-02 (200 mL resin volume, 50 × 4 mm) column. The Cu species were retained in the column at pH values of 6.0 to 8.0 and further eluted to the ICP-MS detector by lowering the pH around 1. Two mobile phases consisted of 100 mmol L^{-1} NH_4OAc, pH 7.4 (mobile phase A) and 10% nitric acid v/v (mobile phase B) were employed. Applying a two-step gradient, bound Cu species were eluted first using 100% eluent A. Afterwards, the mobile phase composition was then changed to 100% eluent B to allow the elution of extractable copper. The developed method allowed the authors to determine extractable Cu in serum in less than 6 minutes. Samples obtained from controls or Wilson disease rats were clearly distinguishable based on the ratio of extractable Cu : bound Cu with the ratio found to be 6.4% and 38% in control and Wilsons disease rats, respectively. Consequently, the developed procedure could be an interesting tool for fast diagnosis of Wilsons disease and possibly other Cu-related diseases. Similarly, Cu speciation in relation with Wilson disease was performed by Solovyev *et al.* by using SAX-ICP-MS/MS.[123] The method was applied to determine ceruloplasmin (Cp) in blood serum samples from Wilson's disease patients. In the blood, functional Cp contains six Cu atoms per molecule (holoceruloplasmin, holo-Cp) but the protein may also be present without bound Cu (apoceruloplasmin, apo-Cp). Copper bound to Cp is not exchangeable under physiological conditions and is considered non-toxic and nonbioavailable. Separation of Cu compounds was achieved using a SAX analytical column (100 × 4.6 mm ID, 7 μm particle size) with quaternary ammonium groups. A combination of 50 mM Tris, pH 7.4 (A) and 50 mM Tris, 1 mol L^{-1} NH_4OAc, pH 7.4 (B) were employed as the mobile phase under gradient elution with a flow rate of 0.7 mL min^{-1}. The proposed method allowed the authors to determine Cp in blood serum of Wilson's disease patients and a healthy control with a LOD value of 0.1 μg L^{-1}. The Cp values were compared with those provided by immunonephelometry and enzymatic activity assay with good correlation values.

The distribution and *chemical state of Co and Cu in three metallophyte species*, *Persicaria capitata*, *P. puncata* (*Polygonaceae*), *Conyza cordata* (*Asteraceae*) from mineral wastes in the Zambian copper–cobalt belt have been studied by XRF and XANES.[121] The aim of this study was to gain understanding of the mechanisms behind the tolerance of these hyperaccumulator plants to the presence of high concentration of these elements. The data obtained by micro-PIXE, SEM-EDS synchrotron XFM and XAS revealed the different response of the plants species when growing in soils with high levels of Co and Cu. *Persicaria puncata* is a Co hyperaccumulator (up to 1060 mg g^{-1} in leaves), while *Persicaria capitata* and *Conyza cordata* are Co-excluders. In contrast all three species were found to be Cu-accumulators. A Co^{II}–tartrate complex was the predominant component identified in all plants and tissues, along with a minor component of a Co^{III}- compound with oxygen donor ligands whereas for Cu there was a considerable variation in the species present in different plants and tissues.

Finally, the *interaction between Cu and Chlorophyll degradation products* (CDPs) has been evaluated. These CDPs are the main cause of discoloration of table olives (from a green to a pale or brown colour) which made them less attractive for consumers. This discolouration occurs during industrial processing and the storage of table olives and can be reversed by the addition of inorganic salts. In this context, the re-greening of table olives can be achieved by complexation of CDP with Cu^{2+}, to form stable bright green copper CDP (Cu-CDP) complexes. To study this process a novel method was developed to separately extract lipophilic and hydrophilic Cu-CDP

 This journal is © The Royal Society of Chemistry 2021

and quantify Cu-CDP by UHPLC-ICP-MS using post-column isotopic dilution with ^{65}Cu as the spike isotope.[124] Table olives spiked with Cu were prepared by boiling commercial pale yellow olives in aqueous $CuSO_4$ (50, 100, and 250 mg L^{-1}) while table olives spiked with sodium copper chlorophyllin (SCC) were obtained by leaving table olives overnight at 20 °C in 1 L of SCC solution (1000 mg kg^{-1}). All the spiked olives were homogenised, freeze-dried, extracted with hexane, methanol, and DMF/H_2O and centrifuged. The lipophilic extracts (top hexane layer) were purified by SPE while the lower hydrophilic layer was filtered through PTFE (0.45 μm). Both, lipophilic and hydrophilic CDP/Cu-CDP extracts were analysed with the same column (Ascentis Ex-press C_{18}, 2.1 × 150 mm, 2 μm) but with different mobile phases. Lipophilic CDP/Cu-CDP were separated with an elution gradient of (A) 0.1% HAc : MeOH and (B) 50 : 50 ACN/acetone whereas Hydrophilic CDP/Cu-CDP were submitted to an elution gradient of (A) 0.1% formic acid in water and (B) acetonitrile. The column effluent was mixed with a ^{65}Cu solution. Quantification of Cu-CDP in both fractions was performed by measuring the ^{63}Cu : ^{65}Cu isotope ratio although no mention is made of how mass bias was corrected for, if at all. Identification of Cu-CDP compounds was achieved by UHPLC-HR-MS. Around 13 Cu-CDC compounds were identified and quantified in the different types of table olives and the authors concluded that the ratio between Cu isochlorin e4 and Cu-15 2-Me-chlorin e6 could be applied to discriminate between table olives re-greened by processing with copper salts or with SCC.

3.7 Gadolinium

Gadolinium-based contrast agents have been used for the past 3 decades in magnetic resonance imaging (MRI) recently however, several papers have pointed out a *potential risk of Gd accumulation in different tissues* after multiple applications. In this context, two papers have been published this year on the accumulation of Gd compounds in rat brain using two methodologies: HPLC-ICP-MS and synchrotron X-ray techniques. In the first paper, HPLC-ICP-MS was employed to determine Gd compounds in rat brain samples after a long term study (1 and 5 months) consisting of a single injection of a clinically relevant dose of 3 different Gd-based contrast agents (GBCAs) (gadoterate meglumine, gadobenate dimeglumine and gadodiamide).[125] At the completion of each treatment period, the rats were euthanised, the brain removed and dissected to sample a half cerebellum. These were stored at −80 °C before further sample preparation which involved homogenisation and centrifugation. The resulting supernatant was collected from the pellet and stored at −80 °C before speciation analysis by SEC-ICP-MS and total Gd content by ICP-MS. The extraction efficiencies of the water-soluble fraction of cerebellum varied depending on the Gd compounds administered. The highest extraction efficiency was found for gadoterate (greater than 50%) while for gadobenate and gadodiamide it was much lower (not greater than 25%). Speciation analysis also evidenced that the presence of Gd compounds in brain was dependent on the Gd form supplemented. The SEC-ICP-MS chromatograms showed that after injection of the macrocyclic gadoterate, Gd was still detected only in its intact chelated form 5 months after injection. In contrast, after a single dose of linear GBCAs (gadobenate and gadodiamide) 2 different forms of Gd were detected: intact GBCA and Gd bound to soluble macromolecules (above 80 kDa). Unfortunately, SEC-ICPMS did not allow identification of the chemical nature of the macromolecules and therefore it was not possible to demonstrate whether the intact linear GBCA or transmetalated Gd^{III} ion were bound to the macromolecules. In the second paper Gd retention in inflamed rat brain after repeating injections of Gd-DTPA was evaluated by means of ICP-MS and μ- and nano-SR-XRF.[126] The results showed that mice with autoimmune encephalomyelitis (EAE) retained a higher concentration of Gd in the brain than healthy mice. Consequently, the occurrence of neuroinflammation may facilitate the retention of Gd in brain tissues. The location and quantification of Gd deposits were evaluated by quantitative μ- and nano-SR-XRF and Gd seemed to be present in hotspots that contained up to several milligrams of Gd per gram of tissue. The size of hotspots was further investigated by SR-nano XRF and it was found to be as small as 160 nm in diameter.

3.8 Gold

Two papers on *the use of Au in biomedical applications* have appeared this year. The first work describes the characterisation of the bimetallic oncology metal complex Titanocref. 127 Titanocref has two metal centres (Au and Ti) and has exhibited good results in tumour reduction but its capability to reach target tissues intact is still unknown. To get insights into its stability, human plasma samples were spiked with Titanocref. After 5 and 60 minutes of incubation, samples were injected onto a SEC column: Superdex™ 200 Increase High Resolution SEC (30.0 × 1.0 cm I.D. particle size: 8.6 μm; fractionation range ∼600–10 kDa) with a mobile phase of PBS buffer (pH = 7.4) flowing at 0.75 mL min^{-1}. The eluate from the column was directed to an ICP-OES instrument. The coupling of HPLC to ICP-OEs is unusual and the instrumental and data acquisition parameters are not given but the reader is referred to a cited reference. The results revealed that around 30% of the compound was transformed into Ti and Au degradation products while about 70% of the parent bimetallic complex remained intact after 60 min, suggesting the stability of Titanocref. In the other interesting paper, DNA-conjugated AuNPs were employed to selectively label graphene oxide (GO) with the aim of evaluating GO distribution in rat tissues using ICP-MS.[128] Graphene oxide is a promising material for drug delivery, bioimaging and biomedical applications however, knowledge of its distribution in the organism once administered is of special importance to assess its safety. The developed analytical protocol involved the following steps: (1) tissue solubilisation, (2) separation of DNA-AuNP-labelled GO from unbound DNA-AuNPs by using a C_{18} packed microcolumn and (3) ICP-MS measurements of Au intensities. The paper provides a detailed description on the experimental factors affecting labelling (DNA length, incubation pH, DNA-AuNP concentration, and incubation time) and separation conditions (sample loading flow rate, rinsing

volume, and eluent composition). Separation of the DNA-AuNP-labelled GO from non-labelled DNA-AuNPs was achieved in a hyphenated system consisting of (1) an automated FI system which included a C_{18}-packed mini-column (2) three eight-port valves and (3) three four-channel peristaltic pumps. The mini-column was fabricated by packing C_{18} resin (30 mg from a Sep-Pak C_{18} classic cartridge; particle size: 55–105 μm) into a 12 cm piece of PTFE tubing. Following sample loading into the FI system, a stream of pure water (0.1 mL min^{-1}) was used to remove the residual biological matrix and the unbound DNA-AuNPs. The GO bound DNA-AuNPs retained in the mini-column were then eluted using a thiol containing solution (100 μmol L^{-1} cysteine in 5 mmol L^{-1} NH_4Ac buffer solution, pH 9) and transported directly into the ICP-MS system. Under optimal conditions a LOD of 9.3 μg L^{-1} was obtained. The approach revealed that GO is mainly accumulated in liver and spleen at 1 and 12 h of post-administration. The authors highlighted the applicability of the method for the quantification of GO of different sizes and other carbon-based materials.

3.9 Halogens

The *speciation of dissolved I in seawater* can be used oceanographically as a tracer/proxy for the redox state of modern and ancient regional seawater masses. The major I species of interest in this context are iodate (IO_3^-), iodide (I^-) and dissolved organic iodine (DOI), with a typical total I concentration in seawater of 450–500 nmol L^{-1}. Validation work on modern water systems has shown the usefulness of IO_3^- and other I species as potential seawater redox tracers; IO_3^- requires O_2 for accumulation and is quantitatively reduced to I^- in reducing settings such as O_2 deficient zones and anoxic basins. This application of the biogeochemical characteristics of I speciation has however been limited by a general lack of observations of IO_3^- and I^- in the marine environment. In an effort to address this gap in knowledge, an off-line column packed with an AE resin (AG1-X8) was used for I species separation and a novel sparge-interface MC-ICP-MS technique was developed for sample introduction and analysis.[129] This approach used isotopic spiking of the samples with ^{129}I, a radiogenic isotope of I with a suitable half-life and ID-MS calibration to measure the redox formations of I in seawater incubations. The main advantage of the sparge method was that it increased the transmission efficiency of I by approximately 10 fold relative to wet-plasma conditions. The measurement of isotope ratios also helped to correct the time-resolved drift of the two isotopic signals used, *m*/*z* 127 and 129. The sparging method also facilitated the introduction of Te as a means of correcting instrumental mass fractionation and the ^{131}Xe isotope could be used for ^{129}Xe interference correction, so that high accuracy isotope ratio measurements were achievable. The I species recovery obtained was similar to that obtained in other studies, being in the range 80–98%. The main drawback included the complex sequential elution and collection protocol from the columns used and the requirement for using two separate AE columns to separate all the I species studied.

The research group led by Goessler has been active in *the development of methods for the analysis of halogenated acetic acids (HAAs), a common group of water disinfection by-products, by HPLC coupled to ICP-MS/MS.*[130,131] Due to their serious human health risks, the presence of five different HAAs in drinking water including: monochloro-, dichloro-, trichloro-, monobromo-, and dibromo-acetic acid have been regulated by the US EPA to a combined maximum contaminant level of 60 μg L^{-1}. In the EU a proposed maximum concentration of 80 μg L^{-1} for the sum of nine HAAs is currently under consideration. To cover the requirements of both jurisdictions, a RP separation based on a YMC Triart-C_{18} column was used and the eluent was switched from 22 mmol L^{-1} oxalic acid (pH = 1.8) at 0.5 mL min^{-1} for the nine component mixture, to one containing 0.15% TFA, pH = *ca.* 1.8 at a flow rate of 0.8 mL min^{-1} for the separation of six HAAs, including those regulated by US EPA plus tribromoacetic acid. The accuracy and the repeatability of the developed method for the determination of six HAAs in tap, river, and groundwater matrices were validated by recovery experiments at four different concentration levels based on external standardisation, whereas for the nine HAAs a 1 + 999 dilution of the EPA 552.2 CRM in pure water was used. The linearity of the method was tested over the concentration range of 10 to 1000 μg per Cl/Br per L (r^2 = 0.9996–0.9999). The calculated instrumental LOD values (based on 3× S/N) were 1.4 to 1.6 μg per Cl per L for the chlorinated acetic acids and 0.8 to 1.5 μg per Br per L for the brominated acetic acids (injection volume 50 μL), both suitable for the legislative requirements mentioned earlier. It was noted that ICP-MS/MS offers better flexibility in some aspects of mobile phase selection compared with ES-MS/MS, the conventional method used in the regulation of HAAs. For example, involatile eluents such as oxalic acid, malonic acid and citric acid are compatible with ICP-MS/MS and even buffers containing chloride, sodium, phosphate, and sulfate are better tolerated provided that the mobile phase contains <0.2% total dissolved solids, which is not the case with ES-MS/MS which requires volatile buffers to be used. However, the disadvantages of HPLC-ICP-MS/MS, include the background signal and the LOD/LOQ being significantly affected by the presence of the element in question in the mobile phase. Therefore, high-purity reagents for mobile phase preparation are required where possible. This is especially true for the analysis of non-metals, as commercially available buffer salts usually contain chloride, phosphate and sulfate impurities which leads to concentrations between 0.5–50 mg L^{-1} of these species when used in a mobile phase. During the development of this HPLC-ICP-MS/MS method, the novel use of fluorinated carboxylic acids as "ion-repelling agents" in RP chromatography was investigated.[130] In an analogous way to the use of ion-pairing reagents, which increase the retention of ionic or hydrophobic compounds in RP chromatography, the addition of fluorinated carboxylic acids can also decrease the retention of similarly charged analytes. The effects of trifluoroacetic acid (TFA), pentafluoropropionic acid (PFPA) and heptafluorobutyric acid (HFBA) on the retention and selectivity of the separation of chloro- and bromo-carboxylic acids, as well as sulfonic acids was investigated. The results showed a consistent decrease in

 This journal is © The Royal Society of Chemistry 2021

the retention factors (up to *ca.* 9-fold with HFBA) in a concentration dependent manner and significant improvement of the peak symmetry was observed. This approach gives another option to investigate when developing separations that might require gradient elution with an organic modifier for the elution of well retained compounds and is particularly advantageous when using ICP-MS as the detector, which has limited compatibility with organic solvents. It may be possible to replace the organic modifier by the use of an ion-repelling agent and reduce the plasma load of organic material.

Interest in the speciation of organofluorine compounds has increased over the last few years as a greater understanding of the health risks associated with F containing POPs such as polyfluoroalkyl (PFA) substances has meant that suitable analytical methods are now being developed. *A review of recent methods for the chemical characterisation of organofluorine compounds in consumer products and environmental samples* included eight different analytical techniques that are suitable for application to the measurement of this difficult to access element.[132] These ranged from solid sampling techniques to those requiring sample extraction. However, because of the difficulty experienced in the measurement of F due to the generally poor LOD/LOQ and the difficulty in determining the individual species, only two papers out of the 74 reviewed covered approaches based on atomic spectrometry and which could be readily applied to speciation analysis, specifically ICP-MS/MS. These two related reports used HPLC-ICP-MS/MS and the simultaneous analysis of target PFAs by ES-MS to investigate spiked river water (sub-μg L^{-1} level) using sample extraction prior to instrumental analysis. Detection of F directly with ICP-MS is not feasible for two main reasons: the high first ionisation potential of fluorine (17.4 eV), which leads to insufficient formation of F^+ ions in the argon plasma; and the isobaric interferences from commonly occurring polyatomic ions such as $^{38}Ar^{2+}$, $^{16}O^1H^{3+}$ and $^{18}O^1H^+$. The novel strategy developed to overcome this lack of ionisation was the formation of specific F-containing polyatomic ions by mixing either a Ba or Al solution with the sample prior to introduction into the nebuliser and measurement of BaF^+ or AlF^+ as surrogate markers for F-containing species. After considering the state-of-the-art methods the reviewers suggested an analytical work-flow based on a top-down approach for the comprehensive assessment of OF, where OF/extractable-OF is first measured, followed by target analysis to obtain unquantifiable OF concentrations using a mass balance. The authors noted that neither inter-laboratory comparison on OF analysis nor suitable CRMs have been used for method validation, which makes data comparability between studies challenging.

The speciation *of Br-containing POPs in relation to human health and exposure has been investigated using significantly different methods*, *illustrating the range of sophisticated approaches that can be used*. An HPLC-ICP-MS method was developed for the simultaneous determination of four polybrominated diphenyl ethers (BDE-47, -99, -153 and -209) and four hydroxylated analogues (3-OH-BDE-47, 5-OH-BDE-47, 6-OH-BDE-47, 5′-OH-BDE-99) in human serum.[133] Extraction and purification used SPE with additional UAE to extract the target analytes from the solid residue produced after protein precipitation of the serum. The recoveries of the investigated analytes ranged from 79.0% to 90.0%. The LOQ ranged from 0.060 to 0.081 ng mL^{-1} and the inter-/intra-day RSDs were all below 4%. In addition, compound-independent calibration was investigated, and the spray chamber efficiency shown to be a key factor for its application to different kinds of brominated chemicals. The method was used for the analysis of 20 human serum samples collected from Tianjin City, China. The use of SR-XRF for the analysis of brominated flame retardants (BFRs) has been shown to have a low LOD (<1 μg g^{-1}) which is suitable for BFRs and can be combined with XANES to speciate the Br-containing species present in household dust.[134] The study investigated twenty indoor dust samples from rural homes in Newfoundland, Canada and identified Br in all the samples, with concentrations ranging from 2 to 19 μg g^{-1}. The XANES analysis identified organic-based Br-containing species in several samples, proposed to be BFRs based on the spectral line shape. The accuracy of using XANES to identify BFRs was highly dependent on the source and size of the dust samples and so it would be necessary to take this into account when applying the method more widely.

3.10 Iron

Analytical *methods for Fe speciation continue to be developed* and reported due the important biological role of this element. In CE, the lack of a stationary phase can help to maintain species integrity, which can be challenging for redox speciation methods. Thus, a CE-ICP-MS method has been developed to separate and quantify Fe^{II} and Fe^{III} in 1 : 2 diluted lysates of human neuroblastoma (SHSY5Y) cells.[135] The background electrolyte was 20 mmol L^{-1} HCl with an applied voltage of +25 kV. The peak shapes and LOD values were improved by conductivity-pH-stacking. For the negation of the $^{56}Ar^{16}O^+$ polyatomic interference NH_3 was used as a reaction gas. The method LOD was found to be 3 μg L^{-1}, the LDR was up to 600 μg L^{-1} and the precision was 2.2% for Fe^{III} and 3.5% or Fe^{II}. Migration time precision was <3% for both species, determined in 1 : 2 diluted lysates of human neuroblastoma (SH-SY5Y) cells. Spike recoveries were 97 and 105% for Fe^{II} and Fe^{III}, respectively. The authors point out that for real-life bio-samples like CSF, the migration time can vary according to varying conductivity, *i.e.* that caused by differing salinities, and that peak identification needs to be confirmed by standard addition. The Fe^{III} and Fe^{II} concentrations in a cell lysate sample analysed were found to be 330 μg L^{-1} and 84 μg L^{-1}, respectively, resulting in a Fe^{II} : Fe^{III} ratio of 0.25. Superparamagnetic iron oxide nanoparticles (SPIONs) are used in cancer diagnosis and therapy and a CE-ICP-MS/MS method for their determination has been reported to assess changes in these NPs after incubation with proteins under simulated physiological conditions.[136] The SPIONs were added to a 10 mmol L^{-1} phosphate buffer, pH 7.4, containing 100 mmol L^{-1} NaCl and 1 mg mL^{-1} albumin, to give a final SPION concentration of 30 μg mL^{-1} and the mixture incubated at 37 °C. A polyimide coated fused silica capillary (i.d. 75 μm; o.d. 375 μm; length 70 cm) was used for the

CE separations with ammonium bicarbonate (20 mmol L^{-1}, pH 7.4) as the running buffer and an applied voltage of +18 kV. Oxygen was used as the ICP-MS cell gas to allow $^{32}S^{16}O$ to be monitored as a marker for proteins and V was added to the sheath liquid for use as an internal standard. Under these conditions the repeatability of migration times and peak areas ranged from 0.23–4.98% RSD, spike recoveries were 93 to 97% and the LOD values were 54 ng mL^{-1} and 101 ng mL^{-1} for SPIONs with carboxyl and amino terminal groups, respectively. The carboxyl coated SPIONs were found to be stable in the buffer solution for 24 hours whilst some of the amino coated SPIONs transformed into a form with higher electrophoretic mobility which matched the retention time of $FeCl_2$. Monitoring of the $^{32}S^{16}O$ signal led the authors to conclude that the majority of the carboxyl SPIONs and albumin present in the sample formed a conjugate. An HPLC-ID-ICP-MS for the absolute quantification of haemoglobin (HGB) in whole blood by measuring content of iron, through two specific methods, has been published.[137] In the first method, following the separation of HGB by HPLC, a ^{54}Fe enriched spike was continuously mixed with the eluate from HPLC prior to nebulisation by the ICP-MS instrument and quantification was by the $^{56}Fe : ^{54}Fe$ ratio and the usual species unspecific IDMS approach. In the second method, the total Fe concentration was quantified by ID-ICP-MS after digesting the spiked whole blood sample. The results obtained with the two methods were 115.3 ± -2.4 mg g^{-1} and 115.5 ± 2.1 mg g^{-1}, respectively and the RSDs were 3% or lower. Both of the proposed methods were validated for by the analysis of a human blood CRM (IRMM/IFCC-467) with the found mass fractions being better than 97% of the certified value for both methods. Further details of the procedure are contained in the paper which is in the Chinese language. The authors also state that the methods can be used as the main reference method to quantify HGB in clinic which suggests that clinical laboratories in China are very well equipped.

A method based on the use of *SEC-ICP-MS and HILIC-electrospray-Orbitrap MS has been developed for the speciation of nutrient elements* (Cu Fe, Mn and Zn) in coconut water.[138] With the aim of preserving species integrity, sample preparation was limited to dilution with the chromatographic mobile phase followed by centrifugation. The distribution of the metal complexes in the coconut water was evaluated by SEC-ICP-MS. Separation was performed by using a HPLC system equipped with a Superdex-75 10/300 GL SEC (separation range 3000 and 70 000 Da, 10 × 300 mm) column with 100 mmol L^{-1} NH_4Ac as the mobile phase flowing at 0.7 mL min^{-1}. The chromatograms for Cu, Mn and Zn showed a single well shaped peak in the low molecular weight (LMW) zone of the chromatogram whereas in the case of Fe two peaks were observed. The fractions were subsequently analysed by HILIC-ES-MS in order to identify the nature of the metal complexes present in the coconut water. Separation was achieved on a Kinetex (150 × 2.1 mm × 2.6 μm) column with ACN or water as the mobile phase under gradient elution. The metal species identified included: Fe complexes with citrate and malate: ($Fe^{III}(Cit)_3(Mal)$, $Fe^{III}(Cit)_2(Mal)_2$ and $Fe^{III}(Mal)_2$), glutamine: ($Fe^{III}(Glu)_2$) and nicotianamine: ($Fe^{II}(NA)$); copper complexes with phenylanaline: ($Cu^{II}(Phe)_2$ and $Cu^{II}(Phe)_3$) and nicotianamine: ($Cu^{II}(NA)$); zinc complexes with citrate: ($Zn^{II}(Cit)_2$) and nicotianamine ($Zn^{II}(NA)$) and a manganese complex with asparagine ($Mn^{II}(Asp)_2$).

The *speciation of Fe in water samples* is usually undertaken using a FI chemiluminescence approach or the coupling of the same FI methodology with an ICP-MS instrument. A solvent-free method for determining ferrocene and five of its derivatives (1,1′-dimethylferrocene, ferrocenecarboxaldehyde, acetylferrocene, ferroceneacetonitrile and benzoylferrocene) in seawaters and soils has been developed.[139] For seawaters, Fe species were directly extracted onto a divinylbenzene/carboxen/polydimethylsiloxane SPME fibre, using a 15 min exposure time at 25 °C, with subsequent separation and detection by GC-MP-AED. For soil samples the analytes were first extracted into 7 mL of a 0.1 mol L^{-1} acetate/acetic buffer solution, pH 4, and UAE before application of the SPME procedure. Conventional external calibration using aqueous standards was used for the seawaters whilst a standard additions approach was required for the soils. The LOD values were in the 3–110 pg mL^{-1} and 0.9–4 ng g^{-1} ranges for seawater and soils, respectively. Ferrocene was only detected in one seawater sample and the amount detected was close to the lower LOD value of 3 pg mL^{-1}. Spike recoveries from seawater and soil, at 70 and 500 pg mL^{-1}, ranged between 99 and 102%. A method for separating Fe^{II} and Fe^{III} species from aqueous solutions using an iminodiacetic acid functionalised resin followed by detection with LIBS has been developed.[140] Solutions of either Fe^{II} and Fe^{III} were pumped into a vessel containing the resin and after optimisation of the flow rate, loading time and solution pH, the resin was extracted, ground and subjected to analysis by LIBS with 5 separate Fe emission lines being monitored. The optimal loading pH was found to be 4 for Fe^{II}, at which value no Fe^{III} was retained, and 1.7 for Fe^{III}. The method LOD values were 0.12 and 0.14 mg L^{-1} for Fe^{II} and Fe^{III}, respectively. These LOD values were too high for the quantification of any Fe present in a natural water sample but spike recoveries, at 6 mg L^{III} for each Fe specie, were 99 to 100%. The method needs further work to be of use for natural samples but may be applicable to polluted waters.

Three papers covered here report on *X-ray based methods for Fe speciation*. The first of these assesses the bioleaching of arsenopyrite, an iron arsenic sulfide, by the moderately thermoacidophilic strain *Sul fobacillus thermosulfidooxidans YN-22*.[81] A number of analytical techniques were used including As/S K- and Fe L-XANES, SR-XRD, and SEM, and FTIR and ICP-OES were also used in the determination of the leaching parameters. The results showed that the presence of bacteria significantly promoted the dissolution of arsenopyrite. The As and Fe in the bioleaching solutions mainly existed as As^{V} and Fe^{III}, whilst in the chemical leaching tests they were found mainly as As^{III} and Fe^{II}. The surface of the arsenopyrite was gradually corroded, and some secondary products were formed during bioleaching. In the sterile control experiment, the mineral surface was only slightly corroded, and only a few products were found after 10 days of chemical leaching. In the second paper Fe species were determined in the awns, bristle-like structures extending from the lemmas, in wheat (*Triticum aestivum* L.).[141] Compared to

 This journal is © The Royal Society of Chemistry 2021

awned cultivars, awnletted cultivars produce more grains per unit area and per spike, resulting in significant reduction in grain size. Nine awned and 11 awnletted cultivars were grown simultaneously and the samples harvested for analysis. The total Fe concentrations in the awned wheat ranged between 50.8 to 94 mg kg^{-1} whist the range for the awnletted wheat was found to be 67.3 to 103 mg kg^{-1}. Micro X-ray absorption near edge structure analysis of different tissues of frozen-hydrated grain cross-sections revealed that differences in total Fe concentration were not accompanied by differences in Fe speciation (Fe^{II} 36% and Fe^{III} 64%) or Fe ligands (53% were phytate and 47% were non-phytate ligands). However, a distinct tissue-specificity, with the pericarp containing the largest proportion (86%) of ferric species and the nucellar projection (49%) the smallest proportion was observed. The phytate ligand was predominant in the aleurone, scutellum and embryo (72%, 70%, and 56%, respectively), while the nucellar projection and pericarp contained only non-phytate ligands. If it is assumed that Fe bioavailability depends on the ligand Fe is bound to, the authors concluded that the bioaccessibility of Fe in wheat grain is tissue specific. The third paper in this analytical area presents experimental and theoretical X-ray emission spectroscopy (XES) data of the Fe K beta line for FeS and FeS_2.[142] In comparison to X-ray absorption spectroscopy (XAS), XES offers different discrimination capabilities for chemical speciation, depending on the valence states of the compounds probed and, more importantly in view of a broader, laboratory-based use, greater flexibility with respect to the excitation source used. The experimental Fe Kβ XES data were recorded using polychromatic X-ray radiation and a compact full-cylinder von Hamos spectrometer, with an energy window of up to 700 eV and a spectral resolving power ($E/\Delta E$) of 800, while subsequent calculations were made using OCEAN code. To validate the reliability of the OCEAN package for the two sample systems, near edge X-ray absorption fine structure measurements of the Fe K absorption edge were compared to theory using the same input parameters as in the case of the X-ray emission calculations. Based on the example of iron sulfide compounds, the combination of XES experiments and OCEAN calculations allowed the electronic structure of different transition metal sulfides to be assessed and qualifying XES investigations for the speciation of different compounds to be realised.

3.11 Lead

Once again there are few reports on *Pb speciation* in this review period, continuing the decline in of recent years. The speciation of ultra-trace organolead compounds at sub ng L^{-1} levels in environmental water samples has been reported by Yang *et al.*[143] An online SPE coupled HPLC-ICP-MS method was used. Graphene oxide bounded silica particles were utilised as the SPE adsorbent because of their superior performance over graphene bounded silica particles and commercial C_{18} packing materials. High enrichment factors (1603 for TML and 1376 for TEL) were obtained when Pb species in 10 mL sample were adsorbed by 1 mmol L^{-1} sodium dodecyl benzene sulfonate (SDBS) preconditioned graphene oxide bounded silica at 10 mL min^{-1} and then eluted by 5 μL of 5 mmol L^{-1} SDBS. The LOD values obtained were 0.018 ng L^{-1} for TML and 0.023 ng L^{-1} for TEL with RSDs below 5%. Separation of Pb^{II}, TML and TEL was achieved in 8 min using a mobile phase consisting of aqueous solutions of 5 mmol L^{-1} sodium 1-pentanesulfonate at pH 2.5, with and without 4 mmol L^{-1} TBAH. Recoveries from river water and tap water samples were between 93 and 106%. A sorbent based on 2,3-dimercapto-1-propanol immobilised on multi-wall carbon nanotubes has been developed for the separation and speciation of organic and iPB (alkyl-Pb, Pb^{2+}) in human blood, urine, and water samples by dispersive IL suspension-μSPE.[144] The Pb^{2+} was back-extracted from the sorbent/IL at pH 6.5 following ultrasonication and centrifugation with final measurement by atom trap AAS. The organic Pb was converted to Pb^{II} and the total Pb was then determined in the same way. Under optimal conditions, a linear range of 9.5 to 480 μg L^{-1}, LOD of 3.2 μg L^{-1} and enrichment factor of 10.4 were achieved (RSD <5%). The method was validated using CRM 1643d (trace elements in water), SRM 955 (caprine blood), and SRM 2668 (human freeze-dried urine). Lead species (Pb^{II}, TML and TEL) have also been included in a study of the simultaneously determination of As, Hg and Pd species in lotus seeds.[49] Using HPLC-ICP-MS, four arsenicals (As^{III}, DMA, MMA and As^{V}), four mercurials (Hg^{II}, MeHg, EtHg and PhHg) and the three lead compounds were simultaneously determined within 8 min with acceptable resolution. The LOD values for the Pb species were between 0.0076 and 0.14 μg L^{-1}.

3.12 Manganese

There are two reports of *Mn speciation in plant-derived materials by HPLC-ICP-MS*, in both of which results for the speciation of other elements were also given. Essential nutrient trace elements (Cu Fe, Mn and Zn) in coconut water were speciated by SEC- and HILIC-ICP-MS and HILIC-ESI-MS.[138] According to the researchers, coconut water (the juice found inside a young fruit of the palm tree *Cocos nucifera* that accounts for 25% of the mass), has become a popular beverage, known for its nutritional properties and a good source of fibre, vitamin C and several important minerals, especially K and Mn. To minimise species interconversion, sample preparation manipulations were confined to dilution with the chromatographic mobile phase and ultracentrifugation (which did not cause analyte loss). But, due to reported difficulties in sample preservation, several methods of storage were investigated, including freezing, cooling to 4 °C and the addition of ascorbic acid (as an antioxidant). The first two procedures were satisfactory, but ascorbic acid changed the speciation. Two chromatographic systems were used: (1) a Superdex-75 10/300 GL SEC column (separation range 3000 and 70 000 Da), with isocratic elution by ammonium acetate at pH 7.5, and (2) a Kinetex HILIC column (150 × 2.1 mm, 2.6 μm) with a Security Guard (2.1 mm × 3 μm) precolumn with a multi-step gradient elution program comprising ammonium acetate at pH 5.5 and ACN. The species identified were Fe complexes with citrate and malate ($Fe^{III}(Cit)_3Mal$, $Fe^{III}(Cit)_2(Mal)_2$ and $Fe^{III}(Mal)_2$), glutamine ($Fe^{III}(Glu)_2$), and nicotianamine ($Fe^{II}NA$); Cu complexes with

phenylamine ($Cu^{II}(Phe)_2$ and $Cu^{II}(Phe)_3$) and nicotianamine ($Cu^{II}NA$); Zn complexes with citrate ($Zn^{II}(Cit)_2$) and nicotianamine ($Zn^{II}(NA)$); and the Mn complex with asparagine ($Mn^{II}(Asp)_2$). Total element concentrations were measured and the contributions of the some of the species to the overall concentration of each elements were estimated. Ebrahim *et al.* determined Cr and Mn species in 14 plants traditionally used for anti-diabetes treatment by SEC-ICP-MS.[118] Analytes were separated on two columns connected in series: first a Toyopearl TSK HW 55S to separate in the 1 to 700 kDa mass range, followed by Toyopearl TSK HW 40S to separate masses of <2 kDa. The isocratic elution was with a mobile phase consisting of ammonium acetate, Tris, and MeOH, whose composition was based on previously published work (reference given) with a flow rate of 0.7 mL min^{-1}. Ammonia was used as a cell gas. Species were extracted by shaking in acidic hot water (pH 4, 80 °C) for 24 h, followed by centrifugation and filtration. The researchers also examined the extract fractions for Cr and concluded that there was no Cr-related health risk. For Mn, which was found in all SEC fractions with the exception of the 100–120 and 1.3–3.7 kDa mass ranges, they concluded that the dominant accessible species were bound to what they called the "inorganic protein fraction".

3.13 Mercury

The recent trend of an increase in the number of papers *reporting on Hg speciation* has been reversed this year. A reference method has been developed for the determination of Hg species in seafood by ss-HPLC-ICP-MS.[145] The procedure was then applied to a fish homogenate candidate RM and for the provision of the assigned values for the IAEA-476 interlaboratory comparison. After the addition of a ^{201}Hg enriched MeHg spike Hg species were extracted from homogenised seafood samples in 30 minutes, with 15% HCl and heating to 50 °C, followed by centrifugation, filtration, and dilution with H_2O prior to quantification by HPLC-ICP-MS. The separations were performed on a RP C_{18} column, with a mobile phase of 0.05% v/v 2-mercaptoethanol, 0.4% w/v L-cysteine, 0.06 mol L^{-1} ammonium acetate and 2% methanol flowing at 1 mL min^{-1}. Under these conditions iHg, which elutes first, and MeHg were separated in five minutes with a retention time (RT) difference of one minute between the two Hg species. This RT difference allowed complete baseline separation despite the well-known memory effect for Hg, which was negated due to the S ligand concentration in the mobile phase. The separation was more rapid with higher amounts of MeOH in the mobile phase, but plasma perturbation was observed as no O_2 was added to the plasma. Three isotopes, ^{200}Hg, ^{201}Hg, and ^{202}Hg, were monitored to allow for the calculation of two reference : spike isotope ratios to assess for the effect of polyatomic interferences, from *e.g.* WO, on the accuracy of the measurements. No interferences were observed using this approach as the mass fractions of MeHg calculated from each isotope ratio agreed within uncertainty limits. Mass bias correction was undertaken using the natural Hg isotope ratios from repeat injections of a MeHg standard and to different concentrations to account for natural Hg mass fraction variations in the seafood samples analysed. Total Hg content was also determined by IDMS after a MAE procedure. The LOD values obtained for iHg and MeHg (as Hg) were 0.15 ng kg^{-1} and 0.42 μg kg^{-1}, respectively with LOQ values of 0.22 ng kg^{-1} and 0.64 μg kg^{-1}, respectively. The estimation of an uncertainty budget was also undertaken. The main uncertainty source was the precision of the measured isotope ratios for MeHg in the sample extracts and mass bias correction solutions and the relative expanded uncertainty was <4%. The LDR of the protocol for MeHg contents in seafood products was found to be from 5 μg kg^{-1} to over 530 μg kg^{-1}. The results obtained for MeHg in three CRMs, IAEA-461 (clam), IAEA-470 (oyster) and IAEA-476 (fish homogenate) were all within 4.2% of the certified values. The method was then applied to further seafood samples and also to MeHg measurements in marine sediment samples using a selective extraction.[146] For this, sediment samples were spiked with both a ^{202}Hg and ^{201}Hg MeHg spike, H_2SO_4 (0.9 mol L^{-1}), KBr (1.3 mol L^{-1}), $CuSO_4$ (1.0 mol L^{-1}) and $CHCl_2$ added and the mixture allowed to equilibrate for 30 minutes. This was then followed by vortex mixing, 45 minutes, centrifugation, removal of a portion of the organic phase and back extraction of the Hg species in to $Na_2S_2O_3$ (0.1 mmol L^{-1}). Recovery of iHg and MeHg from CRM IAEA-461 clam was >98% for both Hg species and for the IAEA-475 sediment candidate CRM the found mass fractions for iHg and MeHg, 30.1 ± 1.6 μg kg^{-1} and 196 ± 8 ng kg^{-1}, respectively were within 1.5% of the consensus value from the IAEA certification campaign. There is a wealth of information in these two papers, and they are recommended reading for workers in this field or more generally for the detailed approach undertaken towards method validation. A different group of workers have also reported on a conventional external calibration based method for the quantification of Hg species in fishery products.[147] In this procedure Hg species were extracted from fresh or freeze dried samples with a mixture of L-cysteine, HCl and H_2O and MAE at 60 °C for 15 minutes. The exact composition of the extraction mixture, and the HPLC mobile phase, is difficult to determine from the report. A RP 'peptide mapping' HPLC column of 150 mm length, with a mobile phase of 5% MeOH, 95% L-cysteine, HCl and H_2O at a pH of 2.3, was used to separate the Hg species in 3 minutes. The authors state that baseline resolution was obtained but, as no chromatogram is presented, it is not possible to assess the degree of separation or indeed the elution order. An attempt was made to use EtHg as an internal standard, but it was found that this compound degraded to iHg and MeHg during the HPLC process and therefore work in this direction was not continued with. The focus of the paper is on method validation using an accuracy approach. It was found that, for seven measurement series in duplicate on seven different days, over 2-month period by two different operators, the measurement bias ranged from −0.2 to 2%, repeatability varied from 1.5 to 8.3%, and the LOQ was 3.2 μg kg^{-1} (wet weight). The recovery of MeHg from three CRMs, ERM CE-464, DOLT-5 and TORT-3, was 92% or better and Z-scores from three different FAPAS RMs were −0.4 or better. The method was subsequently applied to fresh and tinned fish products and iHg ranged from 0.13 to 0.85 mg kg^{-1} and MeHg from 0.11 to

This journal is © The Royal Society of Chemistry 2021

0.79 mg kg^{-1} with the MeHg content being about 80 to 90% of the total Hg present.

The *generation of a Hg vapour* is often used to either improve sensitivity for detection by ICP-MS or for direct analysis using AFS. One such report details the use of a 10 mg L^{-1} Fe^{3+} solution, dissolved in 10% v/v HCl and continuously pumped into the gas liquid separator along with a flow of 0.5% w/v KBH_4 in a 0.2% m/v KOH solution and the HPLC eluent, to catalytically oxidise organoHg species to Hg^{2+} before these were reduced to Hg^0.[148] A previously reported UAE based method was used to extract Hg species from CRMs and fish tissue samples and these species were subsequently separated using RP HPLC. The mobile phase for this was A: 0.5 g L^{-1} L-cysteine and 0.06 mol L^{-1} ammonium acetate and B: 5% v/v acetonitrile, 0.01% mercaptoethanol, and 0.06 mol L^{-1} ammonium acetate in a gradient elution flowing at 1 mL^{-1}. Under these conditions three Hg species, iHg EtHg and MeHg were eluted in 12 minutes although the chromatography looks as if it need improvement as two of the peaks, probably iHg and MeHg although no peak identities are given, are barley baseline resolved. The LOD values for the method were reported as 0.13, 0.06 and 0.09 μg L^{-1} for iHg, MeHg and EtHg, respectively with a LDR of 0.3 to 500 μg L^{-1}. Recoveries of MeHg from two CRMs, DORM-4 and TORT-3, were 101 and 103%, respectively. The developed method was compared with a HPLC-UV-CV-AFS method and no differences in the fluorescence intensities, within uncertainty limits, were observed between the two methods. The use of Cu^{2+} as a catalyst was also investigated, and the fluorescence intensities for both organoHg species were about half of those obtained when Fe^{3+} was the catalyst used. There is a considerable amount of optimisation data in the paper and this work shows another alternative to the use of Mn based oxidants in this type of work although the simplest set-ups seem to be tending towards UV based oxidation in the presence of low molecular mass organic acids.

Speciation analysis is often applied to foodstuffs and the quantification of *Hg species in wild mushrooms* has been reported on ref. 149. The Hg species were extracted from dried mushrooms with a 12 g L^{-1} L-cysteine solution and UAE for 40 min at 40 °C followed by centrifugation and filtration before injection on to an HPLC-ICP-MS system. The Hg species, iHg, MeHg, EtHg and PhHg, were gradient eluted from a C8 column with a mobile phase of (A) methanol and (B) 10 mmol L^{-1} ammonium acetate and 0.8 g L^{-1} L-cysteine at pH 4 flowing at 1.2 mL min^{-1} in 11 minutes. Full details of optimisation of the extraction procedure and mobile phase are given in the paper and it is worth reading for insights into signal suppression due to organic mobile phase content for example. The LOD and LOQ values of the method ranged between 0.6–4.5 μg kg^{-1} and 2.0–15 μg kg^{-1}, respectively. As no mushroom CRM certified for Hg species is available a fish tissue CRM, GBW 10029, was used for this purpose and the recoveries for both MeHg and THg were greater than 98%. Spike recoveries from *Boletus edulis*, of all four Hg species analysed for, ranged from 93 to 104%. Seven different mushroom species were then subjected to the developed and validated method and the THg content ranged from 0.13 to 7.5 mg kg^{-1}. The main Hg species in the mushrooms was found to be iHg, ranging from 0.12 to 6.1 mg kg^{-1} whilst MeHg was only detected in a few samples (0.01–0.1 mg kg^{-1}). For most samples the sum of the Hg species content matched the total Hg content to within a few percent.

There are numerous studies looking at *Hg species in blood* and a further method on this topic has been described.[150] Human whole blood samples (0.2 mL) were placed in 1.5 mL polypropylene test tubes and mixed with 0.02 mL of a solution containing 1 ng mL^{-1} of ^{196}Hg as an internal standard for iHg. This mixture was incubated at 37 °C with gentle shaking (100 rpm) for 5 min. After incubation, 0.25 mL of 7% v/v HCl solution containing 1.5% w/v L-cysteine and 50 ng mL^{-1} of Tl as an internal standard for MeHg was added, and the solution was mixed briefly using a vortex mixer. Then, the samples were subjected to UAE for 20 min centrifuged at 4 °C and the supernatant with a 10% w/v trichloroacetic acid solution to remove proteins, mixed briefly using a vortex mixer, centrifuged at 4 °C and filtered. Calibration standards were prepared in the same way after adding the Hg species to whole rabbit blood. The extracted Hg species were separated on C_{18} column, with 5% v/v methanol, 0.1% v/v 2-mercaptoethanol, and 0.018% v/v hydrochloric acid as the mobile phase flowing at 1 mL min^{-1}. The HPLC eluent was directed to a gas/liquid separator, where the hydride form of iHg and MeHg was produced using $NaBH_4$, and these were swept to the ICP-MS detector. The Hg species were separated in nine minutes with good baseline resolution in the order MeHg then iHg. The method LOD values were 0.04 ng mL^{-1} (MeHg) and 0.02 ng mL^{-1} (I–Hg), the linear ranges were 0.08–60 ng mL^{-1} for MeHg and 0.05–2.5 ng mL^{-1} for I–Hg. And the internal standard recoveries were 95% and 80% for Tl and ^{196}Hg. For MeHg, the intra- and inter-day precisions (coefficient of variation, %) ranged from 1.3% to 10.2% and the accuracy varied between 90.8% and 98.7%. For I–Hg, the intra- and inter-day precisions ranged from 0.0% to 10.1% and the accuracy was between 93.3% and 102.6%. Recoveries from Seronorm L1 were better than 97% for both Hg species. The results were also within 10% of those obtained using a MeHg in blood by dithizone extraction/GC-ECD method. Upon application of the method to 20 human blood samples the average concentrations of MeHg and I–Hg were 1.85 ng mL^{-1} and 0.18 ng mL^{-1}, respectively which is generally similar to those reported in the literature.

Three papers report on *multi-element speciation methods involving Hg* this year. The simultaneous speciation analysis of As^V, As^{III}, AB, DMA, MMA and MeHg in edible oil by HPLC-ICP-MS has been reported.[55] A RP C_{18} ODS column was used for the separation, with a single mobile phase containing 5 mmol L^{-1} sodium 1-butanesulfonate, 2 mmol L^{-1} $NH_4H_2PO_4$, 4 mmol L^{-1} TMAH, 5 mmol L^{-1} L-cysteine, and 0.1% methanol (pH 2.3). Under these conditions eight water-soluble As species eluted between 160 to 390 s, and iHg, MeHg, EtHg and PhHg eluted at 300, 700, 1600 and 2100 s, respectively. As these latter two Hg species are unlikely to be found in the samples under test the chromatographic run was stopped at 900 s thereafter. The LOD values for iAs and MeHg were 0.05 ng g^{-1} as As and 0.09 ng g^{-1} as Hg, respectively. The simultaneous extraction from the edible oil was achieved using 2% w/w TMAH solution at 80 °C for one

hour. The proposed method was also applied to several CRMs (NMIJ CRM 7402-a cod fish tissue, NMIJ CRM 7503-a white rice flour, NMIJ CRM 7533-a brown rice flour, and NMIJ CRM 7405-a hijiki seaweed) and recoveries ranged from 96 to 103%. Finally, five types of edible oil were analysed (fish liver oil, krill oil, whale oil, whale fat and sardine oil). The iAs and MeHg were in the concentration range from 0.001 mg kg^{-1} to 0.010 mg kg^{-1} and from 1.21 ng g^{-1} to 10.18 ng g^{-1}, respectively. All of the iAs was found as As^{V}, DMA was found in all of the samples, and MMA and AB at low levels in three of the samples. For Hg the sum of the species was found to agree with the total Hg content. A method has also been reported for the simultaneous determination of As^{III}, As^{V}, DMA, MMA, Hg^{II}, MeHg, EtHg and PhHg, Pb^{II}, TML and TEL, which were separated and analysed within 8 minutes.[49] The resolution using a 15 cm Diamonsil C_{18} column (4.6 mm i.d. × 5 μm) was reasonable, although the composition of the mobile phase proved critical for separation of the species. Various mobile phase compositions were evaluated and 2 mmol L^{-1} TBAH + 20 mmol L^{-1} Cys + 1 mmol L^{-1} Na 1-pentanesulfonate at pH 5.0 offered promising results. The method offered LOD values from 0.036 to 0.20 μg L^{-1} for As-species, from 0.023 to 0.041 μg L^{-1} for Hg-species, and from 0.0076 to 0.14 μg L^{-1} for Pb-species. The method was applied to speciation measurements of the above species in five lotus seed samples, indicating the presence of DMA (19.6 to 28.2 μg kg^{-1}), TML (1.4 to 2.9 μg kg^{-1}), MeHg (1.2 to 4.8 μg kg^{-1}) and EtHg (0.8 to 2.2 μg kg^{-1}). Parallel methods have been developed for the determination of Hg and Sn species in red wine (see Section 3.23 for details of the Sn method).[151] The MeHg quantification was by ID-GC-ICP-MS, using a ^{201}Hg enriched MeHg spike. The spike was added directly to the wine samples followed *in situ* ethylation, at pH 4.5, with $NaBEt_4$ (1%, w/v final concentration) vigorous mixing for 20 min, extraction into isooctane and recovery of the organic layer. The LOD and LOQ values for MeHg were found to be 0.03 and 0.1 μg Hg L^{-1}, with spike recoveries of 104 to 112% and a measurement uncertainty of 4.7% relative and of the 122 wine samples analysed all had MeHg concentrations <LOD whilst total Hg was detected in 85 samples and ranged between 0.1 to 0.6 μg L^{-1}. Table 3 shows examples of other applications of Hg speciation presented in the literature during the time period covered by this ASU.

3.14 Nickel

An analytical procedure based on the use of off-line and on-line 2D chromatography (SEC × RP) coupled to ICP-MS/MS was developed to *simultaneously determine Ni, S and V compounds in petroleum products.*[159] The first part of the work is devoted to the selection of appropriate conditions for the first and second dimensions, in both off- and on-line modes. In SEC × RPLC, an Acquity APCXT125 (150 × 4.6 mm, 2.5 μm) column and an Acquity BEHC18 (50 × 2.1 mm, 1.7 μm) column were used in the first (1D) and second (2D) dimensions, respectively. The column temperature was set at 30 °C in both dimensions. The 1D mobile phase was THF while the 2D mobile phase consisted of (a) ACN/H_2O, 80/20 v/v, and (b) THF under gradient elution. Both off-line and on-line 2D LC separations were compared using a pareto-optimality approach with the aim of maximising the peak capacity while minimising the dilution factor in a given analysis time. The best 2D-conditions in term of peak capacity were found in off-line SEC-RP-LC. Additionally, the use of ICP-MS/MS, with oxygen as reaction gas to negate interferences and or enhance sensitivity; ^{51}V was shifted to mass 67 ($^{67}VO^+$) and ^{32}S to mass 48 ($^{48}SO^+$) whilst Ni was analysed at $m/z = 58$ (58Ni$^+$). The O_2 flow rate was fixed at 0.3 mL min^{-1} for the analysis of the three elements within one single run. Asphaltenes (the heaviest fraction of crude oils) were separated by the developed off-line SEC × RPLC method. The results evidenced that heavy mass compounds are not well separated in SEC whereas they are partly separated in RP making the combination of both techniques of great interest. This 2D method hyphenated to ICP-MS/MS allowed the authors to speciate of Ni, S and V containing asphaltenes within a single run.

3.15 Phosphorus

One of the significant advantages of ICP-MS/MS compared to ICP-MS is that the mass analyser configuration can improve the LOD/LOQ for elements with significant polyatomic interferences. One such example is *^{31}P, a mono-isotopic element which suffers significant interferences from the highly abundant polyatomic ions formed from O, N and H in the plasma*. Commonly O_2 is used as the reaction gas, Q1 is set to m/z 31 to allow for the transmission of the stable isotope of P and the product ion $^{31}P^{16}O^+$ produced in the cell is selected by Q3, which is set to m/z 47. The heteroatom P is present in a number of important compounds, in particular as phosphodiester bonds, which are central to all life on Earth as they make up the backbone of the strands of nucleic acid. This element features in oligonucleotides, nucleosides, as well as many other industrial chemicals such as the herbicide glyphosate and its primary degradation products. Examples of the application of ICP-MS/MS detection to the speciation of P-containing compounds have been published in this review period.

The use of *HPLC coupled to ICP-MS/MS for the simultaneous and direct determination of the herbicide glyphosate and its primary degradation product, aminomethylphosphonic acid (AMPA)* in water samples from artesian wells, dams, water springs and cisterns has been reported on ref. 160. The separation was carried out using standard HPLC conditions including: a C_8 column (Zorbax SB-C_8, 4.6 × 150 mm, 5 μm); an injection volume of 50 μL; a mobile phase composed of 50 mmol L^{-1} acetic acid/ammonium acetate solution, 5 mmol L^{-1} tetrabutylammonium, 1% (v/v) methanol at pH 4.7, and isocratic elution at 1.0 mL min^{-1}. The lack of a suitable chromophore in these types of molecules mean that the conventional detection method, HPLC-DAD, requires derivatisation of the analytes to add a suitable group to make them amenable to spectrophotometric detection. Derivatisation is still considered the main sample preparation disadvantage, since this procedure increases the number of sample preparation steps, requires expensive reagent use and may cause analyte loss when reaction efficiency is low. In addition, all these factors may contribute to an increase in imprecision and cost of analysis.

 This journal is © The Royal Society of Chemistry 2021

Table 3 Applications of speciation analysis: Hg

Analyte species	Technique	Matrix	Sample treatment	Separation	LOD	Validation	Reference
Total Hg, (THg), organoHg (OHg)	CV-AAS	Plants, soils	Plants: THg; acidic BrCl. OHg; KOH, CH_2Cl_2, H_2O, ethylation. Soils: THg; aqua regia, H_2O, BrCl, $KBrO_3$. OHg; $CuSO_4$, HNO3, CH_2Cl_2, H_2O, ethylation	Selective extraction	THg 6 ng g^{-1} and OHg 0.003 ng g^{-1}	THg: GBW07405 101–121% recovery. GBW10020 96–107% recovery OHg: ERM-CC580 83–106% recovery. ERM-464CE 95–101% recovery	152
Total Hg, organoHg	ET-OES	Fish, mushroom, sediment	Adapted JRC IRMM Technical Report – Determination of Methylmercury In Seafood By Elemental Mercury Analyser	Selective extraction	THg 7.0 μg kg^{-1}, OHg 3.5 μg kg^{-1}	BCR463, ERM-CE464, TORT-2, NIST SRM2976, CS-M-3 Boletus edulis, ERM-CC580. Recoveries 95–104%	153
iHg, EtHg, MeHg	GC-CV-AFS	Blood, dried blood spots (DBS)	Hg species extracted with 25% HNO_3, 0.02% L-cysteine, 60 °C, 24 h, ethylation	Not given	Blood: iHg 1.1 μg L^{-1} MeHg 0.2 μg L^{-1} DBS: iHg 1.9 μg L^{-1} MeHg 0.3 μg L^{-1}	PC-B-M1510 RM 93–128% recovery	154
organoHg	CV-AFS, SEC-ICP-MS,	Mammary cells	MAE, 1000 W, 110 °C, 10 min, 30% HCl and toluene	SDS-PAGE. SEC: BioSep-S-2000, 0.01 mol L^{-1} PBS, pH 6.8	None given	None used	155
iHg, MeHg	GC-ICP-MS, LA-ICP-MS	Glass eels	Exposed to $i^{199}Hg$ and $Me^{201}Hg$. Freeze dried, MAE, tissues sectioned	Not given, cited reference	Not given	Not given	156
MeHg	GC-ICP-MS	Hair	Not given ISO17025 laboratory used	Not given, cited reference	Not given	IAEA-085 used, no results given	157
HgS, HgO, Hg^0, $HgCl_2$	CV-AFS, HPLC-ICP-MS	Sand, soil	None for thermal desorption. Sequential extraction scheme prior to HPLC-ICP-MS	CV-AFS: Selective thermal desorption. HPLC: RP. Mobile phase 0.06 mol L^{-1} $NH_4CH_3CO_2$, 5% MeOH and 0.1% $HOCH_2CH_2SH$, pH 6.8	CV-AFS: 30 μg kg^{-1} HPLC-ICP-MS not given	None given	158

The advantages of using ICP-MS/MS as an HPLC detector, rather than DAD, were investigated and resulted in a LOD of 8.2 μg L^{-1} compared to that for the conventional DAD detection approach of 300 μg L^{-1}. This method was further developed for the simultaneous and direct determination of glyphosate and AMPA in water samples from the hydroponic cultivation of eucalyptus seedlings using HPLC-ICP-MS/MS. In a second paper the same method was employed to investigate the levels of herbicide in botanical and hydroponic samples, with the aim of establishing a method that was appropriate for use at the Brazilian maximum residue limit for glyphosate in drinking water of 65 μg L^{-1}.[161] This required SPE of the glyphosate and AMPA using an AE resin (3 g) with an active quaternary ammonium functional group, particle size of 600–750 μm and packed into a glass column (20 cm × 1.5 cm id). Spiked and unspiked samples were applied to the resin at a flow rate of 1.0 mL min^{-1} and the analytes eluted off with HCl (6 mol L^{-1}). The collected eluate containing the target analytes was completely evaporated under continuous airflow heating at 60 °C and the residue was re-suspended using the mobile phase. The percentage recovery ±RSD% values were 103.9 ± 7.9 and 99.4 ± 9.9, with a LOQ of 1.09 and 0.29 μg L^{-1} for glyphosate and AMPA, respectively. One noticeable difference to the earlier work looking at water, was a significant baseline P signal of 100 000 cps in the chromatograms for the herbicide applied to eucalyptus seedlings, which would hamper measurements at the lower level and may imply that the ICP-MS/MS reaction cell parameters require further optimisation to reduce the background and allow for a lower signal baseline.

3.16 Platinum

A paper on the *use of monolithic chromatography utilising convective interaction media (CIM) disks* for Pt-drug speciation in human samples investigated the cisplatin, carboplatin and oxaliplatin protein-adducts formed in spiked and real human

serum samples from patients being treated for cancer.[162] This followed on from work covered in last year's Elemental Speciation ASU[1] for the speciation of carboplatin-protein adducts in spiked serum. The same affinity protein G and weak anion exchange diethylamine (DEAE) disks were used in series, highlighting the applicability of this approach for the investigation of a range of Pt-drugs with different chemical properties. The separated serum proteins were detected on-line by UV and the Pt-containing species by ICP-MS. Quantification of the drug–protein adduct species formed with Tf, HSA and IgG were determined using ID-ICP-MS and a ^{194}Pt enriched spike added post column. Column recoveries, calculated as a ratio between the sum of concentrations of Pt species eluted and concentration of total Pt in serum samples, were close to 100%. The advantages of this approach centre around the ability to facilitate the use of multi-column chemistry separations easily and on a suitable scale to provide excellent resolution and runtimes. The CIM system can also be easily coupled to elemental detection and the flow rate requirements of both systems are compatible.

3.17 Selenium

One *review has appeared this year on Se speciation in plant foods*.[163] The first part of the review is dedicated to a description of the techniques and sample treatment methods applied to carry out Se speciation in plant tissues. The second section is devoted to the characterisation of Se species and their bioaccessibility in Se-biofortified plants. Special attention is paid to the effect of Se treatment on chemical composition and antioxidant properties of plants. The review inc1udes 150 references.

The interest in *evaluating Se nanoparticles in environmental and biological* samples is ongoing. The phytotoxicity, accumulation, and transformation of Se^{IV}, Se^{VI} and SeNPs was evaluated in Se-enriched garlic by XANES spectroscopy.[164] Garlic seedlings were grown in a hydroponic system containing Se^{IV}, Se^{V} or SeNPs (40 nm diameter) at concentration levels ranging from 0.01 to 50 mg L^{-1} for one month. The phytotoxicity of the different Se chemical forms was assessed by the biomass (dry weight) of garlic seedlings of each group whilst the spatial distribution of Se in the roots was imaged using SR-μXRF. The chemical forms of Se in different plant tissues was assessed using SR-XAS. The study demonstrated that toxicity of the administered Se species was $Se^{VI} > Se^{IV} >$ SeNPs. The SR-μXRF and SR-XAS results showed that SeNPs and Se^{IV} were mainly accumulated in roots and easily transformed to organic species such as MeSeCys and SeCys whereas Se^{VI} was relatively stable but easily translocated from root to leaf which correlates with the greater toxicity of this Se specie. Due to the lack of information on the impact of SeNPs in the environment, the work opens new insights into the metabolisms of SeNPs in plant ecosystems.

Selenium *speciation in supplements and metabolism in plants and animals remains of research interest*. In this line, the use of AF^4-ICP-MS is presented for first time for the determination of SeMet in selenised yeast.[165] Selenium was released from samples by using different sample treatment protocols including: extraction with; 4 mol L^{-1} methane sulfonic acid with and without reflux, formic acid, alkaline extraction using SDS, water and UAE (both probe and bath) with water. In order to achieve complete recoveries, the AF^4 membrane pore size and interactions between analyte and membrane were taken into consideration. Separation with the AF^4 system was achieved by using a 350 mm spacer in an asymmetrical channel, regenerated cellulose (RC) separation membranes with different pore sizes (5, 10 or 500 kDa) and 0.05% v/v solution of SDS as the mobile phase. The alkaline extraction with SDS and the 5 and 10 kDa AF^4 separation membranes provided the best recovery/determination conditions for SeMet based on analysis of NRCC CRM SELM-1 as it minimised hydrolysis of the protein peptide bonds optimally required for the AF^4 separation. Under these conditions the SeMet concentration found was in agreement with the certified value (3190 ± 290 mg kg^{-1}). A LOD value of 0.49 μg per Se per L was obtained for SeMet. The accuracy of the proposed method was further evaluated by the determination of SeMet in several commercial Se supplements. The results, using AF^4-ICP-MS were compared with those found when using HPLC-ICP-MS and there was no statistical difference was observed between the two methods. The authors highlighted the advantages of AF^4-ICP-MS for Se speciation studies that included: fast analysis, low solvent consumption and the longer lifetime of AF^4 membranes over chromatographic columns. In an interesting paper Takahashi *et al.* studied the effect of gut microflora on the nutritional availability of Se, in particular of 9 Se species: Se^{IV}, Se^{VI}, SeMet, MeSeCys, $SeCN^{-}$, TMSe, $SeSug_1$, SeHLan and $SeCys_2$.[166] Experiments were performed in microflora-suppressed and healthy rats which were fed with a Se-deficient diet and divided into 2 groups. The former group were treated with 50 mg per kg per day each, of neomycin, metronidazole and vancomycin, and 100 mg per kg per day of ampicillin from day 3 prior to Se administration whilst the healthy rats were not treated with these antibiotics. The rats were then orally treated with 10 μg of Se from each of the Se compounds dissolved in saline once a day for 2 consecutive days. Rat serum was analysed by HPLC-ICP-MS by using a SEC (Shodex GS-520HQ, exclusion size >300 000 Da, 7.5 i.d. $\times$ 300 mm) column with a mobile phase of 50 mmol L^{-1} Tris–HCl, pH 7.4, at a flow rate of 0.6 mL min^{-1}. The eluate was introduced directly into the nebuliser of the ICP-MS instrument to detect Se at 77 and 82 *m*/*z*. Data obtained revealed that MetSeCys, SeCN and SeSug1 were transformed to SeMet by intestinal microflora, demonstrating the relevant role of the intestinal microflora in improving the nutritional availability of selenocompounds. The different Se species in Se-enriched kale and kohlrabi sprouts was assessed by AEC-ICP-MS.[167] Kale and Kohlrabi seeds were immersed in mineral water (controls) or in the same water containing three different Se concentrations (Na_2SeO_3 at 10, 15 and 30 mg L^{-1} as Se) for 3 h. The seeds were then grown for 6 days and the resulting sprouts collected followed by aqueous extraction and enzymatic hydrolysis with Pronase was used to release Se compounds. For the separation and detection of the Se species a Hamilton PRP-X100 (20 mm length $\times$ 2.1 mm i.d., 10 μm) column coupled to ICP-MS was

employed with a mobile phase composed of 20 mmol L^{-1} acetic acid/10 mmol L^{-1} triethylamine (A) and 200 mmol L^{-1} acetic acid/100 mmol L^{-1} triethylamine (B) under gradient elution. The main organic Se species found in both aqueous and proteolytic extracts of the Se-enriched sprouts were SeMet and MeSeCys. Interestingly, Se fortification stimulated the production of phenolic acids (sinapic, chlorogenic, isochlorogenic and caffeic) in the tested sprouts. A PCA analysis revealed strong correlation between antioxidant parameters, the phenolic acids and L-tryptophan, while Se correlated only with caffeic acid. Moreover, cytotoxic activity of the Se-enriched sprout extracts was evaluated using different cell lines: SW 480 Duke's type B primary colorectal adenocarcinoma, SW 620 Duke's type C colorectal adenocarcinoma derived from lymph node as metastatic site, HepG2 hepatocellular carcinoma and SiHa cervical carcinoma cells. A significant decrease in the viability (MTT assay) of SW480 and SW620 colorectal adenocarcinoma cells, differing in metastatic potential, was detected. The authors postulated that Se-enriched kale and Kohlrabi sprout extract could be used as ingredients in functional foods and as promising candidates in the chemoprevention of colon cancer. The capability of hemp (*Cannabis sativa* L.) plants, collected from seleniferous rural areas of the USA, to accumulate Se was studied.[168] Seeds of those plants were cultured in presence of increasing concentrations of Se^{VI} (0, 40, 80, 160, and 320 μmol L^{-1}) under controlled conditions. Synchrotron X-ray fluorescence and X-ray absorption spectroscopies of selenate-supplied hemp showed Se to accumulate mainly in the leaf vasculature and in the seed embryos, with predominant Se speciation in C–Se–C forms (57–75% in leaf and more than 86% in seeds). Analysis of aqueous seed extracts by LC-MS revealed the presence of SeMet and MeSeCys. According to biomass production data, hemp was quite tolerant to Se as it was not affected at exposures of up to 80 μmol L^{-1} Se. The presence of Se did not alter the production of cannabidiol and terpenoids.

With respect to *animal studies*, Se speciation in turkey liver samples from a controlled feeding study was carried out by Bierla *et al.*[169] For this purpose Se-deficient, Se-adequate, and high-Se liver, turkey poults were fed with a diet containing Na_2SeO_3 (Se^{IV}) (0, 0.4, and 5 μg per Se per g for 28 days). Extraction of SeCys, SeMet and Se^{IV} from the resulting samples was achieved by employing enzymatic hydrolysis with protease. As Se-Cys residues are highly reactive a reduction with dithiothreitol (DDT) followed by with iodoacetamide (IAM) was applied before enzymatic hydrolysis (10 mg protease XIV in 0.1 mol L^{-1} Tris buffer at pH 7.5). The Se species were analysed for by HPLC-ICP-MS and HPLC-ES-MS/MS with two columns (C-8 Alltima and C-18 Acclaim RSLC 120) being used. Water-soluble liver Se species were extracted for size-exclusion chromatography, resulting in recovery of 33, 39.9 and 45.5% for the Se in 0, 0.4, and 5 μg per Se per g diets, respectively. Separation of the aqueous extracts was performed by SEC by using an Acquity UHPLC BEH size-exclusion 125 Å column. Analysis by HPLC-ES-MS/MS for low MW species detected the presence of 8 seleno-compounds with masses between 300 and 1000 Da. No SeMet was detected in the livers of turkeys fed either the Se-deficient diet or supplemented with inorganic Se whilst SeCys was also below the LOD in Se-deficient diet liver but double the concentration in high Se liver as compared to Se-adequate liver. Low molecular weight selenometabolites: glutathione-, cysteine- and methyl-conjugates of the selenosugar, selenonacetylgalactosamine (SeGalNac) increased in the high Se diet livers whilst Se in Se-adequate diet livers was present as selenosugars decorating general proteins *via* mixed-disulfide bonds. In high-Se diet livers, these "selenosugar-decorated" proteins comprised ~50% of the Se in the water-soluble fraction, in addition to low MW selenometabolites. All selenometabolites detected led to the formation of methyl-SeGalNac, the urinary Se excretion species.

The detection of *selenospecies in biological samples is also of interest due to the beneficial effects of selenocompounds*. Speciation of 11 Se species in urine was performed by HPLC-ICP-MS using three chromatographic separation protocols.[170] Seven Se species, MeSeCys, SeMet, MeSeA, $SeSug_1$, SeEt, $SeSug_2$ and MeSeG, were separated using a Phenomenex Luna C_{18} (150 × 4, 6 mm; 3 μm) RP column and a mixture of 4 mmol L^{-1} malonic acid and 0.1% methanol (pH 2.7) as mobile phase. Inorganic Se (Se^{IV} and Se^{VI}) was separated on a Hamilton PRP-X100 (150 × 4.6 mm; 5 μm) column with 10 mmol L^{-1} oxalate and 2% MeOH, 1% formic acid, pH 5.1 as the mobile phase. Finally, TMSe and $SeSug_3$ were separated by using a Shodex RSpak NN-614 (150 × 6 mm, 10 μm) column, at 50 °C, with 30 mmol L^{-1} $NH_3H_2PO_4$, 1% EtOH (pH 6.3) as the mobile phase. The developed procedures enabled the sensitive determination of these species with LOD values between 0.03 and 0.10 μg per Se per L. For TMSe a LOD of 0.02 μg per Se per L was reported. Recovery studies, from spiked human urine, ranged from 87 to 107%. Although Se is mainly excreted in urine, it has been reported that an unknown Se metabolite is excreted in bile and Takahashi *et al.* applied HPLC-ICP-MS and LC-ES-Q/TOF to identify this unknown compound.[171] Bile was collected from rats 10 min after an intravenous injection of 0.2 mL of Se^{IV}, SeMet or SeCN in saline at 50 mg per Se per mL. The collected bile was subjected to Se speciation by HPLC-ICP-MS/MS. Two separation columns were applied: size exclusion (Shodex GS-520HQ, exclusion size >300 000 Da) or RP (Zorbax Stable Bond column (SB-Aq), 4.6 mm i.d. × 250 mm). The columns were eluted with 50 m mol L^{-1} Tris–HCl, pH 7.4, at a flow rate of 0.6 mL min^{-1} or with 25 mmol L^{-1} NH_4Ac, 1.0 mmol L^{-1} TBAH, pH 5.2, and 2.5% v/v methanol at a flow rate of 1.0 mL min^{-1}, respectively. The eluate was introduced directly into the nebuliser of the ICP-MS/MS to detect Se at *m*/*z* 94 and 96 in O_2 mass shift mode. A major peak was detected at a retention time of 16.9 min by SEC from rats administered with Se^{IV} whilst a major peak was detected at a retention time of 36.5 min by RP chromatography. These retention times differed from the retention time of Se^{IV} suggesting that this had been metabolised secreted in bile. When the rats were administered SeCN or SeMet, the selenometabolite had the same retention time as the selenometabolite in bile of rats administered with Se^{IV} on either column. Subsequently, the common biliary selenometabolite was identified as selenodiglutathione (GSSeSG) by LC-ES-Q/TOF. A paper describes for the first time the presence of selenoprotein P (SelP) in human breast milk by using an HPLC

column switching method coupled to ICP-MS.[172] This was achieved by stacking two 5 mL HiTrap® desalting columns (SEC, bed size: 16 mm × 25 mm, ID: 16 mm), connected by means of a six-way valve, to another 5-mL HiTrap® desalting column followed by a 1 mL heparin-sepharose column (HEP-HP, bed size: 7 × 25 mm, column ID: 7 mm). Several selenopeptides which contain SeCys were identified after tryptic acid digestion followed by their separation. Quantification was performed by post-column ID-ICP-MS with a ^{74}Se spike isotope. The identification of SelP was performed by UHPLC-QTOF. The HPLC column switching method allowed the absolute quantification of GPX3, SelP, selenocystamine (SeCA) and other selenometabolites (SeMB), and for the first time the identification of SelP in human breast milk. A mean concentration of 20.1 ± 1.0 ng per Se per g as SelP was determined in colostrum (31% of total Se). The same experimental set up was also reported by the authors in another paper for the determination of selenometabolites and selenoproteins in serum taken from lung cancer patients.[173] Additionally, a method based on the AEC-ICP-MS (Hamilton PRP-X100) was also applied to separate and quantify $SeCys_2$, MeSeCys, SeMet, Se^{IV} and Se^{VI}. The results showed that the amount of Se species (eGPx, SeAlb and Se^{IV}) was significantly higher in serum from lung cancer patients than from a control group. Moreover, the selenoprotein : selenometabolite ratio was calculated for first time in order to be used for potential biomarkers in lung cancer. Rates of eGPx : SelP, SelP : SeAlb, eGPx : Se^{IV} and SelP : Se^{IV} were significantly different between lung cancer patients and control group. Selenium speciation analysis has been also performed in cerebrospinal fluid of patients with Parkinson's disease.[174] Samples from 75 patients were collected and subjected to ICP-MS for total Se determination and ion exchange chromatography (AS14 analytical column (250 × 4 mm ID) hyphenated to ICP-MS for Se speciation analysis. Different Se species were detected but only SelP, human serum albumin–Se (Se-HSA), SeMet and unidentified Se-compounds were above the LOQ. No significant differences in Se species were detected between Parkinson's patients and control groups. Although the study offered new insights into the role of Se in Parkinson's disease, selenoproteins were not useful as diagnostic biomarkers for clinical applications.

Finally, a novel method based on a sequential derivatisation and extraction combined with GC-MS for the simultaneous determination of Se^{IV}, Se^{VI} and selenocyanate ($SeCN^-$) in aqueous mine wastewater samples has been developed.[175] Selenocyanate was derivatised with triethyloxonium tetrafluoroborate ($Et_3OBF_4 : CH_3CN$) to ethylselenocyanate (EtSeCN) which was extracted into chloroform. After EtSeCN extraction, the aqueous solution was divided in two aliquots: One aliquot was acidified and 3,5 bis(trifluoromethyl)-*o*-phenylenediamine was used for the novel derivatisation of Se^{IV} to 4,6-bis(trifluoromethyl)-2,1,3-benzoselenadiazole, for the determination of Se^{IV}. For the second aliquot, HCl was added along with 4-nitro ophenylenediamine to simultaneously reduce Se^{VI} to selenite Se^{IV} and derivatise the combined "selenite + selenate" fraction to 5-nitro-2,1,3-benzoselenadiazole. The benzoselenadiazoles were extracted with chloroform and all extracts were combined for GC-MS analysis. Speciation analysis was performed by an Agilent J&W DB-1701 column (30 m × 0.250 mm inner diameter, 0.25 μm film thickness) with an oven gradient temperature from 40 to 250 °C at 20 °C min^{-1}. Measurements by AEC-ICP-MS were undertaken to assess derivatisation reaction completion. This involved the separation of Se^{IV}, Se^{VI} and $SeCN^-$ on a Thermo Scientific Dionex AS16 guard (4 × 50 mm) and analytical (4 × 250 mm) anion exchange column. The mobile phases were water and 100 mmol L^{-1} NaOH, with both containing 2% methanol to increase ICP-MS signal for Se. The AEC method, with a Hamilton PRP-X100 column, was also employed for direct analysis of the wastewater samples to allow comparison with the results from the developed GC-MS method. A complete study on the stability of $SeCN^-$ that included the effect of light, temperature, oxygen concentration and pH is presented. To preserve SeCN-integrity the authors recommend storage of the samples in cold alkaline conditions. The GC-MS LOD values were found to be 0.35, 0.56, and 1.67 μg L^{-1} Se for $SeCN^-$, Se^{IV}, and Se^{VI}, respectively. The novel methodology was tested on gold mine wastewater samples; compared to total Se, a 63–149% recovery as the sum of species was observed. For the AEC-ICP-MS method a 'reasonable agreement' was found in the species distribution.

3.18 Silicon

Lately, the *use of ICP-MS/MS for Si determination* has focused the attention of several researchers as it offers important advantages in terms of sensitivity and selectivity and exceptional improvement in the detection limits for Si determination. Consequently, three papers on the application of GC-ICP-MS/MS have been published this year for the speciation of silicon compounds. Fopianno *et al.*[176] developed a method based on the use of GC-ICP-MS/MS for determining linear and cyclic siloxane compounds (L2, L3, D3, D4, D5 and D6) in biogas samples, from the anaerobic digestion of manure and mixed organic sources (food, agricultural, manure and green wastes), collected at a biogas production plant in Switzerland with a continuous liquid quench sampling system (LQSS). The LQSS concentrates condensable trace compounds from the biogas into a liquid solvent. Speciation analysis was carried out by employing a 5% phenyl methyl siloxane stationary phase column (HP-5, 30 m × 0.320 mm, 0.25 μm film thickness) and a gradient of temperature from 55 to 200 °C at 3 °C $minute^{-1}$. Under optimal conditions the LOD values ranged from 1, 3, 30 and 75 ng per Si per mL for the siloxane compounds analysed. The LOD and LOQ in the gas for cyclic compounds, such as D5, varied based upon the sampling conditions and were in the range of 0.002–0.004 mg per Si per Nm^3 and 0.007–0.014 mg per Si per Nm^3, respectively, where N stands for normal. The authors claimed that the LOD and LOQ values attained are the lowest reported in the literature, fulfilling the EURAMET (the European Association of National Metrology Institutes) requirements for silicon measurements in biogas and biomethane. In another paper covered here, cyclic volatile methylsiloxanes were measured in fish (filleted) from the Saar River (Germany) collected during the period 1995–2017.[177] The cyclic volatile methylsiloxanes (cVMS) selected in this study were

This journal is © The Royal Society of Chemistry 2021

octamethylcyclotetrasiloxane (D4), decamethylcyclopentasiloxane (D5) and dodecamethylcyclohexasiloxane (D6) which have been identified as substances of very high concern (SVHC) under the REACH regulation. A QuEChERS dispersive solid extraction method was employed for isolating cVMS from the samples. The method is based on the use of ACN and hexane as extractants and tetrakis-(trimethylsilyloxy)silane as the internal standard. Silicon species were chromatographically separated using a polyethylene glycol (PEG) capillary column (length 30 m, ID 0.25 mm and df 0.25 mm) and the GC was coupled to the ICP-MS/MS by means of a stainless-steel transfer line heated to 250 °C. The use of ICP-MS/MS allowed the elimination of interferences, C, N and O based polyatomics, on the main Si isotope ($m/z = 28$) with hydrogen as the reaction gas. The LOD ranges were 3.1–16.8 ng g^{-1} w/w, 2.9–12.3 ng g^{-1} w/w and 3.9–30.9 ng g^{-1} w/w for D4, D5 and D6, respectively. The results evidenced a decrease of cVMS in the samples over the time period studied. This decrease in cVMS in the fish tissues was attributed to a decrease of cVMS concentration in wash-off personal care products and therefore a lower discharge of these compounds to the water bodies *via* WWTP effluents. Finally, a methodology based on the use of GC-ICP-MS/MS was developed for Si speciation (siloxanes, silanols and silanes) in light petroleum products.[178] Species separation was achieved by means of a DB-5 MS UI (30 m × 0.25 mm × 0.25 μm) capillary column. One of the main goals of the work was to minimise the influence of the sample matrix and silicon chemical form on sensitivity. For this purpose, a careful optimisation of the GC-ICP-MS/MS operating parameters (carrier gas, optional gas and H_2 cell gas flow rates) was carried out. Optimal gas flows were found to be 2 mL min^{-1} of H_2, 0.15 L min^{-1} of optional gas (Ar/O_2 80 : 20 mixture) and 0.5 L min^{-1} of Ar as the carrier gas. The LOD values ranged from 8 to 60 μg kg^{-1}. The method was applied to the speciation of Si compounds in coker naphtha samples. Four cyclic siloxanes, D3–D6 were identified and quantified according to their retention times and one unknown Si peak was detected which was attributed to column bleed.

3.19 Silver

Three papers report on Ag speciation this year with the first of these reports covering the detection and quantification of Ag_2S and ZnS NPs in water samples.[179] Cloud point extraction (CPE) was used to extract metal-sulfide and nonmetal-sulfide NPs from the waters from 9.5 mL of NP standard or sample solution with the pH adjusted to about 5 with diluted HNO_3 or NaOH solution. Subsequently, 0.15 mL of 10% (m/v) TX-114 aqueous solution, 0.2 mL of 1 mol^{-1} $NaNO_3$ solution, and 0.25 mL of 200 mmol L^{-1} EDTA were added and the mixture agitated and incubated at 45 °C for 15 minutes. This was followed by centrifugation to separate the NP containing surfactant-rich phase which was then removed and combined with 100 μL of 10 mmol L^{-1} bis(*p*-sulfonatophenyl)phenylphosphane dehydrate dipotassium (BSPP) and shaken to selectively dissociate the nonmetal-sulfide NPs into their ionic components while maintaining the original size and shape of Ag_2S and ZnS NPs. This extract was then diluted with 2% (v/v) FL-70 and 2 mmol L^{-1} sodium thiosulfate, at pH 9.5, which was also the HPLC mobile phase, to give a final metal concentration of 0.1 to 50 μg L^{-1}. The diluted analytes were then either analysed directly by ICP-MS to give the total metal content or injected on a Durashell NH_2 column to separate the sulfide NPs and ionic components. The amount of the metal sulfide NPs was calculated by difference. Spike recoveries, into effluent, lake and river waters, ranged between 81 to 97% for Ag_2S NPs and 84 to 94% for ZnS NPs. The LOD values, calculated as three times of the baseline noise, were 8 and 15 ng L^{-1} for Ag_2S and ZnS NPs, respectively with an enrichment factor of about 50 calculated. In unspiked water samples the Ag-based and Zn-based NP contents were reported to be in the range of 0–15 and 61–94 ng L^{-1}, respectively. For lake water and effluent samples, the detected Ag-based NPs were in the form of Ag_2S, whilst the Zn-based NPs were found to be a mixture of ZnS and other Zn-containing NPs.

The two other papers covered here both used X-ray based techniques to investigate Ag NP location and dissolution. Silver NPs are now routinely incorporated into wound dressings to inhibit microbial growth, with the Ag^{+} ion being the active species, and this can be ‘deactivated by complexation with *e.g.* Cl^{-} ions, hence the use of Ag NPs to provide a continuous supply of ionic Ag. The absorption, distribution, metabolism and excretion behaviour of Ag NPs from wound dressings used on burns patients has been systematically investigated Synchrotron radiation μXRF/μXANES and laser ablation-ICP-MS.[180] Full-profile specimens of skin from four hospital patients with mid-to-deep thickness burns or equivalent skin wounds, treated with dressings containing silver nanoparticles or silver sulfadiazine were collected for this purpose. Semi-quantitative/high resolution direct information on the spatiotemporal distribution and speciation of Ag *in vivo* demonstrated that the metal was rapidly released onto the wound surface, followed by a significant structure dependent mm scale penetration into the damaged tissues. Speciation data showed that this was followed by a sequential processes of metallic silver dissolution, chloride complexation, a change in species to metal–thiol protein complexes and finally, mobilisation into the deeper skin layers towards the vascular networks of the tissue. Complete local clearance of silver was observed after 12 days of treatment in the case of full healing. The study concluded that further questions, such as the effects of possible functionalisation of AgNPs in alternative dressing designs, the biochemical mechanisms and clinical relevance of possible toxic effects of Ag during its residence time into the wound, the mechanisms of potential interaction with Zn, and the fate of Ag after entering systemic circulation, remain to be answered. The final paper covered here reports on the exposure of *Lactuca sativa* (lettuce) to Ag NPs with differing coatings (citrate, polyvinylpyrrolidone, polyethylene glycol) and sizes (60, 75, 100 nm) at different concentrations (1, 3, 5, 7, 10, 15 mg L^{-1}). Total Ag measurements in lettuce tissues, by ICP-MS or ICP-OES after an HNO_3/H_2O_2 MAE procedure, indicated that accumulation of AgNPs in the root increased with exposure concentration, but not by nanoparticle coating. Nanosilver translocation to shoots was more pronounced for neutral charged and large sized NPs at higher NP concentrations. After an enzymatic digestion of lettuce

tissues, 2 mL of 50 g L^{-1} Macerozyme R-10 and 8 mL of citrate buffer at pH 3.5–7.0 (no sample mass is given), incubated shaking at 37 °C and filtration through 0.45 μm pore size and dilution to 1 μg L^{-1} Ag, sNP-ICP-MS analysis indicated the dissolution of some NPs. The Ag NP dissolution was corroborated by the use of K-edge X-ray absorption spectroscopy analysis which showed the presence of fewer Ag–Ag bonds and the appearance of Ag–O and/or Ag–S bonds in lettuce roots. Toxicological effects on lettuces were observed after exposure to nanosilver, especially for transpiration and stomatal conductance.

3.20 Sulfur

Considerable interest has been shown within the petroleum industry, in *the use of different chromatographic methods coupled to ICP-MS for the investigation of S heteroatom-containing asphaltenes and the involvement of metals, predominantly chelated forms of Ni and V, in the formation of aggregates*. This group of hydrocarbons cause significant problems in the refining, processing and transportation of products manufactured from crude oil, but little is understood about the mechanisms involved. Asphaltenes are a particularly complex group of super high-molecular-weight aggregates, which are part of the organic portion of oil that is not readily soluble in straight-chain solvents such as *n*-heptane. For this reason, the separation of these mixtures into individual compounds has proved to be a considerable challenge chromatographically. Recent publications have highlighted a number of chromatographic approaches to separating these complex hydrocarbons, as well as the employment and combined use of elemental and molecular detection systems for their measurement and structural characterisation.

In a two part report, the nano-aggregation of asphaltenes was investigated using *GPC coupled to ICP-MS on-line and positive APPI 9.4 T FT-ICR-MS off-line*.[181] Three preparative GPC columns were connected in series and a mobile phase containing xylene at a flow rate of 3 mL min^{-1} was used for elution. Most of the eluent was directed to a fraction collector by a post-column split and the low-flow outlet from the splitter (~40 μL min^{-1}) was diverted to an ICP-MS instrument for elemental detection. Although no significant resolution of the compounds was possible, fractions corresponding to the elution volume were collected. The fractions were then infused off-line into a 9.4 T FT-ICR-MS, *via* a custom-built adapter used to interface the APPI source with the front stage of the purpose built MS. The second report used a single GPC column and THF as eluent at 200 μL min^{-1} for the separation, but this time for structural characterisation it was coupled online with the APPI source of the FT-ICR-MS.[182] This overcame the problems reported in the initial report, which were related to solvent contaminant peaks and dynamic range limitations encountered with the characterisation of the largest aggregate fractions by direct infusion. These were thought to relate to the extremely low ionisation efficiencies of the larger, more aliphatic species. For detection by SF-ICP-MS, most of the eluent was directed to waste by a post-column split and only about ~40 μL min^{-1} was diverted to the detector. Differences in extra-column volumes between the experimental setup for detection with ICP-MS and the FT-ICR-MS were calculated theoretically to align the two chromatograms. The elution time for a tetraphenyl porphyrin standard was also monitored by UV-vis and detected by both ICP-MS and FT-ICR-MS to verify that the elution times of the two systems were aligned. The GPC-SF-ICP-MS method was applied to asphaltenes samples obtained from three different Venezuelan heavy crude oils (Hamaca, Cerro Negro and Boscan) and their corresponding sub-fractions, A1 (insoluble in toluene) and A2 (soluble in toluene).[183] Once again THF was used as the eluent at a flow rate of 0.7 mL min^{-1} with three GPC columns in series. A post-column split (20 : 1) was used to send the low-flow outlet (~40 μL min^{-1}) to the SF-ICP-MS *via* an in-house built interface, comprising a modified total consumption nebuliser mounted within a laboratory-made jacketed spray chamber, thermostated at 60 °C. The isotopes of ^{32}S, ^{51}V, and ^{58}Ni were monitored in medium resolution mode. The results from the use of GPC-ICP-MS showed very clearly the presence of asphaltene clusters in THF solution and the results provided strong support for the current models regarding cluster formation. Further work by the same group specifically investigated the role of V- and Ni-containing petroporphyrins along with S, in asphaltene composition, aggregation and fouling.[184] The work involved sample component fractionation by solid/liquid extraction, which allowed for separation of important structural motifs. High-performance TLC (HPTLC) with cellulose as the stationary phase and DCM/MeOH as the eluent, was used in an attempt at using a high-resolution chromatographic approach to separation of the complex mixture of petroporphyrins. To facilitate MALDI analysis, after HPTLC separation the different samples were scratched from the plates, extracted using THF and mixed with a custom synthesised MALDI matrix which facilitated porphyrin ionisation by electron transfer reaction. For the LA-ICP-MS analysis, plates were cut to dimensions of 9 × 10 cm^2 to fit within the ablation cell. The MALDI FT-ICR-MS analyses showed that in all the samples, porphyrins that migrate until they reach the solvent front are easier to analyse than those that remained at the deposition point. The LA-ICP-MS work showed that the main metalloporphyrins present contained V and that these tended to either stay at the deposition point of the HPTLC plate or migrate completely with the solvent front, effectively showing very little intermediate chromatographic behaviour on the solvent:plate system used. The authors concluded that the combination of molecular and elemental analyses proved that a large quantity of porphyrins remained inaccessible to molecular analyses because of matrix effects.

Similar work in this area by a different group has also investigated the compositional analysis of heavy oil products, including asphaltenes.[159] Illustrating just how complex these samples are, the group developed a comprehensive *two-dimensional liquid chromatography (LC × LC) system coupled to ICP-MS/MS* in an attempt to provide the necessary compound resolution, to characterise the S, Ni and V species present. Initially, the crude oil samples were treated using chemical precipitation followed by column chromatography, to separate

 This journal is © The Royal Society of Chemistry 2021

them into 4 fractions: saturates; aromatics; resins; and asphaltenes. A number of SEC and RP columns of different stationary phase, particle size and dimensions were investigated, including Advanced Polymer Chromatography silica-based SEC columns, with an effective molecular weight separation from 1000 to 30 000 g mol^{-1}, using isocratic elution with THF. A range of conventional C_{18} columns were investigated, using a gradient elution: 80/20 (v/v) ACN/H2O (A) and THF was used as mobile phase (B), with a linear gradient from 1% B to 99% B. Different column configurations were tested including SEC and RF coupled separately to ICP-MS/MS, but also 2-D on-line hyphenation of SEC to RP. The set-up showing most promise for this application was off-line SEC with fraction collection, followed by RF-ICP-MS/MS of the fractions. Twelve fractions were collected between 1 and 2 min and the gradient time in the second dimension was set at 10.2 min, giving a total analysis time about 150 min. Under such conditions, the calculated effective peak capacity was 2600, much higher than using on-line RPLC × SEC (<1700) whereas the dilution factor was quite similar. For detection $^{51}V^+$ was mass shifted to $^{67}VO^+$, as was $^{32}S^+$ to $^{48}SO^+$, whereas Ni was measured on mass at $^{58}Ni^+$. The resulting 2D-contour plots show that co-elutions could be removed leading, for the first time, to new information on high molecular weight species containing S, Ni and V. The study showed that whereas heavy mass compounds are not well separated in SEC alone, they are partly separated in RPLC making the combination of both techniques of significant interest.

Some *recent applications of S-containing compound analysis by GC-ICP-MS* have involved interesting and novel forensic[185] and industrial[186] applications, which also demonstrate useful calibration approaches for S-containing species. The forensic study focused on the quantitative speciation of volatile S-containing compounds derived from cysteine and methionine from human cadavers and their use as markers to determine post-mortem intervals or decomposition status. The gases emitted from a human body enclosed in an aluminium hood located at an outdoor human decomposition facility, were sampled using a low flow air sampling pump to draw 1 L of headspace at a sampling rate of 100 mL min^{-1} through a dual sorbent tube containing Tenax TA and Carbograph 5TD. The sampling tubes were sealed with brass storage-caps after collection, wrapped in aluminium foil and placed in an airtight glass container for transportation and storage in the laboratory. The sorbent tubes were stored at 4 °C until elution of the trapped VOCs was undertaken using acetone. The samples eluted from the tubes were analysed using pulsed splitless injection (5 μL sample, 1 μL standard) onto a DB5MS capillary column with a thermal programme and coupling to the ICP-MS *via* a commercially available interface held at 300 °C. Calibration used a custom produced standard composed of 5 S-containing pesticides one of which, chlorpyrifos, was spiked into the samples as an IS to mitigate signal drift during acquisition and between re-calibration runs. Because the pesticides used also contained other hetero atoms the LOD/LOQ for all the different compound groups were estimated to be: 0.7/2.2 ng L^{-1} for P; 5.4/16.2 ng L^{-1} for S; and 1.6 ng L^{-1}/4.8 ng L^{-1} for Cl, respectively. For the molecular identification of the species, a qTOF-GC-MS was employed to obtain accurate masses in the range *m*/*z* 50 to 1000. Differences in retention time due to the use of two different GC systems were compensated using Chlorpyrifos as marker. The study showed the most abundant S species were observed between day 9 and 39, with the highest concentration on day 23. Based on accurate mass and the compound specific fragmentation pattern, dimethyltrisulfide was positively identified, whereas identification of the second Se-containing compound was unfortunately affected by co-elution of solvent at the same retention time. The most commonly used technique to measure S isotopes in organic compounds is gas-source IRMS using SO_2 or SF_6 as analyte gas. Over the last 15 years MC-ICP-MS has been developed to measure S isotope ratios in inorganic but not organic compounds. In the second report, using GC-ICP-MS, a method for the simultaneous compound-specific analysis of $\delta^{33}S$ and $\delta^{34}S$ in 4 organic compounds (thiophene, tetrahydrothiophene, diethyl sulfide and dimethyl disulfide) using medium- and low-mass-resolution modes was described.[186] The method was validated using the international isotope reference materials of pure Ag_2S, IAEA-S-1, IAEA-S-2, and IAEA-S-3. Overall analytical uncertainty including normalisation and reproducibility for $\delta^{33}S$ and $\delta^{34}S$ was usually better than ±0.2‰ (sigma) for analytes containing at least 100 pmol of S. The method provided a simpler and faster tool than existing techniques to obtain $\Delta^{33}S$ values for the evaluation of mass-independent isotope effects in organosulfur compounds. However, a major hindrance for adoption of stable S isotope measurement techniques is the current lack of availability of suitable GC amenable organic isotope reference materials.

3.21 Tellurium

One paper on the application of CPE followed by ETAAS determination has appeared this year for the *speciation of Te in environmental samples*.[187] One of the advantages of the reported method is the use of the ionic liquid 1-octyl-3-methylimidazolium chloride (ODMIM) as an additive to improve the extraction capacity of the non-ionic surfactant Triton X-114. The Te^{IV} species in the samples were first complexed with ammonium pyrrolidine dithiocarbamate, extracted into the micellar IL/surfactant phase and then directly measured by ETAAS. The total Te concentration was obtained after a pre-reduction step and Te^{VI} concentration was calculated as the difference between total Te and Te^{IV}. The factors affecting CPE extraction are described in detail: type and concentration of complexing agent, pH, influence of type of non-ionic, ionic strength, temperature and time. Due to the lack of a CRM, the accuracy of the method was evaluated by conducting recovery studies in samples of different complexity (soil, sediments and waters). Recoveries in the ranges of 95.2–106% and 93.8–106% were obtained for Te^{IV} and Te^{VI}, respectively, thus demonstrating the reliability of the proposed IL-CPE method for Te speciation analysis. One interesting approach focused on simultaneous speciation of inorganic Te and Sb in water samples is the work developed by Ou *et al.*[25] For this purpose, a method based on capillary microextraction online hyphenated

with ICP-MS was developed. Microextraction was performed on a poly(glycidyl methacrylate-ethylene dimethacrylate) monolithic capillary functionalised with cystamine. It was found that Sb^{III} and Te^{IV} were selectively retained on the prepared monolithic capillary over a wide pH range (1–8), while Sb^{V} and Te^{VI} were not adsorbed in the pH range of 3–8. Both Sb^{V} and Te^{VI} were pre-reduced simultaneously into Sb^{III} and Te^{IV} and subjected to the proposed method to get the information of total Sb and Te. The content of Sb^{V} and Te^{VI} was calculated by subtracting Sb^{III} and Te^{IV} from total Sb and Te. The repeatability of the in-house columns was assessed by the RSDs of recoveries for 7 runs of microextraction with the monolithic columns constructed in the same and various batches. The RSDs ($n = 7$, $c = 10\ \mu g\ L^{-1}$) of Sb^{III} and Te^{IV} were 3.2 and 4.1% for the same batch and 6.1 and 5.4% for various batches, respectively, demonstrating good repeatability. The method was applied to determine Sb^{III} and Te^{IV} in water samples. The LOD values for Sb^{III} and Te^{IV} were found to be 3.9 and 5.9 ng L^{-1} with RSD values of 5.2 and 4.1%, respectively. The enrichment factor was reported to be 100. The method was validated by using CRMs of environmental water samples (GSB07-1376-2001, GBW(E)080548) certified for total Sb and Te, respectively. The method was applied to the determination of Sb^{III} and Te^{IV} in water samples of different nature (river, lake) with recoveries within 84–108% range.

3.22 Thallium

Only two reports of Tl speciation analysis have appeared during this review period. Rasool *et al.* determined *Tl^{I} and Tl^{III} in a variety of environmental water samples by SPE-ICP-MS*.[188] In this work Tl^{III} was selectively retained as a complex with DTPA (added immediately after sampling) on an anion-exchange column (AG1-X8) and eluted with a solution containing 0.1 mol L^{-1} HCl and 5% (m V^{-1}) SO_2. Spike recoveries, concentrations not given, were quoted as "the average spiking recoveries of Tl^{I} and Tl^{III} in water samples were 99.88 ± 1.05% and 101.17 ± 1.2%, respectively", it is difficult to reconcile these values with the numbers in the relevant table, which ranged from 14 to 89%. Some CRMs were also analysed including NRCC SLRS-5 (river water), NIST SRM 1640a (trace elements in natural water) and "universally confirmed reference materials (OU-6, AMH-1, and GBPG-1)". No details of these latter three were provided and no results for the analyses of these materials were given. The LOD was not given nor was any information about calibration range. The samples contained between 0.01 and 61 $\mu g\ L^{-1}$ Tl^{I} and between 0.23 and 9.7 $\mu g\ L^{-1}$ Tl^{III}.

Kainth and Khandelwal carried out a detailed study of the *effect of speciation on the Tl L_p ($p = l$, alpha, eta, beta) peaks in the X-ray emission spectra* obtained with a conventional laboratory WD XRF spectrometer.[189] The instrument was an AXIOS-DY 6156 (PANalytical, Netherlands) equipped with a rhodium X-ray tube (SST-mAX50, 60 kV and 66 mA), a scintillation counter, and a LiF (220) ($2d = 2.848$ angstrom) crystal. The pure materials studied were elemental Tl, Tl^{I} iodide, chloride and sulfate, and Tl^{III} oxide and nitrate. A large set of physical fundamental parameters, such as X-ray transition energies, natural linewidths and relative transition probabilities, were determined by several spectral fitting procedures. In addition, chemical shifts of between 0.03–3.39 eV relative to the pure thallium target were measured. The researchers observed that the distinct peak profiles of the various Tl compounds, reflected in the linewidths, could be accounted for by different electronegativity values of adjacent ligands, effective charge, changes in the transition probability, mixed oxidation states of thallium and valence-to-core exchange interactions. They concluded that improvements in the geometrical description and data handling procedures in WD spectrometers have led to the possibility of studying the influence of chemical effects on different metal-based compounds, making the laboratory instrument a more versatile tool for routine analysis.

3.23 Tin

Although relatively few in number, publications reporting on Sn speciation within the review period are characterised *by their different methodologies and diverse range of matrix types*. A μTLC method, coupled to LA-ICP-MS, to determine Sn ion species in water and blood plasma samples has been reported, with stationary phase being Sn^{II} imprinted polymer nanoparticles.[190] The polymer particles were prepared from *N*-allylthiourea and ethylene glycol dimethacrylate which were copolymerised in the presence of Sn^{II} and identified using FT-IR, XRD, and field emission SEM. The effects of different variables such as pH of the solution, mobile phase composition, and mass ratio of ion-impregnated polymers to $CaSO_4$ were evaluated with respect to the separation efficiency. The powdered polymer (17.2 mg) was mixed with $CaSO_4$ (8.2 mg) and water (1 mL) to prepare a paste which was applied to a customised TLC plate etched with grooves 1 mm apart. The paste was deposited into the groove and dried at 40 °C for 24 h before 10 μL of sample solution was applied 1 cm above the groove and dried at room temperature. Finally, the plate was stood in a shallow layer of ACN/EtOH mobile phase in a covered beaker. After completion of the separation process on the plate, the separated zones on the surface were scanned by LA-ICP-MS. Under the established optimal conditions, the LOD, RSD and LDR of the method were 0.3 $\mu g\ L^{-1}$, 3.5%, and 0.8 to 900 $\mu g\ L^{-1}$ for Sn^{II} and 0.4 $\mu g\ L^{-1}$, 4%, and 1 to 740 $\mu g\ L^{-1}$ for Sn^{IV}, respectively. An MS based approach has been used by Will *et al.* to study the interactions of environmentally relevant OTCs with proteins.[191] Analytical standards of model proteins, such as beta-lactoglobulin A (LGA), were incubated with different phenyl- and butyltins. For adduct identification and characterisation, the incubated samples were analysed by ICP-MS and ESI-MS coupled to SEC. This approach allowed the preservation of the acid-labile organotin–protein adducts during analysis. The binding of triorganotin compounds, such as TPhT, was shown to be sulfhydryl-directed by using cysteine-specific protein labelling. However, the availability of reduced cysteine residues in proteins did not automatically enable adduct formation. This observation complements previous studies and have indicated the necessity for a highly specific binding pocket, identified for the model protein LGA *via* enzymatic digestion experiments. In

 This journal is © The Royal Society of Chemistry 2021

contrast to the triorganotins, the di- and mono-substituted degradation products, such as DBT, were less specific regarding their binding to proteins. Furthermore, DBT was observed to induce hydrolysis of the protein's peptide backbone. The authors emphasised the importance of future studies on di- and mono-substituted OTCs to elucidate unknown long-term toxic effects. Total Sn and OTCs have been determined by ICP-MS and GC-ICP-MS in 122 red wine samples of worldwide origin.[151] Total Sn concentrations varied considerably from 0.3 to 68 μg L^{-1}. In the absence of CRM for Sn species in wine, a mixture of red wines coming from different origins were pooled together. The RSD ($n = 6$) was below 7%, regardless of the species. To evaluate the recoveries, pooled samples were spiked in two ways. The first spike was made to nearly double the concentration of the species if naturally present in the composite sample, or three times higher than a roughly estimated LOQ if the species were not detected. The second spike was five times higher than the first one. The recoveries were from 86% to 113% for both levels investigated. Methyltins (mainly DMT, but also MMT) were the most abundant OTCs recovered. Methylation seemed to occur biotically during the wine making process and not during bottling and appeared dependent on the geographical origin of the wine. Of the OTCs, MBT was the most regularly found, but DBT and MOctT were also detected in some samples. The origin of the various Sn species was also discussed in the paper. A LC separation and CF-CVG-GD-OES has been reported for the simultaneous determination of DMT and TMT in food samples.[192] The OTCs were separated on an C_{18} column and converted into volatile gases using CVG. The locally constructed GD microplasma was used to excite the Sn atoms and signals were recorded on a CCD at 317.66 nm. Using an injection volume of 1 mL, the linear correlation coefficients were better than 0.99 for the concentration range 0.1 to 10 μg mL^{-1}. The recoveries for the organotin species from spiked samples were from 7 to 103%, with an RSD of from 0.2 to 8.7%. The LOD values were determined to be 0.59 and 0.93 μg L^{-1} for TMT and DMT respectively. Spiked recoveries were reported for a range of fruits, vegetables and meats, but only the two species in spiked samples were evaluated. An analytical method for the simultaneous determination of iSn and organotin in tobacco has also been reported.[193] The extraction efficiencies of methanol, *n*-hexane, dichloromethane, ethyl acetate and the mobile phase were investigated. Inorganic Sn, TMT, MPhT, MBT, DPhT, DBT and TBT were effectively separated and determined within 25 min using HPLC-ICP-MS. The LOD values were from 0.18 to 0.43 ng mL^{-1}, and the recoveries were between 73.9% and 98.4%. The results showed that iSn was the major component of Sn in the tobacco samples with trace quantities of organotins also detected.

3.24 Titanium

A cloud point extraction method has been employed to *separate ionic Titanium and TiO_2NPs* in water samples followed by ICP-MS measurements.[194] Most of the paper is devoted to the optimisation of the parameters affecting extraction efficiency, such as concentrations of Triton X-114 and NaCl and pH. Optimum concentrations were 0.03% w/v and 2.5 mmol L^{-1} of Triton X-114 and NaCl, respectively. Under these optimal conditions TiO_2NPs were extracted in the surfactant rich phase whereas ionic titanium remains in the aqueous phase. The Ti content in both phases was determined with ICP-MS. The surfactant-rich phase containing TiO_2NPs was submitted to an acid digestion procedure before ICP-MS analysis. The analytical characteristics of the method (calibration, limits of detection and quantification, precision and recovery) were evaluated. The LOD and LOQ for Ti determination in the surfactant rich phase were 0.13 and 0.45 μg L^{-1}, respectively. The method was applied for the determination of TiO_2NPs in swimming pool water samples. Extraction efficiencies from spiked water samples were close to 100%. Both species of Ti were detected and quantified in the samples analysed with titanium concentrations ranging from 3.5 to 5.0 μg L^{-1} as NPs, and from 2.5 to 8.3 μg L^{-1} in the ionic form.

3.25 Uranium

The understanding of U reprotoxicity requires a detailed knowledge of its molecular speciation. Sample preparation and *analysis procedures involving SEC- ICP-SFMS*, already developed and reported by Eb-Levadoux and co-workers, were applied to the screening of potential U protein targets in fish ovaries after chronic waterborne exposure.[195] Metal–protein complexes were extracted from freshly frozen gonad samples (approx. 65 mg) with 1800 μL of 25 mmol L^{-1} HEPES + 250 mmol L^{-1} sucrose at pH 7.4 with a Potter–Elvehjem homogeniser for 3 min at 0 °C. The cytosolic metal–protein complexes, contained in the supernatant, were separated by centrifugation, and injected into the chromatographic system consisting of a Superdex 200 10/300 GL column with successive detection by UV spectrophotometry (280 nm) and ICP-MS. The mobile phase was 100 mmol L^{-1} ammonium acetate at pH 7.4 flowing at 0.7 mL min^{-1}. In addition to ^{238}U, ^{63}Cu ^{56}Fe ^{31}P and ^{64}Zn were monitored. The procedures were applied to wild roach and laboratory zebra fish. The researchers concluded that monitoring P and the other endogenous elements (Fe, Zn and Cu), suggested that U was binding to vitellogenin (an egg yolk precursor) fragments including its maturation products.

The reducing conditions and high organic carbon content in wetlands are favourable for U sequestration. In *an on-going study of redox transformations of U phosphate minerals* and mononuclear species in a contaminated wetland, Stetten *et al.*[196] followed changes in speciation, in controlled laboratory studies of the effects of simulated drying or flooding, by several synchrotron X-ray spectrometry techniques. Both XANES and EXAFS spectra at the L_{III}-edge were collected on the 11–2 wiggler beamline at the Stanford Synchrotron Radiation Light source and on the CRG-FAME bending-magnet beamline at the European Synchrotron Radiation Facility. Anoxic incubation samples were analysed at liquid N_2 temperature in fluorescence mode detection using a Si(220) double crystal monochromator and a 100-element solid state Ge array fluorescence detector. The oxic incubation samples were analysed on the FAME beamline at liquid He temperature with a Si(220) double crystal

monochromator and a 30-element Ge fluorescence detector. The model compounds chosen were a U^{IV} humus sample and a synthetic U^{VI} humic acid. In addition, SEM-EDXS, combined with μ-XRF and μ-XANES, indicated that autunite ($Ca(UO_2)_2(PO_4)\cdot 11H_2O$) was reduced to lermontovite ($UPO_4OH\cdot H_2O$), whereas oxidised ningyoite ($CaU(PO_4)_2\cdot 2H_2O$) was dissolved. Analysis of the incubation waters by ICP-MS showed that dissolved organic carbon promoted the dissolution of U even under anoxic conditions.

Analysis of particles from the environment is essential to a range of applications, such as studies of transport, ensuring nuclear safety, and treaty verification. Many of these applications involve U compounds or minerals formed after weathering and many previous studies have involved synchrotron-based X-ray absorption spectroscopy, which renders timely measurements challenging. Researchers at Los Alamos National Laboratory have reported on *the development of a laboratory-scale "hyperspectral X-ray imaging"* approach that has the potential to make this type of analysis routine for many applications.[197] They are building two instruments. One is based on ultra-high-resolution X-ray emission spectroscopy with large transition-edge sensor microcalorimeter arrays in a scanning electron microscope for mapping chemical information (molecular formula, phase, oxidation state, hydration) and, as the ability of the instrument to determine chemical species depends on identification of different compounds from their spectra, they are building a complementary instrument to measure high-resolution X-ray emission spectra from known bulk materials. They are also working on a theoretical basis for the analysis of unknown spectra based on high-fidelity density functional theory and Dirac–Fock–Slater X-ray emission models, to account for the behaviour of weak U M satellites that may be especially sensitive to oxidation state. They reported that preliminary measurements and simulations demonstrated that the approach could identify and map elements and species on the nanoscale in about 10 s by measuring individual point spectra with <5 eV resolution.

3.26 Vanadium

There have been *five different papers published on the speciation of V in asphaltenes and other crude oil fractions this year.* These papers are covered in full in Section 3.20 Sulfur. In brief, the first paper covered the use of three preparative GPC columns connected in series, with xylene as the eluent, coupled to SF-ICP-MS on-line and positive APPI 9.4 T FT-ICR-MS off-line.[181] The second report[182] used a single GPC column and THF as eluent at 200 μL min^{-1} for the separation, with structural characterisation by coupling online with the APPI source of the FT-ICR-MS. The GPC-SF-ICP-MS method was then applied to asphaltenes samples obtained from three different Venezuelan heavy crude oils (Hamaca, Cerro Negro and Boscan) and their corresponding sub-fractions, A1 (insoluble in toluene) and A2 (soluble in toluene).[183] Further work by the same group specifically investigated the role of V- and Ni-containing petroporphyrins along with S, in asphaltene composition, aggregation and fouling.[184] This involved high-performance TLC, with cellulose as the stationary phase and DCM/MeOH as the eluent, and the TLC plates were analysed after further preparation by MALDI and LA-ICP-MS. Similar work in this area by a different group has also investigated the compositional analysis of heavy oil products, including asphaltenes.[159] Illustrating just how complex these samples are, the group developed a comprehensive two-dimensional liquid chromatography (LC × LC) system coupled to ICP-MS/MS, in an attempt to provide the necessary compound resolution, to characterise the S, Ni and V species present.

3.27 Zinc

The research interest on *Zn speciation this year has been focused on its use in its nanoparticulate form*, mainly as quantum dots (QDs). The first paper reports the optimisation of two methods based on CE-ICP-MS and HPLC-ICP-MS to evaluate the intracellular transformation of CdSeS/ZnS-based QDs when applied to the Hep G2 cell cytosol, and under different conditions of the level administered and incubation time.[101] The Hep G2 cells were incubated with QD suspensions containing different QD concentrations (0, 0.585, 0.675, 0.877, 1.17 μmol L^{-1}) for 45 min, 2, 6, 15 or 24 h of incubation. Afterwards, the cytosolic fraction from the Hep G2 cells was subjected to CE- and SEC-ICP-MS examination. Comparing the advantages of the techniques applied, the authors concluded that neither technique exhibited decisive advantages over the other. On the one hand, CE-ICP-MS displayed a better resolution but moderate sensitivity (LOD 4.0×10^{-10} mol per Cd per L) while, on the other, application of SEC-ICP-MS provided a significantly lower LOD (5.4×10^{-12} mol per Cd per L) and revealed the release of Cd ions. In an outstanding paper Zhou *et al.*[179] developed a method based on the use of CPE and LC-ICP-MS to evaluate the transformation of nonmetal S nanoparticles (NMS-NPs) into metal sulfur nanoparticles (MS-NPs) such as Ag_2S-NPsand ZnS-NPs in environmental waters. The developed protocol includes the extraction of NPs into a TritonX-114-rich phase. Under the conditions of 0.15% w/v of Triton X-114, pH 5, 20 mmol L^{-1} $NaNO_3$, incubation temperature of 45 °C for 15 min, MS-NPs and non-MS-NPs were extracted into the surfactant-rich phase. With the subsequent addition of 100 μL of 10 mmol L^{-1} bis(*p*-sulfonatophenyl)phenylphosphane dehydrate dipotassium (BSPP) into the CPE-obtained extract, the non-MS-NPs were selectively dissociated into their ionic counterparts while maintaining the original size and shape of Ag_2S-NPS and ZnS-NPs making it possible to distinguish MS-NP content from other non-MS-NPs by LC-ICP-MS. The LC-ICP-MS equipment consisted of a Venusil Durashell-NH_2, (1000 Å pore size, 250 × 4.6 mm) column and a mobile phase of 2% v/v FL-70 and 2 mmol L^{-1} sodium thiosulfate (pH 9.5) flowing at 0.5 mL min^{-1}. Under optimal conditions, LOD values of 8 ng L^{-1} for Ag_2S-NPs and 15 ng L^{-1} for ZnS-NPs were obtained. The recoveries were in the range of 81.3–96.6% for Ag_2S-NPs and 83.9–93.5% for ZnS-NPs when they were spiked into three environmental water samples. The authors highlighted the suitability of the method for monitoring transformation of AgNPs and ZnONPs in environmental samples. In the second

 This journal is © The Royal Society of Chemistry 2021

paper covered here a method based on the use of SEC-ICP-MS and HILIC-electrospray-Orbitrap MS was developed to carry out the speciation of essential nutrient trace elements in coconut water.[138] With the aim of preserving species integrity, sample preparation was limited to dilution with the chromatographic mobile phase followed by centrifugation. The distribution of the metal complexes in the coconut water was evaluated by SEC-ICP-MS. Separation was performed by using a HPLC system equipped with a Superdex-75 10/300 GL SEC (separation range 3000 and 70 000 Da, 10 × 300 mm) column with 100 mmol L^{-1} NH_4Ac as the mobile phase flowing at 0.7 mL min^{-1}. The chromatograms for Cu, Mn and Zn showed a single well shaped peak in the low molecular weight (LMW) zone of the chromatogram whereas in the case of Fe two peaks were observed. The fractions were subsequently analysed by HILIC-ES-MS in order to identify the nature of the metal complexes present in the coconut water. Separation was achieved on a Kinetex (150 × 2.1 mm × 2.6 μm) column with ACN or water as the mobile phase under gradient elution. The metal species identified included: Fe complexes with citrate and malate: ($Fe^{III}(Cit)_3(Mal)$, $Fe^{III}(Cit)_2(Mal)_2$ and $Fe^{III}(Mal)_2$), glutamine: ($Fe^{III}(Glu)_2$) and nicotianamine: ($Fe^{II}(NA)$); copper complexes with phenylamine: ($Cu^{II}(Phe)_2$ and $Cu^{II}(Phe)_3$) and nicotianamine: ($Cu^{II}(NA)$); zinc complexes with citrate: ($Zn^{II}(Cit)_2$) and nicotianamine ($Zn^{II}(NA)$) and a manganese complex with asparagine ($Mn^{II}(Asp)_2$).

4 Biomolecular speciation analysis

A comprehensive review detailing many aspects of microbial metallothioneins, a class of relatively small (3.5 to 14 kDa) S-rich proteins involved in metal homeostasis and detoxification has described many aspects of their properties, including: their origin; nomenclature; historical timeline of their discovery; the types associated with different micro-organisms (bacteria, fungi, algae, protozoa); structural aspects; type of metal co-factor; genetic regulation; metal detoxification mechanisms; and interaction with other metalloproteins.[198] The review, containing 196 references, also has a short section (21 references) detailing analytical methods and approaches that have been use for their measurement and characterisation, which covers most of the usual speciation platforms, including: HPLC; MALDI-TOF-MS; ES-MS/MS; ICP-MS; ICP-OES. The use of a number of more unusual techniques that have been used for structural determination, are reviewed including: ^{1}H and ^{113}Cd NMR spectroscopy, Raman spectroscopy; EPR; circular dichroism; and Mossbauer spectroscopy techniques. In general, the review was quite weak on the analytical methods, although it did stress the important point that this class of metalloprotein is difficult to measure because of its propensity to change structure if close control of the redox conditions is not maintained during sample preparation and analysis. This is certainly an area that needs a greater focus for the analytical speciation and metallomics community working in the area of metalloprotein research.

Research work focusing on *the quantitation of biomolecules without the use of specific molecular standards*, but instead relying on inorganic elemental standards for so called absolute quantitation, is an important advantage of elemental detection in speciation studies. The group from Oviedo, Spain have published a number of papers and reviews in this area over the years, but their most recent work calls into question whether the response factors for the measurement of biomolecules *via* their S signal using inorganic standards, are reliable when using conventional sample introduction systems in ICP-MS.[199] Studies on 14 different S-containing compounds including three peptides, four proteins, one amino acid, two cofactors, three polyethylene glycol (PEG) derivatives, and a sulfate standard, showed important differences in recovery between nebulisers when using inorganic sulfate as calibrant. The response factors were determined through calibration curves and IDMS analysis was used to normalise the results. No statistical differences were found for low-molecular-weight biomolecules *e.g.* PEGs and non-hydrophobic peptides when using any of the nebulisers tested. However, while statistical differences were negligible (96–104%) for the proteins and hydrophobic peptides using the total consumption nebuliser (TCN), significantly lower response factors (87–40%) were obtained using regular flow nebulisers, such as conventional concentric and cross-flow. This difference was thought to be related to the hydrophobicity of the analytes and only partially to the molecular weight of the molecules. Recovery findings were validated using IDA in intact and digested bovine serum albumin solutions using the TCN (98 and 100%, respectively) and the concentric nebuliser (73 and 97%, respectively). In a similar calibration approach, but this time using inorganic metal standards to calibrate the amount of Cu-bound to specific proteins, a team from the UK developed a method to investigate the "accurate non-ceruloplasmin bound Cu" (ANCC) in human serum samples, an important disease marker in patients with Wilson's disease.[123] In general, routine biomedical analytical methods for protein analysis rely on indirect measurement techniques, such as immunoassays, which can lack effective metrological traceability. However, by using inorganic MS, direct quantification of biomolecules *via* hetero-atoms is a potential game changing approach to improvements in traceability in clinical laboratory assays. Using SAX-ICP-MS/MS with elution *via* a Tris pH 7.4 buffer with an ammonium acetate gradient and standards based on a Cu–EDTA complex, the method provided relatively simple quantification of ANCC with an LOD of 0.1 μg per Cu per L. This paper focused on a slightly different area compared to the Spanish group's work, related specifically to the Cu co-factor and its distribution between protein-bound and the toxic exchangeable form associated with proteins such as albumin. The method was also used to investigate the Cu species separated by using a 30 kDa cut-off ultrafiltration device, often used to generate the so-called "exchangeable" Cu fraction, which is considered to be an alternative clinical biomarker of Wilson's disease. Using the developed speciation approach, it was shown that the ultrafiltration method can overestimate the "exchangeable" Cu fraction due to the removal of Cu from ceruloplasmin, probably due to EDTA during the sample preparation steps. This was confirmed by comparing the enzymatic activity of the fractions, which decreased when EDTA

was used indicating that it removed Cu from ceruloplasmin as well as albumin and showed that the specificity of the "exchangeable" Cu test would only be ensured only under strict maintenance of ultrafiltration conditions.

Although direct biomolecular measurements of metalloproteins using speciation methods involving chromatography coupled to an elemental or molecular MS detector have been widely published over a number of years, *studies of a more practical nature, comparing the different buffers used as eluents and SEC column materials*, are particularly useful for highlighting problems. In this vein, a useful study compared the effect of several different buffer compositions and chromatographic materials on the peak shape and resolution of metalloprotein standards and a brain homogenate sample.[200] Initially, a silica based column (Bio SEC-3 column) with the following characteristics: 3 μm particle size; 150 Å pore structure; 4.6 × 300 mm dimensions; 500–150 000 Da protein MW separation range; was characterised, with one of six different mobile phases, of up to 200 mmol L^{-1} and adjusted to pH 7.5 with ammonia. The eluents/buffers investigated included: ammonium salts of nitrate, acetate, and sulfate; HEPES; MOPS; and Tris–HCl; at a flow rate of 0.4 mL min^{-1}. Recovery studies were undertaken to determine if the column retained any metal from the metalloproteins under the different mobile phase compositions and it was determined that Fe and Zn (or their associated metalloproteins) were retained by the column when ammonium nitrate was used. Also, the contribution of Cu from the column artificially increased the amount recovered when using one buffer. A reduction in signal for Cu in brain homogenate samples regardless of the mobile phase used and a lack of deterioration or change in Fe or Zn proteins was also observed. This was hypothesised as being due to the relative instability of Cu-proteins, as Cu may be able to transition from *a* +1 oxidation state to +2, which could uncouple it from the protein, ultimately resulting in a loss of signal. However, it is unclear why this would not also be a problem for the other trace elements with similar redox characteristics and further studies would be required to confirm this suggestion related to Cu. Additionally, a comparison was made with the use of a similar sized column, containing a non-silica based dextran stationary phase (Superdex 200), on recovery, response and peak resolution, when using either ammonium nitrate or Tris–HCl, the two most promising eluents. The results indicated that both columns were similar in terms of recovery but that the silica-based column was a source of Cu contamination when measuring SOD-1, effectively metallating the apo-form of this protein during the chromatographic run. To confirm this finding, all parts of the SEC-ICP-MS system, including, column injector, connecting tubes and separation column were tested and the column confirmed as the source of the Cu contamination. In summary, the study found that in terms of the peak resolution and response, ammonium nitrate, ammonium acetate and Tris–HCl were all optimal choices for use in the determination of metalloprotein interactions in complex samples. The choice of which of these three buffers to employ being dependent on the particulars of the experimental design. One unfortunate omission from the study, which would have been useful in terms of completeness, was a comparison to a resin-based SEC column.

An important trend for *using orthogonal chromatography systems with markedly different separation mechanisms, followed by elemental detection and structural elucidation by molecular MS* is apparent in recent applications in the biosciences. Li *et al.*[201] measured the Cd-binding proteins in human blood plasma in unexposed subjects and a small number of foetal-umbilical cord samples, which is a significant analytical challenge when taking into consideration the very low concentration of total Cd found in normal populations, being of the order of <50 nmol L^{-1}. Blood plasma samples were first depleted of the two most abundant proteins – albumin and immunoglobulin G, which allowed for a greater amount of sample to be loaded onto the GE column without compromising the chromatographic resolution or masking neighbouring peaks of lower abundance. The use of the commercially available albumin and IgG removal kit enabled 4.7-fold more treated plasma (about 380 μg) to be loaded onto the GE-ICP-MS system for analysis, compared to the ~80 μg of crude/untreated plasma sample that the system was able to handle. Both the crude and depleted plasma samples were analysed using an analytical platform comprising a column GE separation split *via* a T-connector to a fraction collector and an ICP-MS detector. The collected fractions were concentrated using 3 kDa MW cut-off filters and separated by 1D PAGE, followed by visualisation with silver staining. The selected protein bands were excised from the gels manually, and then digested with trypsin at 37 °C overnight. The trypsin-digested peptides were analysed using a TOF-HR-MS instrument and the mass spectra acquired in the range 350–2000 *m*/*z*. The peptide mass data obtained was searched against a peptide database through Mascot. One Cd-binding protein peak corresponding to apo-lipoprotein A-I was detected in 11 of the 29 normal plasma samples and all three paired maternal and cord plasma samples. This protein has been identified previously as binding Cd by this group using an approach based on using immobilised metal-affinity chromatography. Further studies will be required to determine the mode of action for Cd-toxicity involving this particular protein. Work on the characterisation of Ni containing biomolecules in a commonly studied plant species, *Arabidopsis thaliana*, using an orthogonal separation system based on SEC-ICP-MS followed by fraction collection and analysis of the Ni-containing fractions by using AEC coupled to ICP-MS detection, identified at least 5 Ni-containing peaks.[202] Molecular LC-MS/MS was then used for identification of the Ni-containing species after digestion with trypsin to liberate peptides for classification using instrumental software and comparison to the reference genome sequence data for this plant species. Using this procedure five different Ni chelators were present both in the wild type and a urease-defective mutant plants, indicating the presence of Ni-containing proteins other than urease. One of the Ni peaks showed a significant correlation with an Fe-containing peak, suggesting that a protein contained in this peak incorporated both Fe and Ni. Proteome analysis identified acireductone dioxygenase-2, which has two distinct metalloforms containing either Ni or Fe. The approach in these papers used a combination of

 This journal is © The Royal Society of Chemistry 2021

different separation modalities which are mechanistically very different, but which can both operate successfully at physiological pH values. These were used in combination with MS methods that can identify the metal co-factors present in difficult matrices and then what is effectively a proteomic approach, involving database searches to identify candidate proteins based on their peptide sequence and potential metal-binding motifs. Clearly a potentially very successful generic type of analytical platform for direct biomolecular speciation.

5 Abbreviations

1D	one dimensional
2D	two dimensional
AAS	atomic absorption spectrometry
AB	arsenobetaine
AC	alternating current
AE	atomic emission
AEC	anion-exchange chromatography
AES	atomic emission spectrometry
AF^4	asymmetric flow field flow fractionation
AFS	atomic fluorescence spectrometry
AMPA	aminomethylphosphonic acid
APCI	atmospheric pressure chemical ionisation
APDC	ammonium pyrrolidine dithiocarbamate
APL	acute promyelocytic leukemia
apo-Cp	apoceruloplasmin
APPI	atmospheric pressure photoionization
AS3MT	As^{III} methyltransferase
ASU	atomic spectrometry update
ASV	anodic stripping voltammetry
Aβ	amyloid-beta
BARGE	Bioaccessibility Research Group of Europe
BCR	Community Bureau of Reference
BDE	brominated diphenyl ether
BET	Brunauer–Emmett–Teller
BSPP	bis(*p*-sulfonatophenyl)phenylphosphane dehydrate dipotassium
CCD	charge coupled device
CDP	chlorophyll degradation product
CE	capillary electrophoresis
CEC	cation-exchange chromatography
CF	continuous flow
CIM	convective interaction media
CP	ceruloplasmin
CPE	cloud point extraction
CRM	certified reference material
CSCI	spectral component identified
CSIRO	Commonwealth Scientific and Industrial Research Organisation
CV	cold vapour
CVG	chemical vapour generation
cVM	cyclic volatile methylsiloxane
Cys	cysteine
D4	octamethylcyclotetrasiloxane
D5	decamethylcyclopentasiloxane
D6	dodecamethylcyclohexasiloxane
Da	discriminant analysis
DAD	diode array detector
DBD	dielectric barrier detector
DBT	dibutyltin
DCM	dichloromethane
DDT	dithiothreitol
DDTC	diethyldithiocarbamate
DES	deep eutectic solvent
DMA	dimethylarsenic
DMAV	dimethylarsinic acid
DMF	dimethylformamide
DMT	dimethyltin
DNA	deoxyribonucleic acid
DOI	dissolved organic iodine
DPhT	diphenyltin
EC	elemental carbon
ECD	electron capture detector
EDTA	ethylenediaminetetraacetic acid
eGPx	extracellular glutathione peroxidase
EPA	Environmental Protection Agency
EPR	electron paramagnetic resonance
ERM	European Reference Material
ES	electrospray
ET	electrothermal
Et_3OBF_4	triethyloxonium tetrafluoroborate
ETAAS	electrothermal atomic absorption spectrometry
EtHg	ethylmercury
EtOH	ethanol
EtSeCN	ethylselenocyanate
ETV	electrothermal vaporisation
EU	European Union
EURAMET	European Association of National Metrology Institutes
FAO	Food and Agriculture Organization
FAPAS	Food Analysis Performance Assessment Scheme
FFF	field flow fractionation
FI	flow injection
FIA	flow injection analysis
FT	Fourier transform
FTGCNC	fibrous nanocomposite
GBCA	Gd-based contrast agent
GC	gas chromatography
GD	glow discharge
GF	graphite furnace
GO	graphene oxide
GPC	gel permeation chromatography
GSSeSG	selenodiglutathione
HAA	halogenated acetic acid
HAS	human albumin serum
HCL	hollow cathode lamp
HEPES	4-(2-hydroxyethyl)piperazine-1-ethanesulfonic acid
HFBA	heptafluorobutyric acid
HG	hydride generation
HILIC	hydrophilic interaction liquid chromatography
holo-CP	holoceruloplasmin
HPLC	high performance liquid chromatography
HPTLC	high performance thin layer chromatography
HR	high resolution
IAM	iodoacetamide
iAs	inorganic arsenic

ICP	inductively coupled plasma
ICR	ion cyclotron resonance
ID	internal diameter
IDA	isotope dilution analysis
IDMS	isotope dilution mass spectrometry
IE	ion exchange
IgG	immunoglobulin G
iHg	inorganic mercury
IL	ionic liquid
iPb	inorganic lead
IR	infrared
IRMS	isotope ratio mass spectrometry
iSb	inorganic antimony
iSn	inorganic tin
LA	laser ablation
LADD	lifetime average daily dose
LC	liquid chromatography
LDR	linear dynamic range
LGA	beta-lactoglobulin
LLE	liquid–liquid extraction
LMW	low molecular weight
LOD	limit of detection
LOQ	limit of quantification
LQSS	liquid quench sampling system
MAE	microwave-assisted extraction
MALDI	matrix-assisted laser desorption ionisation
MBT	monobutyltin
MC	multicollector
Me	microextraction
MeHg	methyl mercury
MeSeA	methylselenic acid
MeSeCys	methylselenocysteine
MeSeG	methylselenoglutathione
MFC	metal–organic framework composite
MMA	monomethylarsenic
MMT	monomethyltin
MOctT	monooctyltin
MOPS	3-morpholinopropane-1-sulfonic acid
MPhT	monophenyltin
MRI	magnetic resonance imaging
MS	mass spectrometry
MTHFR	methylenetetrahydrofolate reductase
MTR	methionine synthase
MW	molecular weight
NCS	National Analysis Centre for Iron and Steel (China)
NIST	National Institute of Standards and Technology
NMIJ	National Measurement Institute of Japan
NP	nanoparticle
NRCC	National Research Council of Canada
ODMIM	1-octyl-3-methylimidazolium chloride
ODS	octadecylsilane
OES	optical emission spectrometry
OF	organofluorine
OHg	organic mercury
OTC	organotin compounds
PAGE	polyacrylamide gel electrophoresis
PCA	principal component analysis
PCR	polymerase chain reaction
PEG	polyethylene glycol
PFA	perfluoroalkyl
PFPA	pentafluoropropionic acid
PhHg	phenylmercury
PIXE	particle-induced X-ray emission
PM_{10}	particulate matter (with an aerodynamic diameter of up to 10 μm)
POP	persistent organic pollutant
PTFE	poly(tetrafluoroethylene)
Q	quadrupole
QD	quantum dot
QuEChERS	quick, easy, cheap, effective, rugged, and safe
REACH	registration, evaluation, authorisation and restriction of chemicals
RM	reference material
RP	reversed phase
RSD	relative standard deviation
RT	retention time
SAX	strong anion exchange
SCC	sodium copper chlorophyllin
SCGD	solution cathode glow discharge
SCX	strong cation exchange
SDBS	sodium dodecylbenzene sulfonate
SDS	sodium dodecylsulfate
SeAlb	selenoalbumin
SEC	size exclusion chromatography
SeCA	selenocystamine
SeCys	selenocysteine
$SeCys_2$	selenocystine
SeEt	seleno-D,L-ethionine
SeGalNac	seleno-nacetylgalactosamine
SeHLan	selenohomolanthionine
SelP	selenoprotein
SEM	scanning electron microscopy
SeMB	selenometabolites
SEM-EDS	scanning electron microscopy energy dispersive (X-ray) spectrometry
SeMet	selenomethionine
$SeSug_1$	methyl-2-acetamido-2-deoxy-1-seleno-*b*-D-galactopyranoside
$SeSug_2$	methyl-2-acetamido-2-deoxy-1-seleno-*b*-D-glucosopyranoside
SF	sector field
SOD	superoxide dismutase
Sp	single particle
SPE	solid phase extraction
SPION	superparamagnetic iron oxide nanoparticle
SR	synchrotron radiation
SRM	standard reference material
SSID	species specific isotope dilution
TBAH	tetrabutyl ammonium hydroxide
TBT	tributyltin
TCN	total consumption nebuliser
TEL	tetraethyllead
Tf	transferrin
TFA	trifluoroacetic acid
THF	tetrahydrofuran
THg	total mercury
TLC	thin layer chromatography
TMA	tetramethylarsenic

This journal is © The Royal Society of Chemistry 2021

TMAH	tetramethylammonium hydroxide
TMAO	trimethylarsine oxide
TML	tetramethyllead
TMSe	trimethylselenium
TMSe	trimethylselenium
TMT	trimethyltin
TOF	time-of-flight
TPhT	triphenyltin
Tris	tris(hydroxymethyl)aminomethane
UAE	ultrasound-assisted extraction
UBM	unified bioaccessibility method
UHPLC	ultra high performance liquid chromatography
UV	ultraviolet
VAME	vortex-assisted microextraction
VG	vapour generation
Vis	visible
WD	wavelength dispersive
WHO	World Health Organisation
XAFS	X-ray absorption fine structure spectroscopy
XANES	X-ray absorption near-edge structure
XAS	X-ray absorption spectroscopy
XES	X-ray emission spectroscopy
XFM	X-ray fluorescence microscopy
XRD	X-ray diffraction
XRF	X-ray fluorescence

6 Conflicts of interest

There are no conflicts of interest to declare.

7 References

1 R. Clough, C. F. Harrington, S. J. Hill, Y. Madrid and J. F. Tyson, *J. Anal. At. Spectrom.*, 2020, **35**(7), 1236–1278.

2 J. R. Bacon, O. T. Butler, W. R. L. Cairns, J. M. Cook, C. M. Davidson, O. Cavoura and R. Mertz-Kraus, *J. Anal. At. Spectrom.*, 2020, **35**(1), 9–53.

3 A. Taylor, A. Catchpole, M. P. Day, S. Hill, N. Martin and M. Patriarca, *J. Anal. At. Spectrom.*, 2020, **35**(3), 426–454.

4 E. H. Evans, J. Pisonero, C. M. Smith and R. N. Taylor, *J. Anal. At. Spectrom.*, 2020, **35**(5), 830–851.

5 C. Vanhoof, J. R. Bacon, U. E. A. Fittschen and L. Vincze, *J. Anal. At. Spectrom.*, 2020, **35**(9), 1704–1719.

6 S. Carter, R. Clough, A. Fisher, B. Gibson, B. Russell and I. Whiteside, *J. Anal. At. Spectrom.*, 2020, **35**(11), 2410–2474.

7 *Sample Introduction Systems in ICPMS and ICPOES*, ed. D. Beauchemin, Elsevier, Amsterdam, Netherlands, 1st edn, 2020, p. 586, Hardcover ISBN: 9780444594822, eBook ISBN: 9780444594839.

8 T. Pluhacek and V. Maier, *Chem. Listy*, 2020, **114**(3), 239–243.

9 X. H. Xu, H. B. Wang, H. Y. Li and H. Z. Sun, *Chem. Lett.*, 2020, **49**(6), 697–704.

10 A. Lores-Padin, P. Menero-Valdes, B. Fernandez and R. Pereiro, *Anal. Chim. Acta*, 2020, **1128**, 251–268.

11 W. Lorenc, A. Hanc, A. Sajnog and D. Baralkiewicz, *Mass Spectrom. Rev.*, 2020, 19, DOI: 10.1002/mas.21662.

12 R. C. Machado, D. F. Andrade, D. V. Babos, J. P. Castro, V. C. Costa, M. A. Speranca, J. A. Garcia, R. R. Gamela and E. R. Pereira, *J. Anal. At. Spectrom.*, 2020, **35**(1), 54–77.

13 S. K. Feng, E. Liotti, M. D. Wilson, L. Jowitt and P. S. Grant, *MRS Bull.*, 2020, **45**(11), 934–942.

14 K. Pyrzynska, *Talanta*, 2020, **212**, 120784.

15 W. I. Mortada, *Microchem. J.*, 2020, **157**, 105055.

16 A. I. C. Ricardo, F. Abujaber, F. J. G. Bernardo, R. C. R. Martin-Doimeadios and A. Rios, *Trends Environ. Anal. Chem.*, 2020, **27**, 14.

17 B. W. Chen, L. G. Hu, B. He, T. G. Luan and G. B. Jiang, *TrAC, Trends Anal. Chem.*, 2020, **126**, 115875.

18 L. H. Liu, Y. G. Yin, L. G. Hu, B. He, J. B. Shi and G. B. Jiang, *TrAC, Trends Anal. Chem.*, 2020, **129**, 115953.

19 T. Narukawa, G. Raber, N. Itoh and K. Inagaki, *Anal. Sci.*, 2020, **36**(2), 233–239.

20 Z. Gajdosechova, P. Grinberg, K. Nadeau, L. Yang, J. Meija, H. Gurleyuk, B. Wozniak, J. Feldmann, L. Savage, S. Deawtong, P. Kumkrong, K. Kubachka and Z. Mester, *Anal. Bioanal. Chem.*, 2020, **412**(18), 4363–4373.

21 L. X. Feng, Z. Z. Huo, J. P. Xiong and H. M. Li, *Anal. Chem.*, 2020, **92**(19), 13229–13237.

22 M. Sargent, *J. Anal. At. Spectrom.*, 2020, **35**(11), 2479–2486.

23 J. Wielinski, F. F. Marafatto, A. Gogos, A. Scheidegger, A. Voegelin, C. R. Muller, E. Morgenroth and R. Kaegi, *J. Anal. At. Spectrom.*, 2020, **35**(3), 567–579.

24 M. Y. Zhao, X. X. Peng, B. C. Yang and Z. Wang, *J. Anal. At. Spectrom.*, 2020, **35**(6), 1148–1155.

25 X. X. Ou, C. Wang, M. He, B. B. Chen and B. Hu, *Spectrochim. Acta, Part B*, 2020, **168**, 105854.

26 S. Z. Chen, Y. X. Liu, C. L. Wang, J. T. Yan and D. B. Lu, *Food Anal. Methods*, 2020, **13**(11), 2102–2110.

27 W. X. Wang, X. Dai, W. Guo, L. L. Jin and S. H. Hu, *At. Spectrosc.*, 2020, **41**(2), 74–80.

28 I. Moreno-Andrade, E. Regidor-Alfageme, A. Durazo, J. A. Field, K. Umlauf and R. Sierra-Alvarez, *J. Environ. Sci. Health, Part A: Toxic/Hazard. Subst. Environ. Eng.*, 2020, **55**(4), 457–463.

29 Z. X. Zhang, Y. Lu, H. P. Li, N. Zhang, J. F. Cao, B. Qiu and Z. G. Yang, *Anal. Lett.*, 2020, 16, DOI: 10.1080/00032719.2020.1788049.

30 M. Jablonska-Czapla and K. Grygoyc, *Environ. Sci. Pollut. Res.*, 2020, **27**(11), 12358–12375.

31 V. S. Ribeiro, S. O. Souza, S. S. L. Costa, T. S. Almeida, S. A. R. Soares, M. G. A. Korn and R. G. O. Araujo, *Environ. Geochem. Health*, 2020, **42**(7), 2179–2193.

32 A. I. G. de las Torres, M. S. Moats, G. Rios, A. R. Almansa and D. Sanchez-Rodas, *Anal. Methods*, 2020, **12**(14), 1943–1948.

33 M. S. Reid, K. S. Hoy, J. R. M. Schofield, J. S. Uppal, Y. W. Lin, X. F. Lu, H. Y. Peng and X. C. Le, *TrAC, Trends Anal. Chem.*, 2020, **123**, 115770.

34 H. M. Yu, C. H. Li, Y. F. Tian and X. M. Jiang, *Microchem. J.*, 2020, **152**, 14.

35 F. Ardini, G. Dan and M. Grotti, *J. Anal. At. Spectrom.*, 2020, **35**(2), 215–237.
36 D. Banik, S. K. Manna and A. K. Mahapatra, *Spectrochim. Acta, Part A*, 2021, **246**, 119047.
37 M. Welna, A. Szymczycha-Madeja and P. Pohl, *Molecules*, 2020, **25**(21), 4944.
38 C. Luvonga, C. A. Rimmer, L. L. Yu and S. B. Lee, *J. Agric. Food Chem.*, 2020, **68**(7), 1910–1934.
39 C. Luvonga, C. A. Rimmer, L. L. Yu and S. B. Lee, *J. Agric. Food Chem.*, 2020, **68**(4), 943–960.
40 I. Herath, P. Kumarathilaka, J. Bundschuh, A. Marchuk and J. Rinklebe, *Talanta*, 2020, **208**, 120457.
41 Y. F. Wang, S. Y. Chen, D. L. Fang, C. L. Song and L. Y. Zhao, *Microchem. J.*, 2020, **157**, 7.
42 S. Tokalioglu, R. Clough, M. Foulkes and P. Worsfold, *Biol. Trace Elem. Res.*, 2020, **198**(1), 332–338.
43 R. Mudzielwana, M. W. Gitari and P. Ndungu, *Front. Chem.*, 2020, **7**, 913.
44 B. S. Pinheiro, A. J. Moreira, L. L. S. Gimenes, C. D. Freschi and G. P. G. Freschi, *Environ. Monit. Assess.*, 2020, **192**(6), 13.
45 Z. N. Chen, B. B. Chen, M. He and B. Hu, *Microchim. Acta*, 2020, **187**(1), 9.
46 K. K. Jinadasa, E. Pena-Vazquez, P. Bermejo-Barrera and A. Moreda-Pi?eiro, *Anal. Bioanal. Chem.*, 2020, **412**(7), 1663–1673.
47 K. K. Jinadasa, E. Pena-Vazquez, P. Bermejo-Barrera and A. Moreda-Pineiro, *J. Chromatogr. A*, 2020, **1619**, 460973.
48 K. K. Jinadasa, E. Pena-Vazquez, P. Bermejo-Barrera and A. Moreda-Pineiro, *Talanta*, 2020, **220**, 121418.
49 D. Y. Zhang, S. W. Yang, Q. F. Ma, J. N. Sun, H. Y. Cheng, Y. C. Wang and J. H. Liu, *Food Chem.*, 2020, **313**, 8.
50 Z. Z. Yao, M. T. Liu, J. X. Liu, X. F. Mao, X. Na, Z. H. Ma and Y. Z. Qian, *J. Anal. At. Spectrom.*, 2020, **35**(8), 1654–1663.
51 H. Cho, K. B. Dasari, S. Cui, S. H. Choi and Y. H. Yim, *Int. J. Environ. Anal. Chem.*, 2020, 18, DOI: 10.1080/03067319.2020.1807969.
52 Z. Gajdosechova, C. H. Palmer, D. Dave, G. L. Jiao, Y. F. Zhao, Z. J. Tan, J. Chisholm, J. Z. Zhang, R. Stefanova, A. Hossain and Z. Mester, *Environ. Pollut.*, 2020, **266**, 115190.
53 A. I. G. de las Torres, I. Giraldez, F. Martinez, P. Palencia, W. T. Corns and D. Sanchez-Rodas, *Food Chem.*, 2020, **315**, 6.
54 E. Avigliano, J. Schlotthauer, B. M. de Carvalho, M. Sigrist and A. V. Volpedo, *J. Food Compos. Anal.*, 2020, **87**, 103404.
55 T. Narukawa, T. Iwai and K. Chiba, *Talanta*, 2020, **210**, 120646.
56 X. L. Liu, Q. Wang, J. He, M. F. Zhao, L. P. Qiu, L. M. Fan, S. L. Meng, G. Yang, T. Li, Q. Li, C. Song and J. Z. Chen, *J. Food Compos. Anal.*, 2020, **94**, 8.
57 M. J. Clemente, S. Serrano, V. Devesa and D. Velez, *Food Chem.*, 2021, **336**, 127587.
58 W. Lorenc, B. Markiewicz, D. Kruszka, P. Kachlicki and D. Baralkiewicz, *Molecules*, 2020, **25**(5), 1099.
59 M. E. Foulkes, B. A. Sadee and S. J. Hill, *J. Anal. At. Spectrom.*, 2020, **35**(9), 1989–2001.
60 M. R. Dominguez-Gonzalez, M. C. Barciela-Alonso, V. G. Calvo-Milian, P. Herbello-Hermelo and P. Bermejo-Barrera, *Anal. Bioanal. Chem.*, 2020, **412**(13), 3253–3259.
61 M. Z. Zheng, G. Li, Y. L. Hu, J. Nriagu and E. F. Zama, *Environ. Sci. Pollut. Res.*, 2020, 11, DOI: 10.1007/s11356-020-11194-0.
62 Z. Y. Gu, S. de Silva and S. M. Reichman, *Int. J. Environ. Res. Public Health*, 2020, **17**(2), 11.
63 B. M. Freire, V. D. Santos, P. D. F. Neves, J. Reis, S. S. de Souza, F. Barbosa and B. L. Batista, *Anal. Methods*, 2020, **12**(16), 2102–2113.
64 M. Menon, B. Sarkar, J. Hufton, C. Reynolds, S. V. Reina and S. Young, *Ecotoxicol. Environ. Saf.*, 2020, **197**, 8.
65 F. C. da Rosa, M. A. G. Nunes, F. A. Duarte, E. M. D. Flores, F. B. Hanzel, A. S. Vaz, D. Pozebon and V. L. Dressler, *Food Chem.: X*, 2019, **2**, 6.
66 J. Zhang, D. Baralkiewicz, Y. Z. Wang, J. Falandysz and C. T. Cai, *Chemosphere*, 2020, **246**, 11.
67 H. M. Zou, C. Zhou, Y. X. Li, X. S. Yang, J. Wen, S. J. Song, C. X. Li and C. J. Sun, *Food Chem.*, 2020, **327**, 9.
68 Y. L. Li, Y. Liu, X. Han, H. Y. Jin and S. C. Ma, *Front. Pharmacol.*, 2019, **10**, 10.
69 S. Braeuer, J. Borovicka, J. Kamenik, E. Prall, T. Stijve and W. Goessler, *Sci. Total Environ.*, 2020, **736**, 9.
70 W. Lorenc, D. Kruszka, P. Kachlicki, J. Kozlowska and D. Baralkiewicz, *Talanta*, 2020, **220**, 9.
71 S. Wagner, C. Hoefer, M. Puschenreiter, W. W. Wenzel, E. Oburger, S. Hann, B. Robinson, R. Kretzschmar and J. Santner, *Environ. Exp. Bot.*, 2020, **177**, 12.
72 A. van der Ent, M. D. de Jonge, K. M. Spiers, D. Brueckner, E. Montarges-Pelletier, G. Echevarria, X. M. Wan, M. Lei, R. Mak, J. H. Lovett and H. H. Harris, *Environ. Sci. Technol.*, 2020, **54**(2), 745–757.
73 E. M. Kroukamp, T. W. Godeto and P. B. C. Forbes, *Chemosphere*, 2020, **250**, 9.
74 Y. L. Yu, A. V. Navarro, A. Sahuquillo, G. M. Zhou and J. F. Lopez-Sanchez, *J. Chromatogr. A*, 2020, **1609**, 10.
75 Y. Xu, X. J. Xie, Y. Feng, M. A. Ashraf, Y. Y. Liu, C. L. Su, K. Qian and P. Liu, *Bioresour. Technol.*, 2020, **304**, 8.
76 E. Byeon, C. Yoon, J. S. Lee, Y. H. Lee, C. B. Jeong, J. S. Lee and H. M. Kang, *J. Hazard. Mater.*, 2020, **391**, 11.
77 A. Penezic, M. L. Tercier-Waeber, M. Abdou, C. Bossy, L. Dutruch, E. Bakker and J. Schafer, *Mar. Chem.*, 2020, **223**, 13.
78 J. Yang, J. Bertram, T. Schettgen, P. Heitland, D. Fischer, F. Seidu, M. Felten, T. Kraus, J. N. Fobil and A. Kaifie, *Chemosphere*, 2020, **261**, 9.
79 S. Tanda, K. Gingl, R. Licbinsky, J. Hegrova and W. Goessler, *Environ. Sci. Technol.*, 2020, **54**(9), 5532–5539.
80 Q. Q. Liu, C. Z. Huang and X. C. Le, *J. Environ. Sci.*, 2020, **91**, 168–176.
81 H. R. Chen, D. R. Zhang, Z. Y. Nie, L. Zheng, L. L. Zhang, H. Y. Yang and J. L. Xia, *Spectrosc. Spectral. Anal.*, 2020, **40**(3), 934–940.
82 S. T. Thul, B. Nigam, S. Tiwari and R. A. Pandey, *Indian J. Biotechnol.*, 2019, **18**(1), 34–41.

 This journal is © The Royal Society of Chemistry 2021

83 T. Itabashi, J. N. Li, Y. Hashimoto, M. Ueshima, H. Sakanakura, T. Yasutaka, Y. Imoto and M. Hosomi, *Environ. Sci. Technol.*, 2019, **53**(24), 14186–14193.
84 S. Mitsunobu, T. Hiruta, J. Fukudo, Y. Narahashi, N. Hamamura, N. Matsue and Y. Takahashi, *Geoderma*, 2020, **373**, 8.
85 M. Ataee, T. Ahmadi-Jouibari, N. Noori and N. Fattahi, *RSC Adv.*, 2020, **10**(3), 1514–1521.
86 M. R. Letsoalo, M. A. Mamo and A. A. Ambushe, *Anal. Lett.*, 2020, 25, DOI: 10.1080/00032719.2020.1830103.
87 W. S. Liu, X. Y. Wang, J. Lu, Y. M. Zhang, X. M. Ye, J. M. Li, Q. L. Zhao, Z. Q. Wu, J. Zhou and X. Hai, *Arch. Toxicol.*, 2020, **94**(4), 1203–1213.
88 F. Gonzalez-Martinez, D. Sanchez-Rodas, N. M. Varela, C. A. Sandoval, L. A. Quinones and B. Johnson-Restrepo, *Int. J. Mol. Sci.*, 2020, **21**(14), 21.
89 Y. M. Hsueh, Y. C. Lin, C. J. Chung, Y. L. Huang, R. L. Hsieh, P. T. Huang, M. Y. Wu, H. S. Shiue, S. N. Chien, C. Y. Lee, M. I. Lin, S. C. Mu and C. T. Su, *Arch. Toxicol.*, 2020, **94**(6), 2027–2038.
90 N. Y. Yin, X. L. Cai, L. R. Zheng, H. L. Du, P. F. Wang, G. X. Sun and Y. S. Cui, *Environ. Sci. Technol.*, 2020, **54**(7), 4432–4442.
91 N. Yan, G. W. Xu, C. C. Zhang, X. P. Liu, X. Li, L. Sun, D. Wang, X. X. Duan and B. Li, *Cell Biosci.*, 2020, **10**(1), 10.
92 L. Lopez-Carrillo, B. Gamboa-Loira, A. J. Gandolfi and M. E. Cebrian, *Environ. Res.*, 2020, **184**, 109361.
93 J. T. Wang, W. Hu, H. L. Yang, F. B. Chen, Y. L. Shu, G. W. Zhang, J. Z. Liu, Y. G. Liu, H. W. Li and L. X. Guo, *Environ. Int.*, 2020, **138**, 14.
94 C. G. Howe, S. F. Farzan, E. Garcia, T. Jursa, R. Iyer, K. Berhane, T. A. Chavez, T. L. Hodes, B. H. Grubbs, W. E. Funk, D. R. Smith, T. M. Bastain and C. V. Breton, *Environ. Res.*, 2020, **184**, 109294.
95 G. Desai, A. E. Millen, M. Vahter, E. I. Queirolo, F. Peregalli, N. Manay, J. Yu, R. W. Browne and K. Kordas, *Environ. Res.*, 2020, **189**, 109935.
96 G. A. Borges, G. D. Souza, P. S. F. Lopes, V. S. T. Ciminelli, C. L. Caldeira and G. D. Rodrigues, *Quim. Nova*, 2020, **43**(6), 697–704.
97 P. Sun, Y. L. Gao, X. L. Zhang and R. Yan, *Quim. Nova*, 2020, **43**(8), 1074–1077.
98 A. Kana, M. Sadowska, J. Kvicala and O. Mestek, *J. Food Compos. Anal.*, 2020, **92**, 103562.
99 P. F. Rodriguez, R. M. Martin-Aranda, J. L. L. Colon and J. H. de Mendoza, *Talanta*, 2021, **221**, 121494.
100 Y. Gu, P. Wang, S. Zhang, J. Dai, H. P. Chen, E. Lombi, D. L. Howard, A. van der Ent, F. J. Zhao and P. M. Kopittke, *Environ. Sci. Technol.*, 2020, **54**(19), 12072–12080.
101 J. Kruszewska, M. Matczuk, S. Skorupska, I. Grabowska-Jadach, E. P. Hernandez, A. Timerbaev and M. Jarosz, *Anal. Biochem.*, 2019, **584**, 113387.
102 R. Milacic and J. Scancar, *TrAC, Trends Anal. Chem.*, 2020, **127**, 115888.
103 M. Fasihi, M. Rajabi, B. Barfi and S. M. Sajjadi, *Int. J. Environ. Anal. Chem.*, 2020, 13, DOI: 10.1080/03067319.2020.1784408.
104 M. Fasihi, M. Rajabi, B. Barfi and S. M. Sajjadi, *J. Iran. Chem. Soc.*, 2020, **17**(7), 1705–1713.
105 F. Elahi, M. B. Arain, W. A. Khan, N. Shah and T. G. Kazi, *Chem. Pap.*, 2020, 8, DOI: 10.1007/s11696-020-01337-5.
106 S. Fouladlou, H. Faraji, H. Shahbaazi, A. Moghimi and F. Azizinezhad, *Int. J. Environ. Anal. Chem.*, 2020, 12, DOI: 10.1080/03067319.2020.1727462.
107 B. Barfi, A. Asghari and M. Rajabi, *Arabian J. Chem.*, 2020, **13**(1), 568–579.
108 P. Vasileva, I. Dakova, T. Yordanova and I. Karadjova, *Open Chem.*, 2019, **17**(1), 1095–1104.
109 W. Zou, C. H. Li, J. Hu and X. D. Hou, *Talanta*, 2020, **218**, 121128.
110 W. C. Nugraha, H. Nagai, S. I. Ohira and K. Toda, *Anal. Sci.*, 2020, **36**(5), 617–620.
111 J. J. Shi, W. B. McGill, N. Chen, P. M. Rutherford, T. W. Whitcombe and W. Zhang, *Environ. Sci. Technol.*, 2020, **54**(12), 7226–7235.
112 F. Hernandez, N. Bemrah, F. Seby, L. Noel and T. Guerin, *Food Addit. Contam., Part B*, 2019, **12**(3), 209–215.
113 S. Q. Zhang, S. H. Cheng, S. Shen, B. Y. Luo and Y. Zhang, *Biol. Trace Elem. Res.*, 2021, **199**(1), 338–343.
114 R. Pechancova, J. Gallo, D. Milde and T. Pluhacek, *Talanta*, 2020, **218**, 121150.
115 M. Bergant, J. Scancar and R. Milacic, *Talanta*, 2020, **218**, 121199.
116 B. H. Chen, S. J. Jiang and A. C. Sahayam, *Food Chem.*, 2020, **324**, 5.
117 O. Mihai, M. S. Kawamoto, K. L. LeBlanc, P. Grinberg, A. R. D. Nogueira and Z. Mester, *J. Food Compos. Anal.*, 2020, **87**, 103421.
118 A. M. Ebrahim, A. M. Idris, A. O. Alnajjar and B. Michalke, *J. Trace Elem. Med. Biol.*, 2020, **62**, 126645.
119 A. Knoop, P. Planitz, B. Wust and M. Thevis, *Drug Test. Anal.*, 2020, **12**(11–12), 1666–1672.
120 J. Wojcieszek and L. Ruzik, *J. Anal. Sci. Technol.*, 2020, **11**(1), 26.
121 A. van Der Ent, R. Vinya, P. D. Erskine, F. Malaisse, W. J. Przybylowicz, A. D. Barnabas, H. H. Harris and J. Mesjasz-Przybylowicz, *Metallomics*, 2020, **12**(5), 682–701.
122 C. D. Quarles, M. Macke, B. Michalke, H. Zischka, U. Karst, P. Sullivan and M. P. Field, *Metallomics*, 2020, **12**(9), 1348–1355.
123 N. Solovyev, A. Ala, M. Schilsky, C. Mills, K. Willis and C. F. Harrington, *Anal. Chim. Acta*, 2020, **1098**, 27–36.
124 B. P. Harp, P. F. Scholl, P. J. Gray and P. Delmonte, *J. Chromatogr. A*, 2020, **1620**, 461008.
125 I. Strzeminska, C. Factor, P. Robert, A. L. Grindel, P. O. Comby, J. Szpunar, C. Corot and R. Lobinski, *Invest. Radiol.*, 2020, **55**(3), 138–143.
126 S. Q. Wang, B. Hesse, M. Roman, D. Stier, H. Castillo-Michel, M. Cotte, J. P. Suuronen, A. Lagrange, H. Radbruch, F. Paul, M. Taupitz, E. Schellenberger,

I. Sack and C. Infante-Duarte, *Invest. Radiol.*, 2019, **54**(10), 617–626.
127 S. Sarpong-Kumankomah, M. Contel and J. Gailer, *J. Chromatogr. B: Biomed. Sci. Appl.*, 2020, **1145**, 5.
128 J. Y. Lin, P. X. Lai, Y. C. Sun, C. C. Huang and C. K. Su, *Anal. Chem.*, 2020, **92**(20), 13997–14005.
129 D. S. Hardisty, T. J. Horner, S. D. Wankel, J. Blusztajn and S. G. Nielsen, *Chem. Geol.*, 2020, **532**, 119360.
130 B. Lajin and W. Goessler, *J. Chromatogr. A*, 2020, **1631**, 461575.
131 B. Lajin and W. Goessler, *Anal. Chem.*, 2020, **92**(13), 9156–9163.
132 A. Koch, R. Aro, T. Wang and L. W. Y. Yeung, *TrAC, Trends Anal. Chem.*, 2020, **123**, 115423.
133 S. J. Song, C. Yang, M. W. Shao, J. B. Chao, N. Zheng, W. H. Wang, Y. J. He and P. H. Li, *J. Chromatogr. B: Biomed. Sci. Appl.*, 2020, **1147**, 7.
134 P. Blanchard, N. Babichuk and A. Sarkar, *Environ. Sci. Pollut. Res.*, 2020, **27**(33), 42168–42174.
135 B. Michalke, D. Willkommen and V. Venkataramani, *J. Visualized Exp.*, 2020, 8, DOI: 10.3791/61055(159.
136 J. Kruszewska, J. Sikorski, J. Samsonowicz-Gorski and M. Matczuk, *Anal. Bioanal. Chem.*, 2020, **412**(29), 8145–8153.
137 M. Y. Pan, L. X. Feng and H. M. Li, *Chem. Res. Chin. Univ.*, 2020, **41**(9), 1983–1988.
138 G. Alchoubassi, K. Kinska, K. Bierla, R. Lobinski and J. Szpunar, *Food Chem.*, 2021, **339**, 127680.
139 R. Penalver, N. Campillo, I. Lopez-Garcia and M. Hernandez-Cordoba, *Microchem. J.*, 2020, **154**, 104630.
140 P. C. Zheng, H. D. Zhao, J. M. Wang, R. N. Liu, N. Ding, X. F. Mao and C. H. Lai, *J. Anal. At. Spectrom.*, 2020, **35**(12), 3032–3038.
141 P. Pongrac, I. Arcon, H. Castillo-Michel and K. Vogel-Mikus, *Plants*, 2020, **9**(1), 79.
142 M. Wansleben, J. Vinson, A. Wahlisch, K. Bzheumikhova, P. Honicke, B. Beckhoff and Y. Kayser, *J. Anal. At. Spectrom.*, 2020, **35**(11), 2679–2685.
143 S. W. Yang, Y. H. Song, Q. F. Ma, H. Y. Cheng, Y. C. Wang and J. H. Liu, *Anal. Chim. Acta*, 2020, **1133**, 30–38.
144 N. Esmaeili, J. Rakhtshah, E. Kolvari, A. Rashidi and H. Shirkhanloo, *Biol. Trace Elem. Res.*, 2020, 12, DOI: 10.1007/s12011-020-02382-7.
145 A. A. Krata, M. Wojciechowski, E. Vassileva and E. Bulska, *J. Food Compos. Anal.*, 2020, **86**, 103381.
146 A. A. Krata and E. Vassileva, *Talanta*, 2020, **217**, 121113.
147 M. Ghosn, R. Chekri, C. Mahfouz, G. Khalaf, T. Guerin, R. Amara and P. Jitaru, *Int. J. Environ. Anal. Chem.*, 2020, 14, DOI: 10.1080/03067319.2020.1767095.
148 X. L. Zhang, D. L. Ji, Y. Zhang, Y. Lu, J. H. Fu and Z. H. Wang, *J. Anal. At. Spectrom.*, 2020, **35**(4), 693–700.
149 H. M. Zou, C. Zhou, Y. X. Li, X. S. Yang, J. Wen, C. X. Li, S. J. Song and C. J. Sun, *Anal. Bioanal. Chem.*, 2020, **412**(12), 2829–2840.
150 Y. Sogame and A. Tsukagoshi, *J. Chromatogr. B: Biomed. Sci. Appl.*, 2020, **1136**, 8.
151 V. Vacchina, E. N. Epova, S. Berail, B. Medina, O. F. X. Donard and F. Seby, *Food Addit. Contam., Part B*, 2020, **13**(2), 88–98.
152 Q. H. Li, L. Tang, G. L. Qiu and C. H. Liu, *Sci. Total Environ.*, 2020, **738**, 8.
153 S. B. Angyus, E. Darvasi, M. Ponta, D. Petreus, R. Etz, M. Senila, M. Frentiu and T. Frentiu, *Talanta*, 2020, **217**, 121067.
154 A. Santa-Rios, B. D. Barst and N. Basu, *Anal. Chem.*, 2020, **92**(5), 3605–3612.
155 M. A. Maniero, R. G. Wuilloud, E. A. Callegari, P. N. Smichowski and M. A. Fanelli, *J. Trace Elem. Med. Biol.*, 2020, **58**, 126441.
156 M. Monperrus, C. Pecheyran and V. Bolliet, *Appl. Sci.*, 2020, **10**(7), 2463.
157 E. V. Walker, Y. Yuan, S. Girgis and K. J. Goodman, *BMC Public Health*, 2020, **20**(1), 13.
158 J. L. R. Gallego, M. A. Lopez-Anton, D. M. de la Rosa, E. Rodriguez-Valdes, N. Garcia-Gonzalez, E. Rodriguez and M. R. Martinez-Tarazona, *Environ. Sci. Eur.*, 2019, **31**(1), 79.
159 M. Bernardin, A. Le Masle, F. Bessueille-Barbier, C. P. Lienemann and S. Heinisch, *J. Chromatogr. A*, 2020, **1611**, 460605.
160 E. M. Pimenta, F. F. da Silva, E. S. Barbosa, A. P. Cacique, D. L. Cassimiro, G. P. de Pinho and F. O. Silverio, *J. Braz. Chem. Soc.*, 2020, **31**(2), 298–304.
161 J. P. F. Tiago, L. C. Sicupira, R. E. Barros, G. P. de Pinho and F. O. Silverio, *J. Environ. Sci. Health, Part B*, 2020, **55**(6), 558–565.
162 K. Markovic, R. Milacic, J. Vidmar, S. Markovic, K. Ursic, M. N. Zakelj, M. Cemazar, G. Sersa, M. Unk and J. Scancar, *J. Trace Elem. Med. Biol.*, 2020, **57**, 28–39.
163 K. Pyrzynska and A. Sentkowska, *Crit. Rev. Food Sci. Nutr.*, 2020, 13, DOI: 10.1080/10408398.2020.1758027.
164 Y. X. Li, N. L. Zhu, X. J. Liang, L. R. Zheng, C. X. Zhang, Y. F. Li, Z. Y. Zhang, Y. X. Gao and J. T. Zhao, *Ecotoxicol. Environ. Saf.*, 2020, **189**, 7.
165 D. B. Alcantara, R. F. Nascimento, G. S. Lopes and P. Grinberg, *Anal. Methods*, 2020, **12**(26), 3351–3360.
166 K. Takahashi, N. Suzuki and Y. Ogra, *Food Chem.*, 2020, **319**, 126537.
167 P. Zagrodzki, P. Pasko, A. Galanty, M. Tyszka-Czochara, R. Wietecha-Posluszny, P. S. Rubio, H. Barton, E. Prochownik, B. Muszynska, K. Sulkowska-Ziaja, K. Bierla, R. Lobinski, J. Szpunar and S. Gorinstein, *J. Trace Elem. Med. Biol.*, 2020, **59**, 126466.
168 G. C. Stonehouse, B. J. McCarron, Z. S. Guignardi, A. F. El Mehdawi, L. W. Lima, S. C. Fakra and E. A. H. Pilon-Smits, *Environ. Sci. Technol.*, 2020, **54**(7), 4221–4230.
169 K. Bierla, R. M. Taylor, J. Szpunar, R. Lobinski and R. A. Sunde, *Metallomics*, 2020, **12**(5), 758–766.
170 J. Hildebrand, A. Greiner, H. Drexler and T. Goen, *J. Trace Elem. Med. Biol.*, 2020, **61**, 8.
171 K. Takahashi and Y. Ogra, *Metallomics*, 2020, **12**(2), 241–248.

 This journal is © The Royal Society of Chemistry 2021

172 A. Arias-Borrego, B. Callejon-Leblic, G. Rodriguez-Moro, I. Velasco, J. L. Gomez-Ariza and T. Garcia-Barrera, *Food Chem.*, 2020, **321**, 126692.
173 B. Callejon-Leblic, G. Rodriguez-Moro, A. Arias-Borrego, A. Pereira-Vega, J. L. Gomez-Ariza and T. Garcia-Barrera, *J. Chromatogr. A*, 2020, **1619**, 460919.
174 F. Maass, B. Michalke, D. Willkommen, C. Schulte, L. Tonges, M. Boerger, I. Zerr, M. Bahr and P. Lingor, *J. Trace Elem. Med. Biol.*, 2020, **57**, 126412.
175 M. G. Bordash, E. Pagliano, K. L. LeBlanc, P. Kumkrong, D. Wallschlager and Z. Mester, *Sci. Total Environ.*, 2020, **745**, 140877.
176 D. Foppiano, M. Tarik, J. Schneebeli, A. Calbry-Muzyka, S. Biollaz and C. Ludwig, *Talanta*, 2020, **208**, 120398.
177 G. Radermacher, H. Rudel, C. Wesch, A. Bohnhardt and J. Koschorreck, *Sci. Total Environ.*, 2020, **706**, 136011.
178 R. Sanchez, F. Chainet, V. Souchon, S. Carbonneaux, C. P. Lienemann and J. L. Todol, *J. Anal. At. Spectrom.*, 2020, **35**(10), 2387–2394.
179 X. X. Zhou, L. W. Jiang, D. J. Wang, S. He, C. J. Li and B. Yan, *Anal. Chem.*, 2020, **92**(7), 4765–4770.
180 M. Roman, C. Rigo, H. Castillo-Michel, D. S. Urgast, J. Feldmann, I. Munivrana, V. Vindigni, I. Micetic, F. Benetti, C. Barbante and W. R. L. Cairns, *Analyst*, 2020, **145**(20), 6456–6469.
181 J. C. Putman, R. Moulian, C. Barrere-Mangote, R. P. Rodgers, B. Bouyssiere, P. Giusti and A. G. Marshall, *Energy Fuels*, 2020, **34**(7), 8308–8315.
182 J. C. Putman, R. Moulian, D. F. Smith, C. R. Weisbrod, M. L. Chacon-Patino, Y. E. Corilo, G. T. Blakney, L. E. Rumancik, C. Barrere-Mangote, R. P. Rodgers, P. Giusti, A. G. Marshall and B. Bouyssiere, *Energy Fuels*, 2020, **34**(9), 10915–10925.
183 G. Gonzalez, S. Acevedo, J. Castillo, O. Villegas, M. A. Ranaudo, K. Guzman, M. Orea and B. Bouyssiere, *Energy Fuels*, 2020, **34**(10), 12535–12544.
184 R. Moulian, M. Chacon-Patino, O. Lacroix-Andrivet, S. Mounicou, A. L. M. Siqueira, C. Afonso, R. Rodgers, P. Giust, B. Bouyssiere and C. Barrere-Mangote, *Energy Fuels*, 2020, **34**(10), 12449–12456.
185 D. Clases, M. Ueland, R. G. de Vega, P. Doble and D. Profrock, *Talanta*, 2021, **221**, 121424.
186 S. Kummel, A. Horst, F. Gelman, H. Strauss, H. H. Richnow and M. Gehre, *Anal. Chem.*, 2020, **92**(21), 14685–14692.
187 M. Llaver and R. G. Wuilloud, *Talanta*, 2020, **212**, 120802.
188 A. Rasool, T. F. Xiao, S. Ali, W. Ali and W. Nasim, *Environ. Sci. Pollut. Res.*, 2020, **27**(9), 9686–9696.
189 H. S. Kainth and D. Khandelwal, *J. Anal. At. Spectrom.*, 2020, **35**(12), 2935–2947.
190 A. S. Kisomi, T. Alizadeh and A. Shakeri, *Microchim. Acta*, 2020, **187**(5), 298.
191 J. M. Will, C. Erbacher, M. Sperling and U. Karst, *Metallomics*, 2020, **12**(11), 1702–1712.
192 B. Qian, J. Zhao, Y. He, L. X. Peng, H. L. Ge and B. J. Han, *J. Chromatogr. A*, 2019, **1608**, 460406.
193 Z. Z. Tian, L. X. Xing, D. K. Li, L. C. Ma, R. X. Wu, N. Tian and C. T. Zhang, *Anal. Lett.*, 2020, **53**(15), 2501–2516.
194 J. Lopez-Mayan, M. C. Barciela-Alonso, M. R. Dominguez-Gonzalez, E. Pena-Vazquez and P. Bermejo-Barrera, *Microchem. J.*, 2020, **152**, 104264.
195 S. Frelon, O. Simon, Y. Eb-Levadoux and S. Mounicou, *J. Environ. Radioact.*, 2020, **222**, 106365.
196 L. Stetten, P. Lefebvre, P. Le Pape, A. Mangeret, P. Blanchart, P. Merrot, J. Brest, A. Julien, J. R. Bargar, C. Cazala and G. Morin, *J. Hazard. Mater.*, 2020, **384**, 121362.
197 M. H. Carpenter, M. P. Croce, Z. K. Baker, E. R. Batista, M. P. Caffrey, C. J. Fontes, K. E. Koehler, S. E. Kossmann, K. G. McIntosh, M. W. Rabin, B. W. Renck, G. L. Wagner, M. P. Wilkerson, P. Yang, M. D. Yoho, J. N. Ullom, D. A. Bennett, G. C. O'Neil, C. D. Reintsema, D. R. Schmidt, G. C. Hilton, D. S. Swetz, D. T. Becker, J. D. Garda, J. Imrek, J. A. B. Mates, K. M. Morgan, D. Yan, A. L. Wessels, R. H. Cantor, J. A. Hall and D. T. Carver, *J. Low Temp. Phys.*, 2020, **200**(5–6), 437–444.
198 S. Chatterjee, S. Kumari, S. Rath, M. Priyadarshanee and S. Das, *Metallomics*, 2020, **12**(11), 1637–1655.
199 L. Cid-Barrio, F. Calderon-Celis, J. M. Costa-Fernandez and J. R. Encinar, *Anal. Chem.*, 2020, **92**(19), 13500–13508.
200 L. Lago, O. R. B. Thomas and B. R. Roberts, *J. Chromatogr. A*, 2020, **1616**, 460806.
201 Y. L. Li, Y. S. Huang, B. He, R. Z. Liu, G. B. Qu, Y. G. Yin, J. B. Shi, L. G. Hu and G. B. Jiang, *Ecotoxicol. Environ. Saf.*, 2020, **188**, 7.
202 S. Nishida, A. Takahashi, L. Negishi, M. Suzuki and N. Furuta, *Soil Sci. Plant Nutr.*, 2020, 6, DOI: 10.1080/00380768.2020.1860645.